

# Journal of THERMOELECTRICITY

International Research

Founded in December, 1993

published 6 times a year

---

No. 5

2018

---

## Editorial Board

Editor-in-Chief LUKYAN I. ANATYCHUK

Petro I. Baransky

Bogdan I. Stadnyk

Lyudmyla N. Vikhor

Oleg J. Luste

Valentyn V. Lysko

Elena I. Rogacheva

Stepan V. Melnychuk

Andrey A. Snarskii

## International Editorial Board

Lukyan I. Anatyshuk, *Ukraine*

A.I. Casian, *Moldova*

Steponas P. Ašmontas, *Lithuania*

Takenobu Kajikawa, *Japan*

Jean-Claude Tedenac, *France*

T. Tritt, *USA*

H.J. Goldsmid, *Australia*

Sergiy O. Filin, *Poland*

L. Chen, *China*

D. Sharp, *USA*

T. Caillat, *USA*

Yuri Gurevich, *Mexico*

Yuri Grin, *Germany*

Founders – National Academy of Sciences, Ukraine  
Institute of Thermoelectricity of National Academy of Sciences and Ministry  
of Education and Science of Ukraine

Certificate of state registration № KB 15496-4068 ИП

Editors:

V. Kramar, P.V.Gorskiy, O. Luste, T. Podbegalina

Approved for printing by the Academic Council of Institute of Thermoelectricity  
of the National Academy of Sciences and Ministry of Education and Science, Ukraine

Address of editorial office:

Ukraine, 58002, Chernivtsi, General Post Office, P.O. Box 86.

Phone: +(380-372) 90 31 65.

Fax: +(380-3722) 4 19 17.

E-mail: [jt@inst.cv.ua](mailto:jt@inst.cv.ua)

<http://www.jt.inst.cv.ua>

---

Signed for publication 26.11.2018. Format 70×108/16. Offset paper №1. Offset printing.  
Printer's sheet 11.5. Publisher's signature 9.2. Circulation 400 copies. Order 5.

---

Printed from the layout original made by “Journal of Thermoelectricity” editorial board  
in the printing house of “Bukrek” publishers,  
10, Radischev Str., Chernivtsi, 58000, Ukraine

Copyright © Institute of Thermoelectricity, Academy of Sciences  
and Ministry of Education and Science, Ukraine, 2016

## CONTENTS

### **Technology**

- B.S. Dzundza* Automated hardware-software system for measurement of thermoelectric parameters of semiconductor materials 5

### **Design**

- L.I. Anatyshuk, L.M., A.V. Prybyla.* Thermoelectric generators with flame heat sources, two-stage thermopiles and electric energy batteries 14
- O.V. Nitsovykh* Computer simulation of  $Bi_2Te_3$  crystallization process in the presence of electrical current 21
- P.V. Gorskiy, V.V. Razinkov* Influence of container geometry on the orientation and the degree of parallelism of cleavage planes of bismuth telluride single crystals 31
- V.S. Zakordonets, N.V. Kutuzova* Calculation of thermoelectric system for cooling LEDs 42

### **Reliability**

- M.V. Maksimuk* Economic aspects of using starting preheaters with thermoelectric heat sources 52

### **Thermoelectric products**

- L.I. Anatyshuk, N.V. Pasechnikova, V.O. Naumenko, O.S. Zadorozhnyi, M.V. Havryliuk, R.R. Kobylanskyi* Thermoelectric device for determining heat flux from the surface of the eyes 58
- P.D. Mykytiuk., O.Yu. Mykytiuk* In reference to the choice of thermocouple material for metrological-purpose thermal converters 73
- S.F. Zaporov, T.V. Zakharchuk* Device for producing rectangular samples of thermoelectric material 81



**B.S. Dzundza**  *cand. phys. - math. sciences*



*Дзундза Б.С.*

Vasyl Stefanyk PreCarpathian National University  
57, Shevchenko Str., Ivano-Frankivsk, 76018, Ukraine,  
*e-mail: bohdan.dzundza@pu.if.ua*

## **AUTOMATED HARDWARE-SOFTWARE SYSTEM FOR MEASUREMENT OF THERMOELECTRIC PARAMETERS OF SEMICONDUCTOR MATERIALS**

---

*A method of measuring Seebeck coefficient, Hall concentration of current carriers, electrical conductivity of semiconductor films has been described. An electric circuit has been presented and a computer program, which enables automation of measurement, registration and initial processing of data with the possibility of charting time dependences for preliminary analysis of experimental data in the process of measurement, has been developed. Fig. 6, Bibl. 6.*

**Keywords:** thermoelectricity, hall measurements, automation, microcontroller, thin films.

### **Introduction**

Problem of automation of measurements of the Seebeck coefficient, the Hall concentration of current carriers, the electrical conductivity and their dependences on temperature and magnetic field for semiconductor thermoelectric materials, in particular IV-VI compounds, is relevant due to the prospect of their use for creation of thermoelectric energy converters [1]. Such measurements require precise stabilization of temperatures, the magnitude of the magnetic field and the current through the sample, the precision and expensive electrometric equipment, and the study of the thermoelectric parameters of such samples is rather time-consuming.

In recent decades, the rapid development of microprocessor and computer technology opens new opportunities for automation of complex technological processes and laboratory research. Specialized microcircuits and microcontrollers with a large amount of memory, well-developed peripherals and low price, combined with mastering simplicity, are optimal for their use in automated measuring systems.

In this paper, the electric circuit is presented and the computer program is developed that provides automation of measurements of the Seebeck coefficient, electrical conductivity and Hall concentration of current carriers depending on temperature and magnetic fields for film thermoelectric materials, as well as registration, visualization and primary processing of the received data.

### **Measurement method**

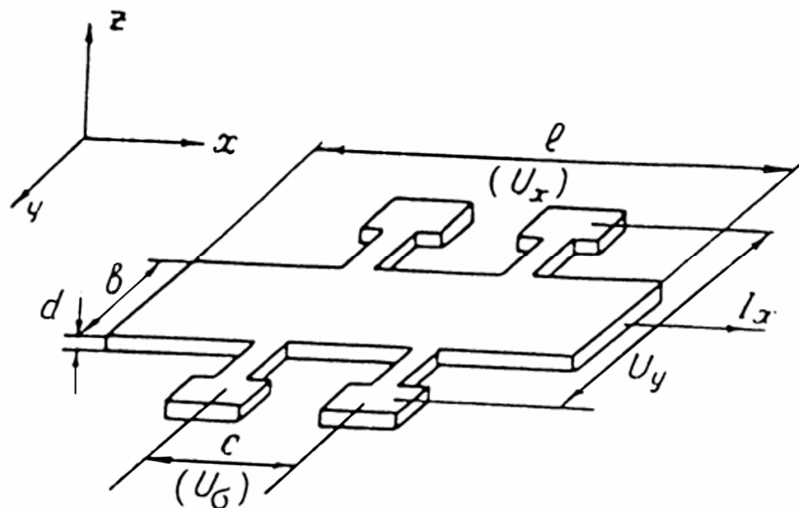
Measurements of the Seebeck coefficient, conductivity, and Hall concentration were carried out in constant magnetic fields up to 2 T. When measuring the film samples were placed in the standard design holders [2] with six measuring probes (two current and four Hall probes). Making reliable ohmic contacts, which do not destroy the film and satisfy all the necessary requirements [2,3], was carried out by silver deposition methods in combination with gilded contact pins or soldering at  $T < 400$  K. The choice of the main contact material was determined by its work output, temperature and mechanical properties. For soldering, indium and its alloys with tin, lead, silver and antimony were used, and silver and copper wires

of (0.01-0.05) mm in diameter were used as connecting elements. In order to ensure ohmicity of contacts and improve adhesion in the soldering places, the gold (for p-type films) or copper (for n-type films) was deposited chemically. Control of the properties of the made contacts was carried out by analyzing the current-voltage characteristics of the samples [2].

The contacts are designed as two massive copper plates; the design ensures a stable temperature gradient of (0.3-1.2) K/mm in the sample. The temperature range in the working area was (77-500) K. The accuracy of the temperature measurement was 0.1-0.2 K and measurement of the magnetic fields –  $\pm 3\%$ . The low temperature cryostats were quartz Dewar flask or styrofoam vessels filled with liquid nitrogen and placed in the gap of the magnet. The intermediate temperatures between liquid nitrogen and room temperatures were reached by heating using a nichrome spiral, bifilarly wound on a tubular cylinder that was hermetically mounted on the sample holder, which allowed measurements in a vacuum of  $10^{-4}$  Pa.



a)



b)

Fig. 1. General view of the measuring cell (a) and configuration of the sample (b) for measuring the electrical parameters of the thin films.

The results averaged measurements in two directions of current and the magnetic field on both pairs of sample contacts (Fig. 1). The thickness of thin films was determined by the optical method using the

micro-interferometer MII-4 with accuracy of  $\sim 0.02$  mkm. Type of conductivity was determined by the sign of thermoEMF [2].

### Schematic of the device

The functional scheme of the device is shown in Fig. 2. The given measuring system is an improved and essentially redesigned version of the previously developed device described by the author in [4]. The basis of the measuring system is a digital multimeter UNI-T UTM1805A, which supports the output of data on the computer and in the mode of voltmeter of constant voltage, provides a resolution of 1 mV with accuracy of 0.015 % and has a mode of automatic selection of measuring range.

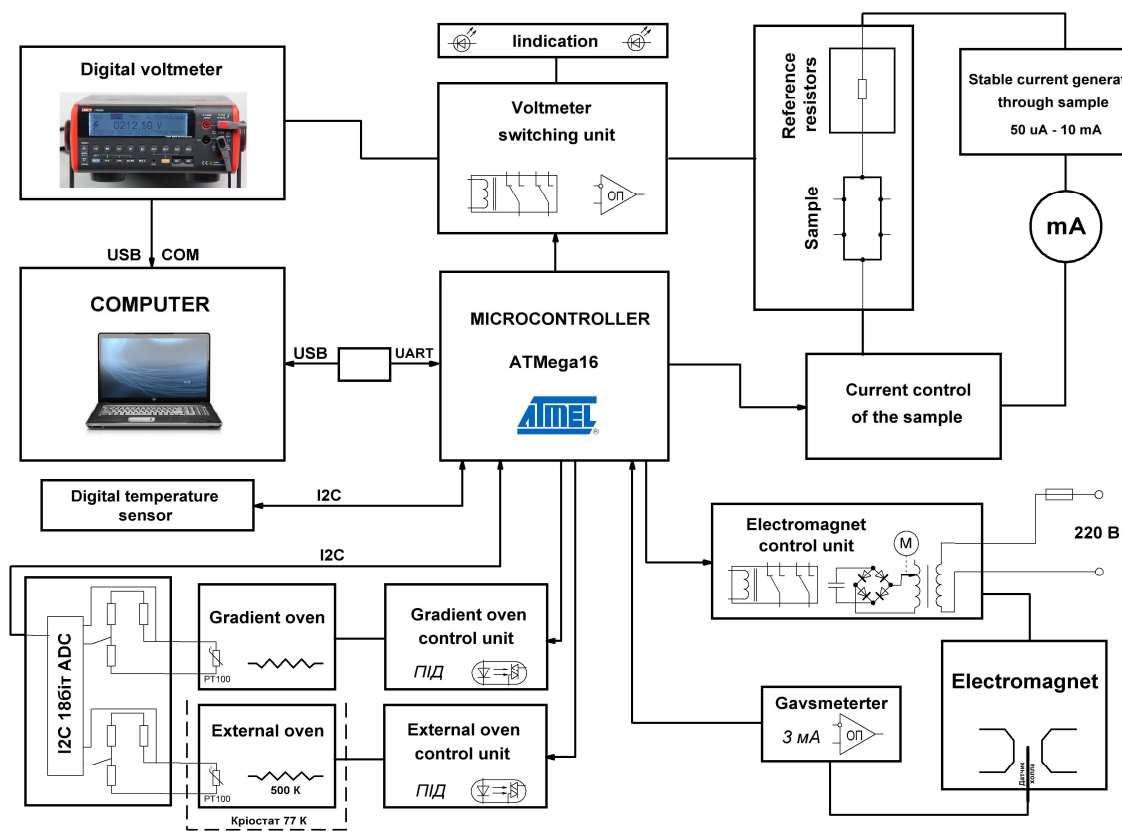


Fig. 2. Functional block diagram of the device of automated measurements of thermoelectric parameters of semiconductors.

Microcontroller ATmega16 was chosen as a controller, which is characterized by enough memory and a well-developed periphery. The use of this microcontroller has made it possible to implement the task and also to leave a resource for further modernization and expansion of functionality. The program for the microcontroller is written in C. Communication with the computer at the hardware level is carried out via USB-UART converter, and at the software level – with the help of the text command interpreter, which provides two-way data exchange between the control program on the computer and the microcontroller of the device.

Measurements of the voltage drop on the sample, reference resistor, Hall and current pairs of

contacts are carried out sequentially with the help of six reed microrelays of the switching unit. The use of reed microrelays provides low contact resistance in the on mode and extremely high (more than 1 G $\Omega$ ) in the off mode, as well as the stability of contacts over time. A generator of stable current through the sample is assembled on a LM234 chip and has 12 discrete values of current, which are controlled by an ammeter. Switching on current and changing polarity are implemented on electromechanical relays controlled by a microcontroller.

The change in the polarity of the magnetic field and the turning on the magnet are implemented on electromagnetic contactors, which are galvanically isolated from the microcontroller using opto-triacs. In order to minimize electromagnetic interference, spark RC chains are installed on all contactors. The control of the magnitude of the magnetic field is carried out smoothly with the help of a motorized laboratory autotransformer. The control of the motor is implemented through opto-triacs and relays for the purpose of galvanic isolation from the control microcontroller. The feedback is carried out by voltage through an isolation transformer TR3 (Fig. 4). In the previous version, an attempt was made to implement the smooth control of the magnetic field by means of pulse-width modulation on high voltage MOS-FET transistors, but due to the large amount of electromagnetic interference and inductive load instability we had to abandon such an implementation.

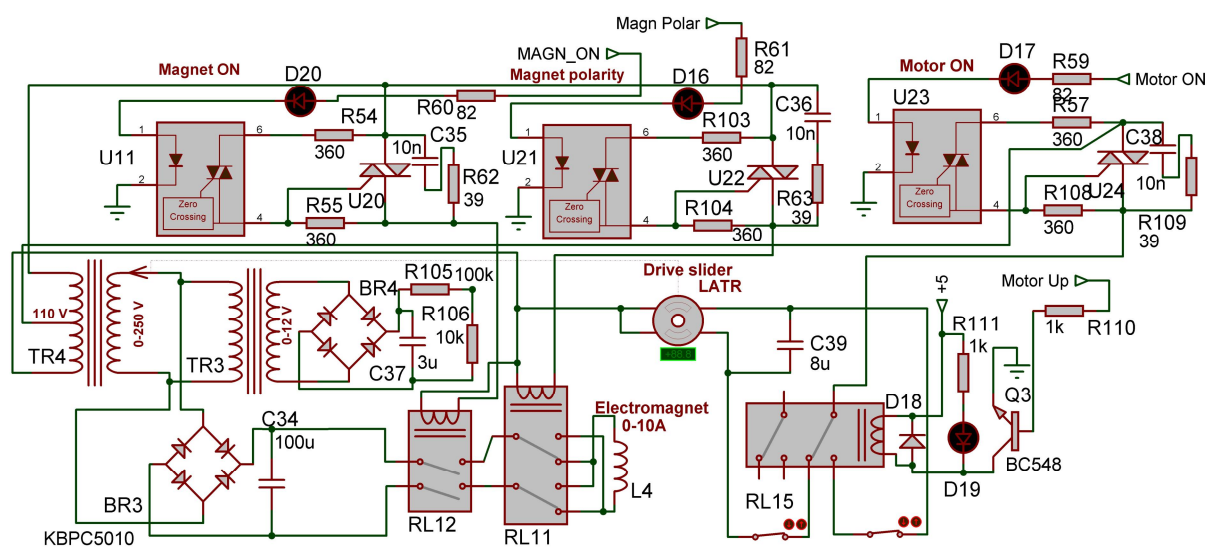


Fig. 3. Electric circuit of the control unit of magnetic induction.

For measuring the magnetic induction, we have used the Hall sensor (ДХК-0.5А, ПХЭ602117Б), which is powered by a stable current of 3 mA and placed on the remote probe in the working area of the magnet (Fig. 3). The signal from the sensor is normalized by the operational amplifier and read by the analog-to-digital converter (ADC) of the microcontroller. Calibration and verification was carried out using a high-precision gaussmeter III1-8 in the range of (0.05-2.0) T with recording the calibration table to the microcontroller memory.

The temperature is measured by platinum thermistors PT100 included in the bridge circuit (Fig. 3), which is powered by a precision reference voltage source AD1583. As resistors in the shoulders of the bridge 0.1 % SMD resistors with low temperature coefficient were used. Bridge imbalance voltage is measured by the discrete I2C delta-sigma ADC MCP3424, placed along with the bridge circuits and the reference voltage source on a separate board in the measuring cell connector. The heater control is provided by the triac regulator with switching at the voltage transition through zero and optocoupler.



Stabilization of the temperature is carried out using proportional-integral-derivative (PID) algorithm with a uniform distribution of periods according to Bresenham's algorithm.

The general view of the device is shown in Fig. 5. In order to minimize electromagnetic interference, functional units are assembled on separate printed circuit boards, which are placed in enclosed aluminum cells of the grounded case and connected together by a shielded wire, and the power unit (magnet and heater control unit) is put into a separate case (Fig. 5).

### Software implementation of the measurement process

The computer program provides automated control of the measurement process, digital voltmeter data recording, data preprocessing and visualization. The program is written in the Delphi environment. The voltmeter data are received and decoded by the program and displayed on the screen, and the average value of the last ten measurements is calculated and displayed. The UNI-T wattmeter is supported both with the new data transfer protocol (UTM1805A) and the previous version (UT804).

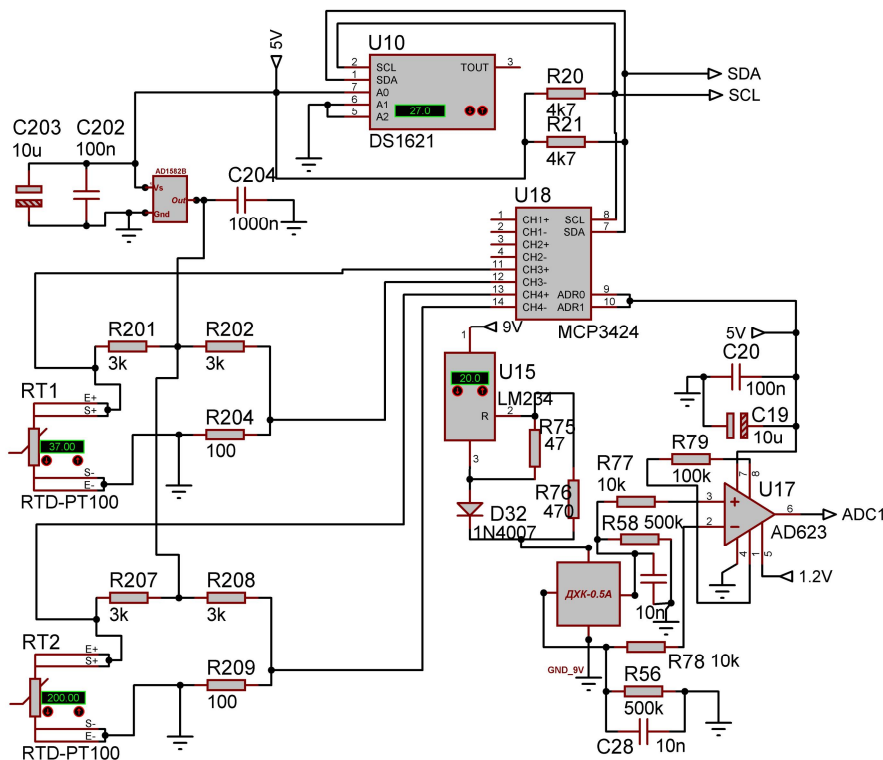


Fig. 4. Electric circuit of the unit for measuring temperature and magnetic induction.

Between the controller and the computer there is a two-way exchange of information via UART (9600 bps, 8 bits), device control and data request are carried out by sending commands and receiving the response after their execution. Validation of the command and its re-sending in the case of error are implemented. Since some commands are executed periodically, in order to avoid failures, the status of waiting for the result of the execution of the current command is monitored.

In manual mode, the program allows you to control separate functional units independently, which makes it possible to set-up and perform a non-standard test with automatic or manual recording of results.



Fig. 5. General view of the device for automated measurements of thermoelectric parameters of semiconductors.

In automatic mode, the program allows both single measurements of electrical parameters with automatic calculation of the Seebeck coefficient, specific conductivity, concentration and mobility of carriers, etc. and a series of measurements of dependences on time, temperature or magnetic field with the construction of the time-temperature diagram of the planned measurements (Fig. 6). During measurements, visualization of the selected parameters in the graphs is possible.

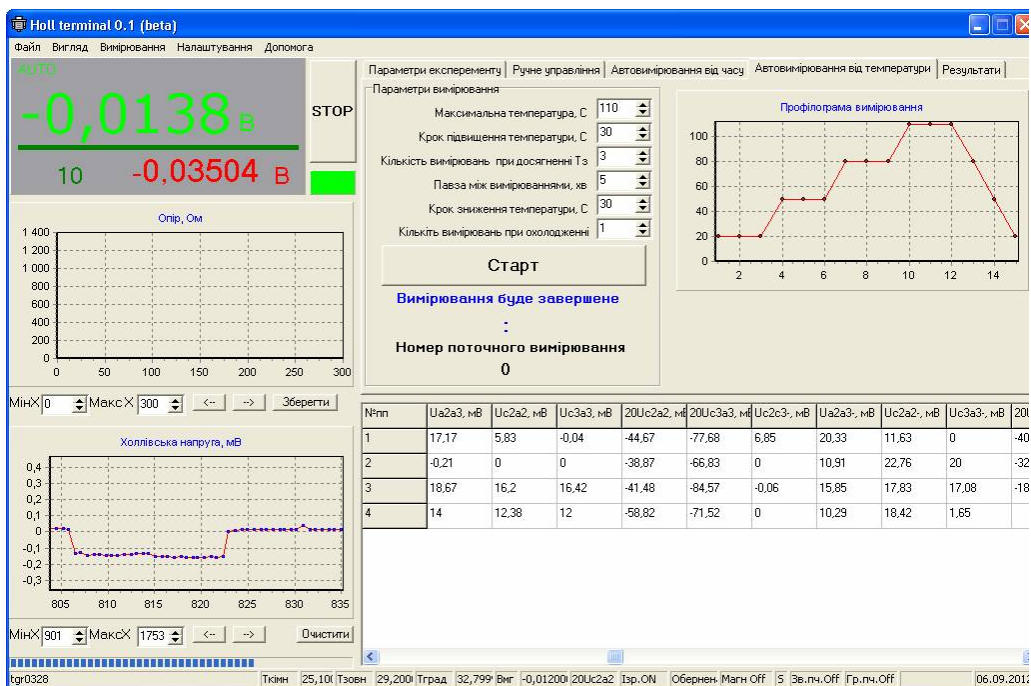


Fig. 6. General view of the window of the control program in the process of automated measurements of thermoelectric parameters of films.

For a series of samples of different thicknesses, the automatic data filtering option and construction

of profiles of electrical parameters are implemented. The measurement results of each sample are stored in a separate MS Excel compatible file with the possibility of further continuation of the experiment.

For estimation of the errors, measurements of samples of different types of conductivity with known parameters have been carried out. The maximum error for  $\sigma$  did not exceed 3 %, for RH – 5 %, and for the value of  $\alpha$  – 10 %. The results of study of thermoelectric semiconductor films obtained on this measuring system are presented in [4-6]. With long-term regular operation, the device has shown high reliability and stability of the results.

## Conclusions

1. An electric circuit has been developed, and an operating device for measuring the Seebeck coefficient, the Hall concentration of current carriers, and the specific conductivity of semiconductor film thermoelectric materials has been designed.
2. A computer program that provides automation of measurements, registration and primary processing of data with possibility of visualization of graphic dependencies has been created.

## References

1. Shperun V.M., Freik D.M., Zapukhliak R.I. Termoelektryka telurydu svyntsiu ta yoho analohiv. Ivano-Frankivsk, Plai, 2000, 250 s.
2. Kuchys E.V. Metod yssledovanyia efekta Kholla. Moskva, Sovetskoe radio, 1974, 328 s.
3. Kovtoniuk N.F.. Yzmerenye parametrov poluprovodnykovykh materiyalov. Moskva, Metallurhiya, 1970, 429 s.
4. Saliy Y.P., Dzundza B.S., Bylina I.S., Kostyuk O.B. The influence of the technological factors of obtaining on the surface morphology and electrical properties of the PbTe films doped Bi// Journal of Nano- and Electronic Physics, Vol 8, N 2, 2016, P. 02045-02051.
5. Dzundza B.S., Kostyuk O.B., Makovyshyn V.I., Pehinchuk M.Iu. Termoelektrychni vlastyvoli tonkykh plivok na osnovi chystoho i lehovanoho pliumbum telurydu // Termoelektryka №6, 2016. S. 55-61.
6. Ruvinskii M.A., Kostyuk O.B., Dzundza B.S., Yaremiy I.P., Mokhnatskyi M.L., Yavorsky Ya.S. Kinetic phenomena and thermoelectric properties of polycrystalline thin films based on PbSnAgTe compounds // Journal of Nano - and Electronic Physics, Vol. 9, N 5, 2017, P. 05004-1 – 05004-6.

Submitted 04.10.2018

**Б.С. Дзундза** канд. фіз.-мат. наук

Прикарпатський національний університет імені Василя Стефаника,  
вул. Шевченка, 57, Івано-Франківськ, 76018, Україна,  
*e-mail: bohdan.dzundza@pu.if.ua*

**АВТОМАТИЗОВАНИЙ ПРОГРАМНО-АПАРАТНИЙ**

## **КОМПЛЕКС ДЛЯ ВИМІРЮВАННЯ ТЕРМОЕЛЕКТРИЧНИХ ПАРАМЕТРІВ НАПІВПРОВІДНИКОВИХ МАТЕРІАЛІВ**

*Описано методу вимірювання коефіцієнта Зеебека, холлівської концентрації носіїв, питомої електропровідності напівпровідникових плівкових термоелектричних матеріалів. Представлена електрична схема та розроблена комп'ютерна програма, що забезпечує автоматизацію вимірювань, реєстрацію і первинною обробку даних, з можливістю побудови графіків часових залежностей для попереднього аналізу експериментальних даних вже в процесі вимірювання. Бібл. 6, Рис. 6.*

**Ключові слова:** термоелектрика, холлівські вимірювання, автоматизація, мікроконтролер, тонкі плівки.

**Б.С. Дзундза канд. физ.-мат. наук**

Прикарпатський національний університет  
імені Василя Стефаника, ул. Шевченко, 57,  
Івано-Франківськ, 76018, Україна  
*e-mail: bohdan.dzundza@pu.if.ua*

## **АВТОМАТИЗИРОВАННЫЙ ПРОГРАММНО-АППАРАТНЫЙ КОМПЛЕКС ДЛЯ ИЗМЕРЕНИЯ ТЕРМОЭЛЕКТРИЧЕСКИХ ПАРАМЕТРОВ ПОЛУПРОВОДНИКОВЫХ МАТЕРИАЛОВ**

*Описана методика измерения коэффициента Зеебека, холловской концентрации носителей, удельной электропроводности полупроводниковых пленочных термоэлектрических материалов. Представлена электрическая схема и разработана компьютерная программа, которая обеспечивает автоматизацию измерений, регистрацию и первичную обработку данных, с возможностью построения графиков временных зависимостей для предварительного анализа экспериментальных данных уже в процессе измерения.*

**Ключевые слова:** термоэлектричество, холловские измерения, автоматизация, микроконтроллер, тонкие пленки.

### **References**

1. Shperun V.M., Freik D.M., Zapukhliak R.I.. Termoelektryka telurudu svyntsiu ta yoho analohiv. Ivano-Frankivsk, Plai, 2000, 250 s.
2. Kuchys E.V. Metody issledovaniya effekta Kholla. Moskva, Sovetskoe radio, 1974, 328 s.
3. Kovtoniuk N.F.. Yzmerenye parametrov poluprovodnikovyykh materyalov. Moskva, Metallurhiya, 1970, 429 s.
4. Saliy Y.P., Dzundza B.S., Bylina I.S., Kostyuk O.B. The influence of the technological factors of obtaining on the surface morphology and electrical properties of the PbTe films doped Bi// Journal of Nano- and Electronic Physics, Vol 8, N 2, 2016, P. 02045-02051.
5. Dzundza B.S., Kostyuk O.B., Makovyshyn V.I., Pehinchuk M.Iu. Termoelektrychni vlastyvoli tonkykh plivok na osnovi chystoho i lehovanoho pliumbum telurudu // Termoelektryka №6, 2016. S. 55-61.

6. Ruvinskii M.A., Kostyuk O.B., Dzundza B.S., Yaremiy I.P., Mokhnatskyi M.L., Yavorsky Ya.S. Kinetic phenomena and thermoelectric properties of polycrystalline thin films based on PbSnAgTe compounds // *Journal of Nano - and Electronic Physics*, Vol. 9, N 5, 2017, P. 05004-1 – 05004-6.

Submitted 04.10.2018

**L.I. Anatyshuk** *acad. National Academy of Sciences of Ukraine*<sup>1,2</sup>

**A.V. Prybyla** *cand. Phys. - math. Sciences*<sup>1,2</sup>



L.I. Anatyshuk

<sup>1</sup>Institute of Thermoelectricity  
of the NAS and MES of Ukraine,  
1, Nauky str., Chernivtsi, 58029, Ukraine;  
<sup>2</sup>Yu.Fedkovych Chernivtsi National University,  
2, Kotsiubynskyi str., Chernivtsi, 58000, Ukraine  
*e-mail: anatysh@gmail.com*



A.V. Prybyla

## THERMOELECTRIC GENERATORS WITH FLAME HEAT SOURCES, TWO-STAGE THERMOPILES AND ELECTRIC ENERGY BATTERIES

---

*This paper presents calculations of the dynamic power of a two-stage thermoelectric generator with flame heat sources of variable power. The results of calculations of such a generator with its stages made of materials based on BiTe and SiGe are given. Bibl. 6, Fig. 2.*

**Key words:** *thermoelectric generator, computer design, physical model.*

### Introduction

*General characterization of the problem.* One of the factors limiting the widespread practical application of thermoelectric generators (TEG) is the low efficiency of thermal into electric energy conversion, due to the use of single-stage modules with a low dimensionless figure of merit of thermoelectric materials in the TEG design,  $ZT = 1.0 - 1.6$  [1 – 3]. One way to increase the efficiency of thermoelectric conversion is to extend the range of operating temperatures of the module by cascading [4]. To create generator modules optimized for the working temperature level of 30-600 °C, it is expedient to use a two-stage circuit with thermoelements based on *Bi-Te* of *n*- and *p*-type conductivity in the low-temperature stage (up to 300 °C) and, accordingly, *Si-Ge* based thermoelements, which provide high efficiency in the high-temperature stage (300 - 600 °C).

The Institute of Thermoelectricity of the National Academy of Sciences and the Ministry of Education and Science of Ukraine developed special thermoelectric modules from such materials for each of the TEG stages. Nevertheless, no calculations have been made yet of the parameters of the TEG using a circuit with thermoelements based on *Bi-Te* in the low-temperature stage and *Si-Ge* in the high-temperature stage, in the mode close to its actual operation. Correct matching of the TEG stages also remains important.

Thus, the purpose of this work is to calculate the dynamic performance of a two-stage thermoelectric generator with heat sources of variable power in the range of temperatures 30-600 °C.

### Physical model

The calculations used a physical model of a thermoelectric generator unit (Fig. 1), which contains the heated surface of a heat source of variable power 1, heat exchangers 2 for supply of heat flux to the module of a high-temperature stage of TEG (made of thermoelectric material based on *Si-Ge* [5]) 3 and heat exchangers 7 for removal of heat flux from the two modules of high-temperature stage of TEG (made of standard thermoelectric material based on *Bi-Te* [5]) 5, heat-leveling plate 4, thermal insulation 6,

electric voltage stabilizer 8 and electric energy battery 9.

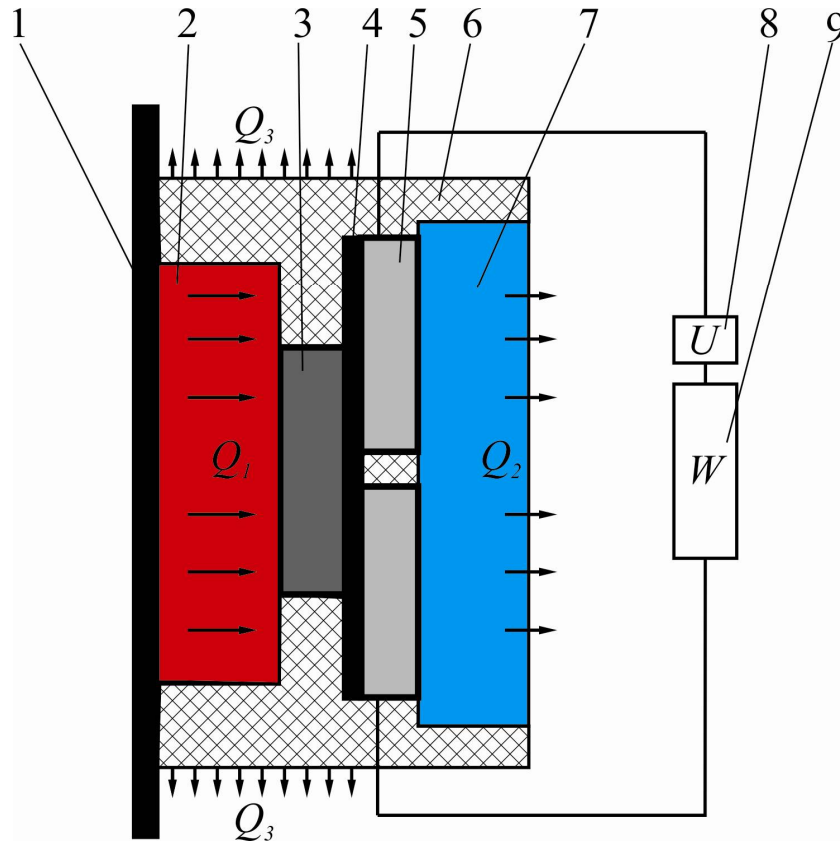


Fig. 1. Physical model of a thermoelectric generator unit:

- 1 – heated surface; 2 – hot heat exchanger; 3 – module of a high-temperature stage of TEG;  
 4 – heat-leveling plate; 5 – modules of a high-temperature stage of TEG;  
 6 – thermal insulation; 7 – cold heat exchanger; 8 – voltage stabilizer;  
 9 – electric energy battery.

Since the generator is installed on a heated surface, the model does not consider the processes of heat transfer from the actual source of combustion of fuel to this surface. Instead, to determine the temperature of the heated surface 1, the experimental temporal dependence of its temperature in the real cycle of using the solid fuel heat source is used [2].

### Mathematical and computer descriptions of the model

Thus, the equation of heat balance is used to calculate the thermoelectric generator in accordance with the physical model (Fig. 1).

On the hot side there is a heat source of variable power  $Q_1[T_1(t)]$ . Its thermal power depends on the temperature of this surface  $T_1$  which, in turn, changes with time  $t$  (Fig. 3), and is given in the form of some function  $f[T_1(t)]$ .

$$Q_1 = f[T_1(t)], \quad (1)$$

Heat supply from the heated surface to the hot side of the thermoelectric module and heat removal to

the cold heat exchanger is described by the equations:

$$Q_1 = \chi_1 [T_1(t) - T_r], \quad (2)$$

$$Q_2 = \chi_2 [T_x - T_2], \quad (3)$$

where  $\chi_1, \chi_2$  are thermal resistances of the hot and cold heat exchangers;  $T_h, T_c$  are the hot and cold side temperatures of thermoelectric module, respectively;  $T_2$  is the temperature of the external surface of the cold heat exchanger.

Thermal power  $Q_2$  is removed from the cold heat exchanger by forced convection of air to the environment:

$$Q_2 = \alpha (T_2 - T_0) S_m, \quad (4)$$

where  $\alpha$  is coefficient of convective heat exchange between the surface of the heat exchanger and the environment;  $S_m$  is the area of heat exchange surface;  $T_0$  is ambient temperature.

The electrical power generated by thermoelectric module is proportional to  $Q_1 [T_1(t)]$  and its efficiency  $\eta$ :

$$W = Q_1 [T_1(t)] \cdot \eta, \quad (5)$$

The main losses of heat  $Q_3$  occur due to thermal insulation:

$$Q_3 = \chi_4 (T_M - T_0), \quad (6)$$

where  $\chi_4$  is thermal resistance of insulation,  $T_M$  is temperature of the internal surface of thermal insulation.

Thus, the equation of heat balance for the chosen model of the thermoelectric generator can be written as:

$$Q_1 = W + Q_2 + Q_3. \quad (7)$$

For the computer representation of the TEG mathematical model, the Comsol Multiphysics software package [6] was used. For this it is necessary to present our equations in the following form.

To describe the flows of heat and electricity, we will use the laws of conservation of energy

$$\operatorname{div} \vec{E} = 0 \quad (8)$$

and electrical charge

$$\operatorname{div} \vec{j} = 0, \quad (9)$$

where

$$\vec{E} = \vec{q} + U\vec{j}, \quad (10)$$



$$\vec{q} = \kappa \nabla T + \alpha T \vec{j}, \quad (11)$$

$$\vec{j} = -\sigma \nabla U - \sigma \alpha \nabla T. \quad (12)$$

Here  $\vec{E}$  is energy flux density,  $\vec{q}$  is heat flux density,  $\vec{j}$  is electrical current density,  $U$  is electrical potential,  $T$  is temperature,  $\alpha$ ,  $\sigma$ ,  $\kappa$  are the Seebeck coefficient, electrical conductivity and thermal conductivity.

With regard to (10) – (12), one can obtain

$$\vec{E} = -(\kappa + \alpha^2 \sigma T + \alpha U \sigma) \nabla T - (\alpha \sigma T + U \sigma) \nabla U. \quad (13)$$

Then the laws of conservation (8), (9) will take on the form:

$$-\nabla [(\kappa + \alpha^2 \sigma T + \alpha U \sigma) \nabla T] - \nabla [(\alpha \sigma T + U \sigma) \nabla U] = 0, \quad (14)$$

$$-\nabla(\sigma \alpha \nabla T) - \nabla(\sigma \nabla U) = 0. \quad (15)$$

From the solution of equation (14) - (15) we obtain the distribution of physical fields, as well as the integral values of the efficiency and power of the TEG.

### Description of the dynamic powers of TEG

To determine the actual temperature conditions on the heated surfaces of furnaces with flame heat sources on solid fuels (wood), experimental studies were carried out and the dependences of the heated furnace surfaces on the time during which the equal amount of wood was added at identical intervals were determined [2].

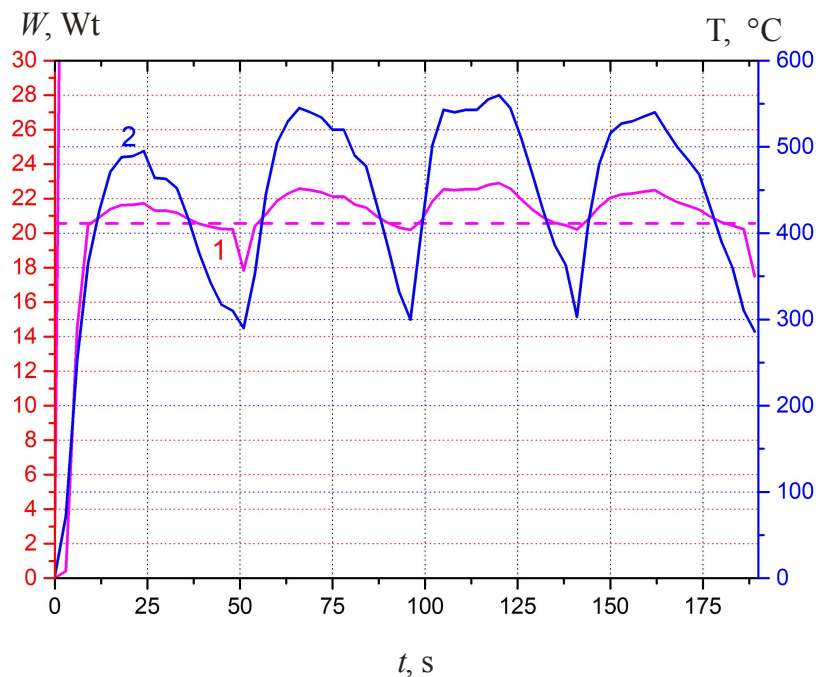


Fig. 2. Temporal dependence of a TEG located on the rear surface of the furnace:  
 1 – TEG power at  $T_c=30^\circ$ , 2 – the surface temperature of the furnace.

The obtained data are processed in the form of functional temporal dependences of the temperatures of heated furnace surfaces and used in the calculations of characteristics of a thermoelectric generator with flame heat sources of variable power on solid fuels.

Thus, using computer methods, the calculation of the dynamic powers of a TEG in terms of its installation on the surface of the furnace was carried out (Fig. 2).

Thus, Fig. 2 shows a temporal dependence of the power of TEG located on the rear surface of the furnace for the cold side temperature of TEG  $T_c = 30^\circ\text{C}$  (1 in Fig.2). The hot side temperature of the TEG is shown by the solid curve 2 in Fig. 2.

As can be seen from Fig. 2, the type of the temporal dependence of the dynamic power though reproduces the dependences of furnace surface temperature, but this dependence on temperature is not so sharp as in the single-stage version of TEG. For the cold side temperature  $T_c = 30^\circ\text{C}$ , the average power of a TEG, consisting of one thermoelectric module in the high-temperature stage (*Si-Ge*) and two in the low-temperature stage (*Bi-Te*) is 20.56 W for a selected period of time. At the same time, the energy generated by TEG per 1 hour is  $\sim 70$  kJ.

Thus, the investigated version of a two-stage TEG made of special materials based on *BiTe* – *SiGe* allows increasing its specific power by  $\sim 12.5\%$  as compared to the single-stage version [2].

## Conclusions

1. Based on the experimental data, the dynamic power of a two-stage TEG with flame sources of heat on solid fuels was calculated using *Bi-Te*-based thermoelements in the low-temperature stage and *Si-Ge* in the high-temperature stage.
2. The average power of a TEG consisting of one thermoelectric module in the high-temperature stage (*Si-Ge*) and two in the low-temperature stage (*Bi-Te*) is 20.56 W for a selected period of time (with its cold side temperature  $T_c = 30^\circ\text{C}$ ). At the same time, the energy generated by TEG per 1 hour is  $\sim 70$  kJ.
3. It is established that the investigated version of a two-stage TEG made of special materials based on *BiTe* – *SiGe* allows increasing its specific power by  $\sim 12.5\%$  as compared to the single-stage version.

## References

1. Anatychuk L.I., Mocherniuk R.M., Havryliuk M.V., Andrusiak I.S. (2017). Thermoelectric generator using the heat of heated surfaces. *J. Thermoelectricity*, 2, C 84 – 95.
2. Anatychuk L.I., Rozver Yu.Yu., Prybyla A.V., Maksimuk M.V. (2018). Thermoelectric generators with flame heat sources of variable power and temperature stabilizers for thermopiles. *J. Thermoelectricity*, 2.
3. Anatychuk L.I., Prybyla A.V. (2018). Thermoelectric generators with flame heat sources of variable power, single-stage thermopiles and electric energy batteries. *J. Thermoelectricity*, 3.
4. Mykhailovsky V.Ya., Bilinsky-Slotylo V.R. (2012). Thermoelectric staged modules of materials based on *Bi<sub>2</sub>Te<sub>3</sub>-PbTe*-TAGS. *J. Thermoelectricity*, 4, 67-74.
5. <http://www.ite.inst.cv.ua>
6. *COMSOL Multiphysics User's Guide* (2010). COMSOLAB, 804 p.

Submitted 22.10.2018

**Анатичук Л.І.,** *акад. НАН України*<sup>1,2</sup>  
**Прибила А.В.,** *канд. физ.-мат. наук*<sup>1,2</sup>

<sup>1</sup>Інститут термоелектрики НАН і МОН України,  
вул. Науки, 1, Чернівці, 58029, Україна;  
<sup>2</sup>Чернівецький національний університет  
ім. Юрія Федьковича, вул. Коцюбинського 2,  
Чернівці, 58012, Україна

### **ТЕРМОЕЛЕКТРИЧНІ ГЕНЕРАТОРИ З ПОЛУМ'ЯНИМИ ДЖЕРЕЛАМИ ТЕПЛА ЗМІННОЇ ПОТУЖНОСТІ, ДВОКАСКАДНИМИ ТЕРМОБАТАРЕЯМИ ТА АКУМУЛЯТОРАМИ ЕЛЕКТРИЧНОЇ ЕНЕРГІЇ**

*У роботі виконано розрахунки динамічної потужності двокаскадного термоелектричного генератора з полум'яними джерелами тепла змінної потужності. Наводяться результати розрахунків такого генератора із каскадами, виготовленими із матеріалів на основі BiTe та SiGe. Бібл. 6, рис. 2.*

**Ключові слова:** термоелектричний генератор, комп'ютерне проектування, фізична модель.

**Анатычук Л.И.,** *акад. НАН Украины*<sup>1,2</sup>  
**Прыбыла А.В.,** *канд. физ.-мат. наук*<sup>1,2</sup>

<sup>1</sup>Институт термоэлектричества НАН и МОН Украины,  
ул. Науки, 1, Черновцы, 58029, Украина,  
*e-mail: anatyuch@gmail.com;*  
<sup>2</sup>Черновицкий национальный университет  
им. Юрия Федьковича, ул. Коцюбинского, 2,  
Черновцы, 58012, Украина

### **ТЕРМОЭЛЕКТРИЧЕСКИЕ ГЕНЕРАТОРЫ С ПЛАМЕННЫМИ ИСТОЧНИКАМИ ТЕПЛА ПЕРЕМЕННОЙ МОЩНОСТИ, ДВУХКАСКАДНЫМИ ТЕРМОБАТАРЕЯМИ И АККУМУЛЯТОРАМИ ЭЛЕКТРИЧЕСКОЙ ЭНЕРГИИ**

*В работе выполнены расчеты динамической мощности двухкаскадного термоэлектрического генератора с пламенными источниками тепла сменной мощности. Приводятся результаты расчетов такого генератора с каскадами, изготовленными из материалов на основе систем Bi-Te и*

*Si-Ge. Библ. 6, Рис. 2.*

**Ключевые слова:** термоэлектрический генератор, компьютерное проектирование, физическая модель.

## References

1. Анатичук Л.И., Мочернюк Р.М., Гаврилюк М.В., Андрусак И.С. Термоэлектрический генератор, который использует тепло нагретых поверхностей // Термоэлектричество. - 2017. №2. - С 84 – 95.
2. Анатичук Л.И., Розвер Ю.Ю., Прибила А.В., Максимук М.В. Термоэлектрические генераторы с пламенными источниками тепла сменной мощности и стабилизаторами температуры термобатарей // Термоэлектричество. - 2018. №2.
3. Анатичук Л.И., Прибила А.В. Термоэлектрические генераторы с пламенными источниками тепла сменной мощности, однокаскадными термобатареями та аккумуляторами электрической энергии // Термоэлектричество. - 2018. №3.
4. Михайловський В.Я. Термоэлектрические каскадные модули из материалов на основе  $\text{Bi}_2\text{Te}_3$ - $\text{pbte}$ -tags. / Михайловський В.Я., Білінський-Слотило В.Р. // Термоэлектричество, 2012, №4, С. 67-74.
5. <http://www.ite.inst.cv.ua>.
6. COMSOL Multiphysics User's Guide // COMSOLAB. - 2010. - 804 p.

Submitted 22.10.2018

---

**O.V. Nitsovykh** *cand. phys.-math. sciences*<sup>1,2</sup>



*O.V. Nitsovykh*

<sup>1</sup>Institute of Thermoelectricity of the NAS and MES of Ukraine,  
1 Nauky str., Chernivtsi, 58029, Ukraine;  
*e-mail: anatykh@gmail.com*

<sup>2</sup>Yuriy Fedkovych Chernivtsi National University,  
2 Kotsiubynsky str., Chernivtsi, 58012, Ukraine;

## **COMPUTER SIMULATION OF $Bi_2Te_3$ CRYSTALLIZATION PROCESS IN THE PRESENCE OF ELECTRICAL CURRENT**

---

*This paper presents an approach to constructing a computer model of the process of growing thermoelectric materials by the method of vertical zone melting taking into account the Peltiereffect which occurs at the interface between the solid and liquid phases of material being grown when passing electrical current through the ingot. The results of visualization of numerical model solution are presented. Bibl. 10, Fig. 4.*

**Keywords:** simulation, vertical zone melting, thermoelectric material, growing in electrical field

### **Introduction**

Thermoelectric power converters - coolers and thermogenerators - are widely used in many branches of modern technology. An urgent task is to increase the efficiency of these devices, including the creation of materials for them with high thermoelectric figure of merit  $Z$ .

The most widely used semiconductor solid solutions are  $Bi_2Te_3$ - $Bi_2Se_3$  and  $Bi_2Te_3$ - $Sb_2Te_3$ , which have the highest figure of merit values in the temperature range 250-500 K. To obtain a thermoelectric material (TEM) based on  $Bi_2Te_3$  with high parameters, the most promising methods are directional melt crystallization and vertical zone melting. Moreover, production of thermoelectric materials with the required properties is possible only under the conditions of a controlled crystallization process. Therefore, it is relevant to model TEM growing processes, which allow optimizing the choice of technological parameters of the installation.

In [1, 5], the possibility of growing single crystals of thermoelectric materials by the method of vertical zone melting in the presence of electrical current passing through an ingot was considered. It is known that the interface between the solid and liquid phases of the same material is the site where the magnitude of the thermoelectric power, electrical conductivity, thermal conductivity and other properties change abruptly. At the interface, the picture of filling energy levels with electrons also changes. This is manifested in the Peltier effect which occurs at the crystallization front of a material when an electrical current is passed through a crystal being grown. The amount of heat released or absorbed at the interface between the liquid and solid phases can affect the course of crystallization.

Thus, the purpose of this work is to create a method for constructing a computer model of the process of growing thermoelectric materials by the method of vertical zone melting, taking into account the Peltier effect that occurs at the interface between the solid and liquid phases of the material being grown by passing electrical current through the ingot.

### Physical model of vertical zone melting process

The physical model of the process of growing single crystals based on  $\text{Bi}_2\text{Te}_3$  by the method of vertical zone melting is shown in Fig.1.

The figure shows an ingot fragment, including polycrystalline material 2, molten zone 6 and single crystal 3. The ingot is placed in quartz ampoule 1. With the help of heater 7 and cooler system 8, molten zone 6 is formed, which, moving with the heater along the sample, provides melting of polycrystal and melt crystallization below boundary 5, which is called the crystallization front.

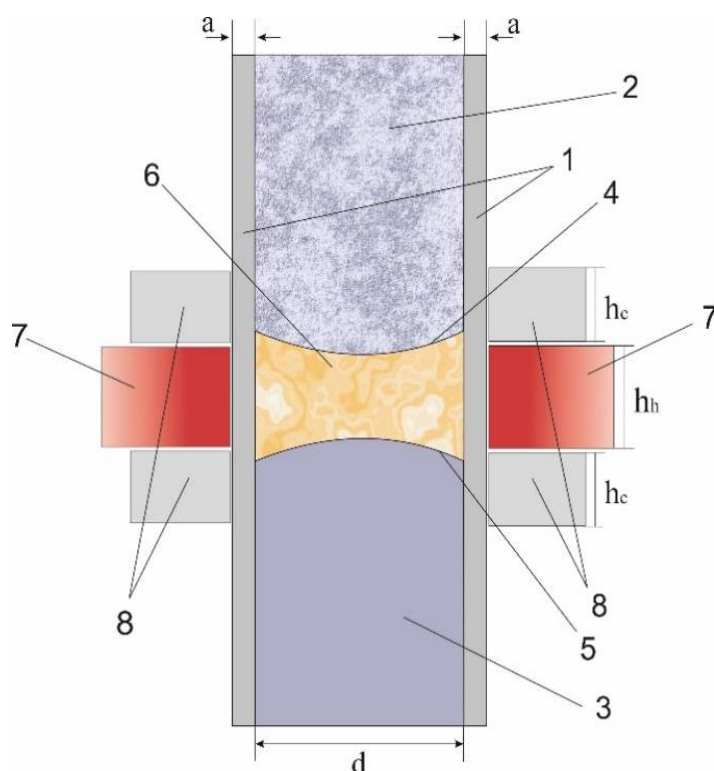


Fig.1. Physical model of installation for growing TEM by vertical zone melting method:  
 1 – quartz ampoule, 2 – material in solid phase (polycrystal), 3 – material in solid phase (single crystal), 4 – melt front boundary, 5 – crystallization front boundary,  
 6 – material in liquid phase (melt front), 7 – heater, 8 – coolers.

Since the boundaries of the solid and liquid phases 4 and 5 of the same material are the site of an abrupt change in the properties of this material, in particular, the values of the thermoelectric coefficient  $\alpha$ , electrical conductivity  $\sigma$  or thermal conductivity  $\kappa$ , when passing through these boundaries of electrical current, in one of them the Peltier heat will be absorbed, and on the other, accordingly, released.

### Mathematical and computer description of the model

When modeling the heat conduction process in a homogeneous medium with a phase transition in the COMSOL Multiphysics software package, the classical system of non-stationary differential heat conduction equations is solved, supplemented by the dependences of the physical properties of the solid under study as a function of the phase state at a given point at a specified temperature

$$\rho C_p \frac{\partial T}{\partial t} + \rho C_p u \nabla T + \nabla q = Q, \quad (1)$$

$$q = -\kappa \nabla T, \quad (2)$$

$$\rho = \theta \rho_{\text{phase1}} + (1-\theta) \rho_{\text{phase2}}, \quad (3)$$

$$C_p = \frac{1}{2} \left( \theta \rho_{\text{phase1}} C_{p_{\text{phase1}}} + (1-\theta) \rho_{\text{phase2}} C_{p_{\text{phase2}}} \right) + L \frac{d\alpha_m}{dT}, \quad (4)$$

$$\alpha_m = \frac{1}{2} \cdot \frac{(1-\theta) \rho_{\text{phase2}} - \theta \rho_{\text{phase1}}}{\theta \rho_{\text{phase1}} - (1-\theta) \rho_{\text{phase2}}}, \quad (5)$$

$$\kappa = \theta \kappa_{\text{phase1}} + (1-\theta) \kappa_{\text{phase2}}, \quad (6)$$

where  $\rho$  is the density,  $\text{kg/m}^3$ ;  $C_p$  is heat capacity of material at constant pressure,  $\text{J}/(\text{kg}\cdot\text{K})$ ;  $\kappa$  is thermal conductivity,  $\text{W}/(\text{cm}\cdot\text{K})$ ,  $u$  is medium velocity,  $\text{m/s}$ , in the investigated problem is zero;  $T$  is temperature,  $\text{K}$ ;  $t$  is time,  $\text{s}$ ;  $\theta$  is the phase ratio at a given temperature;  $\alpha_m$  is mass ratio between phases;  $L$  is the latent heat of phase transition,  $\text{J/kg}$ ;  $Q$  is external heat flux,  $\text{W}$ . The indices *phase1* and *phase2* indicate to what phase the properties, solid phase or liquid, respectively, are related.

The Joule-Lenz heat is in the material due to the passage of electrical current, is taken into account in the right-hand side of Eq. (1) by another term  $Q_e = jE$ .

To account for thermoelectric effects, in particular, the Peltier effect, which occurs at the interfaces between the phases, we write formula (2) as follows:

$$q = -\kappa \nabla T + Pj, \quad (7)$$

here

$$j = \sigma E + j_e, \quad (8)$$

$$j_e = -\sigma \alpha \nabla T, \quad (9)$$

$$P = \alpha T,$$

$$E = -\nabla U.$$

Where  $U$  is the electrical potential,  $\text{V}$ ;  $\alpha$  is the Seebeck coefficient,  $\mu\text{V}/\text{K}$ ;  $\sigma$  is the electrical conductivity,  $(\text{Ohm}\cdot\text{cm})^{-1}$ .

To simulate the effect of the electrical field on the growing process, the following boundary

conditions are set at the upper and lower bounds of the ingot:

$$U|_{z=0} = U_0, \quad U|_{z=l} = 0.$$

The condition of thermal insulation was set on all external walls of the heater and coolers:

$$-n \cdot (-\kappa \nabla T) = 0. \quad (10)$$

On the outer wall of the quartz ampoule (in areas not in contact with the heater and coolers), the boundary condition of the heat flow is set, as a function of:

$$-n \cdot (-\kappa \nabla T) = h \cdot (T_{ext} - T), \quad (11)$$

Where  $T_{ext}$  is the ambient temperature, K;  $T$  is the temperature of the inner wall of the ampoule, K;  $n$  is vector directed along the normal to the surface of the cylinder (ampoule);  $h$  is the heat transfer coefficient,  $\text{W}/(\text{m}^2 \cdot \text{K})$ , which is expressed by the formula [8]:

$$h = \begin{cases} \frac{k}{l} \left( 0.68 + \frac{0.67 Ra_l^{1/4}}{\left( 1 + \left( \frac{0.492k}{\mu C_p} \right)^{9/16} \right)^{4/9}} \right), & \text{if } Ra_l \leq 10^9 \\ \frac{k}{l} \left( 0.825 + \frac{0.38 Ra_l^{1/6}}{\left( 1 + \left( \frac{0.462k}{\mu C_p} \right)^{9/16} \right)^{8/27}} \right), & \text{if } Ra_l > 10^9 \end{cases}$$

here,  $Ra_l$  is the Raleigh number which is defined by the following expression:

$$Ra_l = \frac{g \alpha_p \rho^2 C_p (T - T_{exp}) l^3}{\mu \kappa},$$

where  $g$  is acceleration of free fall,  $\text{m}/\text{s}^2$ ;  $\alpha_r$  is temperature coefficient of volume expansion,  $\text{K}^{-1}$ ;  $l$  is the length of the air layer,  $\text{m}$ ;  $\mu$  is the dynamic viscosity,  $(\text{Pa} \cdot \text{s})$ .

### Computer simulation results

As an example of the use of the developed program, the process of growing the synthesized  $\text{Bi}_2\text{Te}_3$  material was considered, in a quartz ampoule, the wall thickness of which is 3 mm, the length of the ingot is 250 mm, the diameter  $d = 24$  mm. The temperature of the heater varied within  $680\text{-}950$  °C, the height from 24 to 96 mm. To simulate the effect of electrical current on the growing process, a potential



difference from 0 to 4V was created at the ends of the ingot. The appearance of the simulated system is shown in Fig. 2.

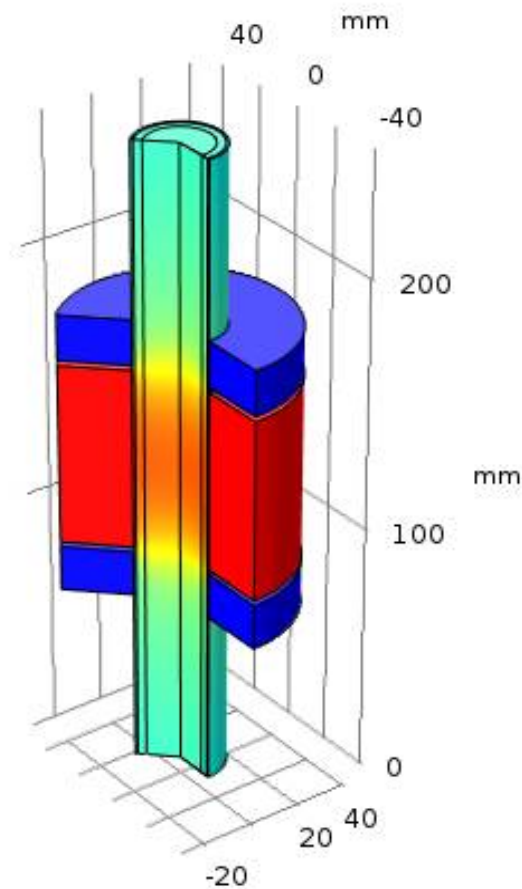


Fig.2. Computer model of installation for growing TEM by vertical zone melting method.

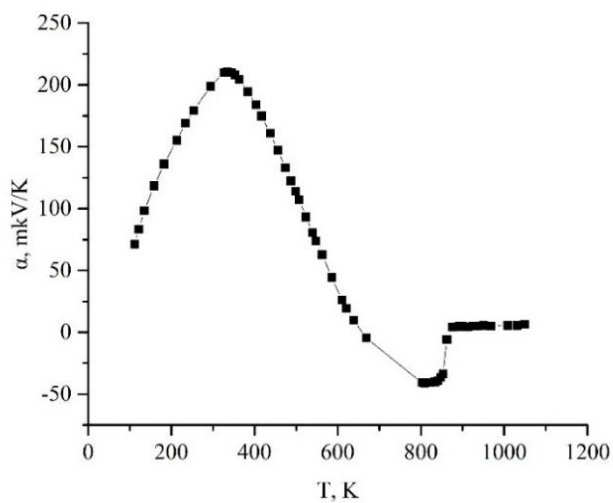
The temperature dependences of thermoelectric coefficient  $\alpha(T)$ , electrical conductivity  $\sigma(T)$  and thermal conductivity  $\kappa(T)$  for  $\text{Bi}_2\text{Te}_3$  are shown in Figs. 3-5. These dependences were constructed according to data obtained from the literary sources [2, 9].

By changing the properties of the material under study, in particular, the magnitude and sign of the Seebeck coefficient  $\alpha$ , electrical conductivity  $\sigma$  or thermal conductivity  $\kappa$ , when an electrical current is passed through the crystal being grown, the Peltier effect actually occurs at the phase boundaries.

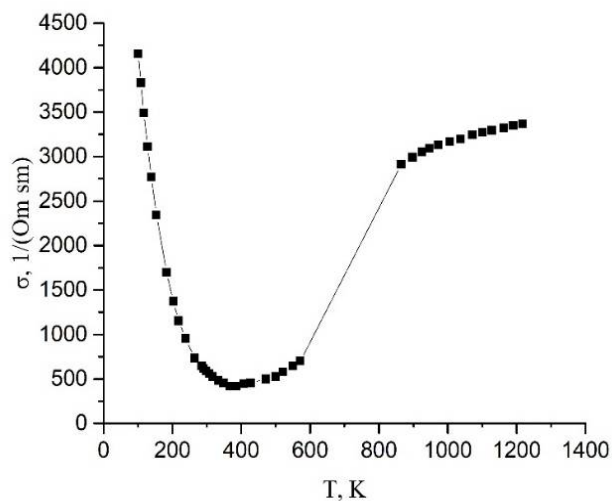
The simulation results showed that the Peltier heat is absorbed when current passes from a solid to liquid phase and vice versa, it is released when a current passes from a liquid to solid phase.

In addition, it was found that changing the magnitude of the potential difference applied to the edges of the grown ingot may affect the crystallization front shape, which is known to have a large impact on the stability of growth of the single crystal and its homogeneity.

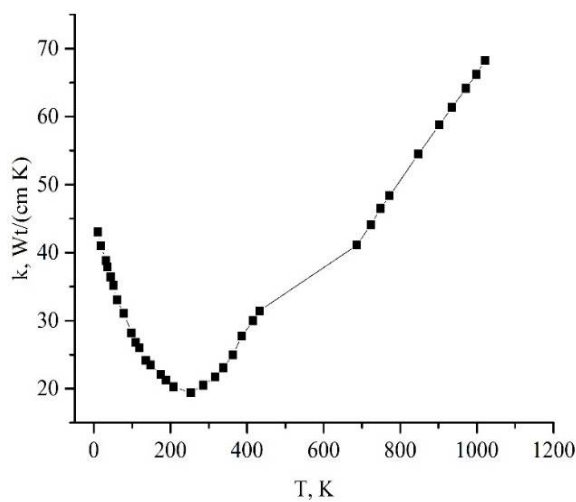
For a given configuration of the installation, without regard to the electrical current, the flat crystallization front was achieved only at temperatures of 900-910K. As is seen from Fig.5, when the electrical current passes through the molten zone, the crystallization front changes its shape, which makes it possible to optimize the growing process.



a)

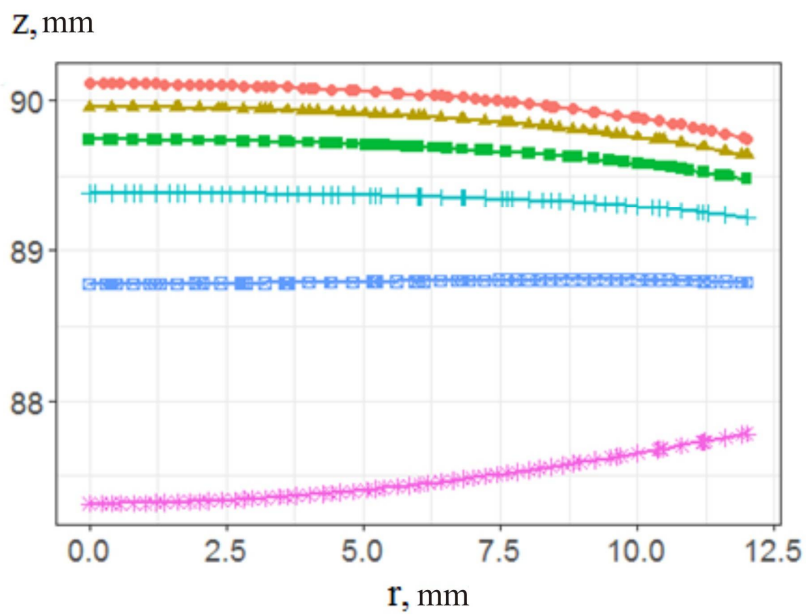


b)

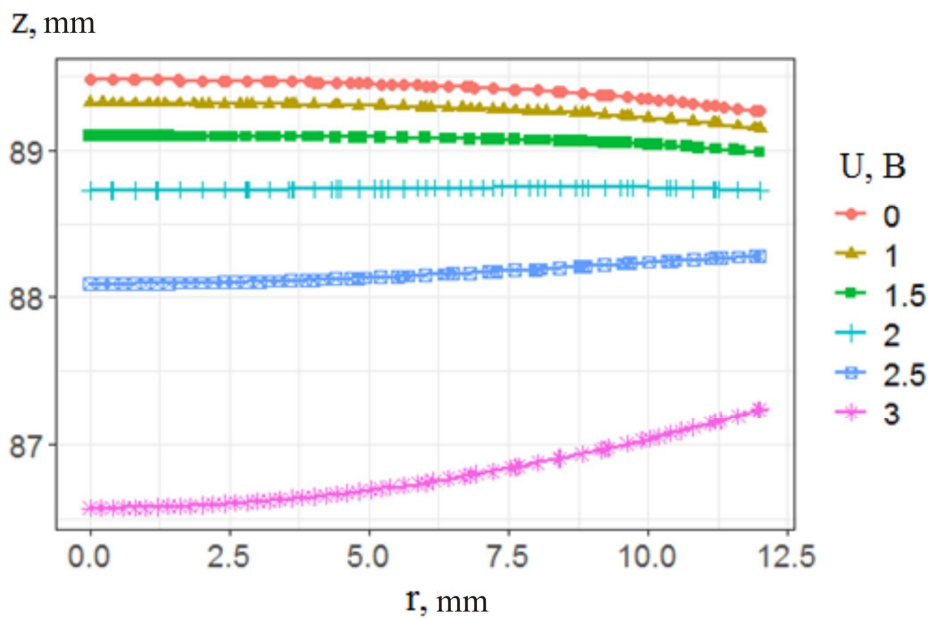


c)

Fig.3. Dependence of the Seebeck coefficient  $\alpha$  (a), electrical conductivity  $\sigma$  (b) and thermal conductivity  $\kappa$  (c) of bismuth telluride on temperature.



a)



b)

Fig. 4. The dependence of the crystallization front shape on the magnitude of the applied potential difference at the heater temperature  $T = 880\text{K}$  (a) and  $T = 890\text{K}$  (b).

The authors of [10] conducted a series of experiments on the effect of electrical current on the properties of materials based on  $\text{Bi}_2(\text{Te}, \text{Se})_3$  doped with  $\text{Hg}_2\text{Cl}_2$  and  $\text{Cd}_2\text{Br}_2$ , grown by the method of directional solidification. The possibility was noted of achieving an increase in the figure of merit of the grown materials by 9% due to the growth of TEM with the optimized distribution of the carrier density

along the ingot, which was achieved by a programmable change in the magnitude and direction of the current flowing through the crystallization front during growth.

## Conclusions

1. A computerized method has been developed for determining the thermal conditions for growing single crystals based on  $\text{Bi}_2\text{Te}_3$  by the method of directional solidification when an electrical current is passed through a sample.
2. An example of using the method confirms the influence of the Peltier effect on the growth conditions of single crystals and control of temperature distribution in the ingot while growing.

The author considers it her pleasant duty to express her gratitude to academician L.I. Anatyshuk for the proposed topic, formulation of the problem and the useful constructive discussion of the results.

## References

1. Pfan U.G. (1970). *Zonnaiaplavka [Zonemelting]*. V.N. Vigdorovich (Ed.). Moscow: Mir [in Russian].
2. Goltsman B.M., Kudinov V.A., Smirnov I.A. (1972). *Poluprovodnikovyye termoelektricheskiye materialy na osnove  $\text{Bi}_2\text{Te}_3$  [Semiconductor thermoelectric materials based on  $\text{Bi}_2\text{Te}_3$ ]*. B.Ya. Moizhes (Ed.). Moscow: Nauka [in Russian].
3. Anatyshuk L.I. (1979). *Termoelementy i termoelektricheskiye ustroystva [Thermoelements and thermoelectric devices]*. Kyiv: Naukova Dumka [in Russian].
4. Vilke K.T. (1977). *Metody vyrashchivaniya kristallov [Methods of crystal growth]*. Leningrad: Nedra [in Russian].
5. Goltsman B.M., Liaschenok V.I., Strekopytova N.I. (1986). Kristallizatsiya v elektricheskom pole termoelektricheskikh materialov na osnove tellurida vismuta [Crystallization in the electrical field of thermoelectric materials based on bismuth telluride]. *Termoelektricheskiye istochniki toka: materialy, konstruktsiya, primeniye. Tezisy dokladov v sesoiuznogo soveshchaniya – Thermoelectric current sources: materials, construction, application. Abstracts of All-Union conference reports*. Ashgabad [in Russian].
6. *COMSOL Multiphysics User's Guide (2010)*. COMSOL AB.
7. Shi D. (1988). *Chislennyye metody v zadachakh teploobmena [Numerical methods in heat exchange problems]*. Moscow: Mir [in Russian].
8. Incropera F.P., DeWitt D.P., Bergman T.L., Lavine A.S. (2007). *Fundamentals of heat and mass transfer. 6th ed.* New York: John Wiley & Sons Ltd.
9. Ivanova L. D., Granatkina Yu.V. (2000). Thermoelectric properties of  $\text{Bi}_2\text{Te}_3$ - $\text{Sb}_2\text{Te}_3$  single crystals in the range 100–700 K. *Inorganic Materials*, 36, 7.
10. Liaschenok V.I., Strekopytova N.I. (1995). Influence of electric current flow during crystallization process on thermoelectric properties of materials. *Proc. of XIV International Conference of Thermoelectrics* (St. Petersburg, Russia, June 27-30, 1995) (pp.112-114).

Submitted 19.10.2018.

**О.В.Ніцович, канд. фіз.-мат. наук<sup>1,2</sup>**

<sup>1</sup>Інститут термоелектрики НАН і МОН України,  
вул. Науки, 1, Чернівці, 58029, Україна,  
e-mail: anatysh@gmail.com;

<sup>2</sup>Чернівецький національний університет  
імені Юрія Федьковича, вул. Коцюбинського 2,  
Чернівці, 58012, Україна

## **КОМП'ЮТЕРНЕ МОДЕЛЮВАННЯ ПРОЦЕСУ КРИСТАЛІЗАЦІЇ $Bi_2Te_3$ ПРИ НАЯВНОСТІ ЕЛЕКТРИЧНОГО СТРУМУ**

*У статті представлений підхід до побудови комп'ютерної моделі процесу вирощування термоелектричних матеріалів методом вертикальної зонної плавки з врахуванням ефекту Пельтьє, що виникає на межі розділу твердої та рідкої фаз вирощуваного матеріалу при пропусканні через злиток електричного струму. Наведено результати візуалізації чисельного рішення моделі. Бібл.10, Рис.4.*

**Ключові слова:** моделювання, вертикальна зонна плавка, термоелектричний матеріал, вирощування в електричному полі.

**О.В.Ницович, канд. физ.-мат. наук<sup>1,2</sup>**

<sup>1</sup>Институт термоэлектричества НАН и МОН Украины  
ул. Науки, 1, Черновцы, 58029, Украина  
e-mail: anatysh@gmail.com;

<sup>2</sup>Черновицкий национальный университет  
им. Ю.Федьковича, ул. Коцюбинского, 2,  
Черновцы, 58012, Украина

## **КОМПЬЮТЕРНОЕ МОДЕЛИРОВАНИЕ ПРОЦЕССА КРИСТАЛЛИЗАЦИИ $Bi_2Te_3$ ПРИ НАЛИЧИИ ЭЛЕКТРИЧЕСКОГО ТОКА**

*В статье представлен подход к построению компьютерной модели процесса выращивания термоэлектрических материалов методом вертикальной зонной плавки с использованием эффекта Пельтье, который возникает на границе раздела твердой и жидкой фаз выращиваемого материала при пропускании через слиток электрического тока. Приведены результаты визуализации численного решения модели. Библ. 10, Рис. 4.*

**Ключевые слова:** моделирование, вертикальная зонная плавка, термоэлектрический материал, выращивание при наличии электрического тока.

**References**

1. PfanU.G. (1970). *Zonnaiaplavka [Zonemelting]*. V.N.Vigdorovich (Ed.). Moscow: Mir [in Russian].
2. Goltsman B.M., Kudinov V.A., Smirnov I.A. (1972). *Poluprovodnikovyye termoelektricheskiye materialy na osnove  $\text{Bi}_2\text{Te}_3$  [Semiconductor thermoelectric materials based on  $\text{Bi}_2\text{Te}_3$ ]*. B.Ya.Moizhes (Ed.). Moscow: Nauka [in Russian].
3. Anatyshuk L.I. (1979). *Termoelementy i termoelektricheskiye ustroystva [Thermoelements and thermoelectric devices]*. Kyiv: Naukova Dumka [in Russian].
4. VilkeK.T. (1977). *Metody vyrashchivaniia kristallov [Methods of crystal growth]*. Leningrad: Nedra [in Russian].
5. Goltsman B.M., Liaschenok V.I., Strekopytova N.I. (1986). Kristallizatsiia v elektricheskom pole termoelektricheskikh materialov na osnove telluride vismuta [Crystallization in the electrical field of thermoelectric materials based on bismuth telluride]. Termoelektricheskiye istochniki toka: materialy, konstruktsiia, primeneniie. *Tezisy dokladov v sesoiuznogo soveshchaniia– Thermoelectric current sources: materials, construction, application. Abstracts of All-Union conference reports*. Ashgabad [in Russian].
6. *COMSOL Multiphysics User's Guide (2010)*. COMSOL AB.
7. ShiD. (1988). *Chislennyemetody v zadachakhteploobmena [Numerical methods in heat exchange problems]*. Moscow: Mir [in Russian].
8. Incropera F.P., DeWitt D.P., Bergman T.L., Lavine A.S. (2007). *Fundamentals of heat and mass transfer. 6th ed.* New York: John Wiley & Sons Ltd.
9. Ivanova L. D., Granatkina Yu.V. (2000). Thermoelectric properties of  $\text{Bi}_2\text{Te}_3\text{-Sb}_2\text{Te}_3$  single crystals in the range 100–700 K. *Inorganic Materials*, 36, 7.
10. Liaschenok V.I., Strekopytova N.I. (1995). Influence of electric current flow during crystallization process on thermoelectric properties of materials. *Proc. of XIV International Conference of Thermoelectrics* (St.Petersburg, Russia, June 27-30, 1995) (pp.112-114).

Submitted 19.10.2018.



*P.V. Gorskiy*

**P.V. Gorskiy**, doctor Phys.-math. Science<sup>1,2</sup>

**V.V.Razinkov**, cand Phys-math . Science<sup>1,2</sup>

<sup>1</sup>Institute of Thermoelectricity of the NAS and  
MES of Ukraine, 1 Nauky str., Chernivtsi, 58029, Ukraine;

*e-mail: anatykh@gmail.com*

<sup>2</sup>Yuriy Fedkovych Chernivtsi National University,  
2 Kotsiubynsky str., Chernivtsi, 58012, Ukraine;



*V.V.Razinkov*

---

**INFLUENCE OF CONTAINER GEOMETRY ON THE  
ORIENTATION AND THE DEGREE  
OF PARALLELISM OF CLEAVAGE PLANES OF BISMUTH  
TELLURIDE SINGLE CRYSTALS**

---

*In the paper, by solving the heat conduction equation for a cylindrical and slotted container, it is shown that, with the same specific power of the heater and the same temperature of container exterior walls, the transverse temperature gradient in the melt is the greater, the larger the diameter of the cylindrical or the width of the slotted container. In addition, it is shown that in the idealized case, the crystallization front when using a cylindrical container has the shape of a paraboloid of revolution, and in the case of using a slotted container, the shape of a parabolic cylinder with generators parallel to the long side of the container cross section, which is significantly closer to flat. But the diameter of the cylindrical container cannot be drastically reduced, while the slot width of the slotted container can be reduced to the minimum value technologically acceptable for further cutting the resulting single-crystal plate in the shape of a rectangular parallelepiped into legs. This circumstance, together with the ability to rotate the Bridgman furnace around the vertical axis with the optimal angular velocity in order to smooth the transverse temperature gradient, makes it possible, under the condition of using slotted containers, to bring the crystallization front as close as possible to the flat one, and therefore to achieve maximum parallelism of the single crystal cleavage planes and maximum homogeneity of the distribution of dopants in the resulting single crystal. Bibl. 8, Fig. 4.*

**Key words:** slotted container, cylinder container, specific power of the heater, crystallization front shape, paraboloid of revolution, parabolic cylinder, maximum temperature gradient, the degree of parallelism of cleavage planes to the wide edges of the slotted container, the degree of homogeneity of the distribution of impurities in a single crystal.

## **Introduction**

It is known that the quality of the thermoelectric material is substantially affected by the concentration heterogeneities that arise in the course of directional crystallization from the melt [1]. As noted earlier, the relationship between the longitudinal gradient of temperature near the crystallization front and the growth rate has a considerable impact on the appearance of these concentration heterogeneities. In accordance with Tiller's approximate estimate [2], concentration overcooling occurs if the ratio ( $G/v$ ) of the longitudinal temperature gradient  $G$  to the growth rate of a single crystal  $v$  in the direction of this gradient is less than a certain critical value:

$$(G/v) < (G/v)_{cr} = \frac{mC_0(1-K_0)}{K_0D_0}, \quad (1)$$

In this formula,  $m$  – the slope of the liquidus line,  $C_0$  – the concentration of impurities in the bulk of the melt,  $K_0$  – the distribution coefficient of the impurity,  $D_0$  – the diffusion coefficient of the impurity in the melt.

Uneven distribution of impurities and concentration of free charge carriers is the main factor influencing the growth conditions on the properties of thermoelectric materials. In [1], it is noted that, all other things being equal, the dimensionless thermoelectric efficiency of a material is greater, the greater the ratio  $(G/v)$ .

It is believed that there are two groups of heterogeneities that differ in the length and causes of their occurrence: macro-heterogeneities with scales comparable to sample sizes and micro-heterogeneities with scales significantly smaller than sample sizes. In particular, the monotonous change in the composition of the material along the section and length of the ingots grown from the melt through directional crystallization belongs to the macro-heterogeneities. The change in the composition of the material along the cross-section is due to the non-planar (usually concave toward the solid phase) crystallization front shape, distorted by emission of the heat of crystallization, and the effect of transverse heat fluxes in the ingot. The growth rate and convection conditions in different parts of the non-planar crystallization front are different, and this leads to a change in the effective distribution coefficient and to a change in the composition of the ingot section. And the transverse temperature gradient and the possibility of controlling it, and, hence, the crystallization front, is significantly affected by the geometry of the cross-section of the container (slotted or cylindrical). Exactly the analysis of various aspects of this influence is the purpose of this paper.

### Description of the physical model of the process of growing bismuth telluride single crystals in a slotted container

The physical model of the process of growing bismuth telluride single crystals in a slotted container is shown in Fig. 1.

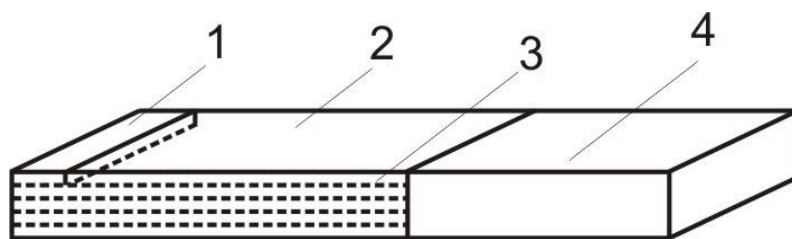


Fig. 1. The physical model of the process of growing bismuth telluride single crystals in a slotted container: 1) growing layer, parallel to cleavage planes; 2) previous layer; 3) cleavage planes of solidified volume; 4) melt

In accordance with this model, the growth of a single crystal of bismuth telluride most intensively occurs along cleavage planes. In addition, each new layer 1 consists of oriented hexagonal "columns". This layer gradually grows on top of the previous layer 2. In this case, the only non-competitive nucleus is a solidified volume with its cleavage planes 3, which grows, absorbing the substance from the melt 4. It is clear from the model that if grown in a slotted container, the crystallization front would be perfectly flat, if there were no transverse temperature gradient in the container section, but only an axial (longitudinal) gradient, and, moreover, the distribution coefficient of dopants would be as close as possible to unity. Then



all layers of a single crystal would grow at the same time and the same speed, and their orientation with respect to the wide edges of the slotted container would be close to ideal. However, in fact, a transverse temperature gradient exists.

In addition, due to more or less heterogeneity of the distribution of dopants in the crystal, the melting temperature, the diffusion coefficients of the components of the solid phase and the melt, the thermal conductivity and their specific heat, the heat of phase transition, the surface tension coefficient at the “solid phase–melt” interface, prove to be dependent on the coordinates in the cross sectional plane of the container. As a result, the crystallization front is not only non-planar and does not even represent some kind of smooth, though non-planar, surface, but also has a peculiar “stepped” structure [1, 2].

It is clear from the above that the shape of the crystallization front and the nature of the distribution of alloying impurities in the grown single crystal essentially depend on the container geometry, that is, on the shape of its cross-section. Consider this point in more detail.

### **Influence of container geometry on temperature distribution in the process of growing bismuth telluride single crystals and on the crystallization front shape**

Fig. 2 shows cross-sections of the slotted and traditional cylindrical containers.

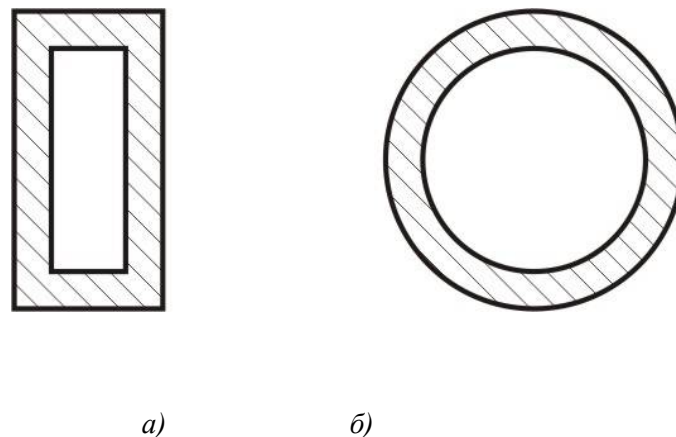


*Fig.2. Cross-sections of containers: a) slotted; b) traditional cylindrical*

Let us consider the problem of steady-state temperature distribution in these containers in a maximum simplified formulation, which, however, will give an opportunity to correctly imagine the crystallization front shape. We will assume that the heat enters the substance contained in the containers from the exterior walls. The power of the heat flowing to the unit volume of a substance will be assumed to be the same in both cases. In the case of a slotted container (Fig. 2a), the steady-state heat equation will have the form:

$$\frac{d^2T}{dx^2} = \frac{q}{\kappa} (q > 0), \quad (1)$$

where  $q$  – thermal power coming to the unit volume of substance in a container,  $\kappa$  – its thermal conductivity.

Solution of this equation under the boundary conditions  $T(l/2) = T(-l/2) = T_0$ , where  $l$  – the width of the slot, will be given by:

$$T = \frac{q}{2\kappa} \left( x^2 - \frac{l^2}{4} \right) + T_0. \quad (2)$$

In accordance with (2), the maximum value of the transverse temperature gradient when using a slotted container is:

$$G_{t \max} = ql/2\kappa. \quad (3)$$

In the case of a cylindrical container, Eq.(1) takes on the form:

$$\frac{d}{dr} \left( r \frac{dT}{dr} \right) = \frac{q}{\kappa}. \quad (4)$$

Its nonsingular solution for the boundary condition  $T(R)=T_0$ , where  $R$  – the inner radius of the container, is given by:

$$T = T_0 + \frac{q}{4\kappa} (r^2 - R^2). \quad (5)$$

In this case the maximum value of the transverse temperature gradient is equal to:

$$G_{t \max} = qR/2\kappa = qD/4\kappa, \quad (6)$$

where  $D$  – the inner diameter of the cylindrical container.

Crystallization fronts in the approximation of a uniform distribution of impurities for the above cases are shown in Figs. 3 and 4.

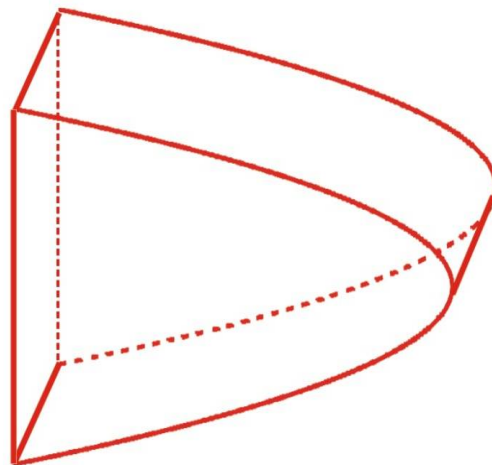


*Fig. 3. Crystallization front shape in the case of a slotted container*

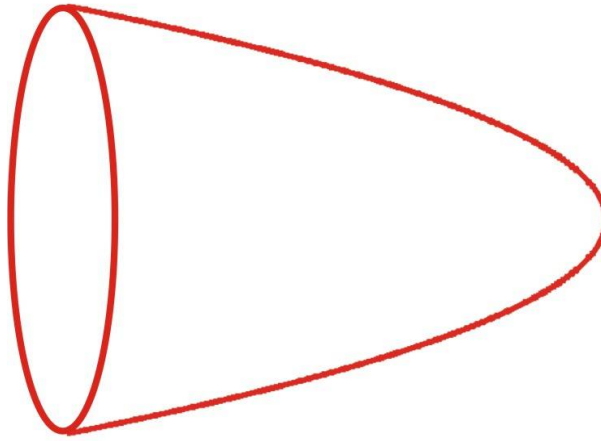


*Fig. 4. Crystallization front shape in the case of a traditional cylindrical container*

Figs. 3 and 4 show that in the case of a slotted container, the crystallization front has the shape of a parabolic cylinder, and in the case of a traditional cylindrical container, the shape of a paraboloid of revolution. It is this difference that creates fundamentally different conditions for the growth of a bismuth telluride single crystal when grown in these containers using the Bridgman method. In the case of a slotted container, a growing single crystal, due to the joint action of the seed and gravity, is a set of layers parallel to the wide edges of the container. Due to the presence of a transverse temperature gradient, these layers grow at slightly different speeds, as a result of which the surface of a parabolic cylinder is their bypass. But it follows from formula (3) that by making the container width small and, therefore, the ratio of the long side of the rectangular cross section of the container to the short one large enough, you can make the maximum of the transverse temperature gradient small and, therefore, to achieve an almost perfect parallelism of the cleavage planes to the wide edges of the container. Thus, the short side of the cross-section of the slotted container should be made minimum acceptable technologically, while the long side of this section, on the contrary, should be made maximum acceptable technologically, so that from the resulting single-crystal plate one could obtain maximum number of thermoelectric legs with given sizes. An additional means of compensating for the transverse temperature gradient can be rotation of the Bridgman furnace around the vertical axis with optimum angular speed. But at the same time, in accordance with ratio (1), which is correct not only for the longitudinal (axial), but also for the transverse temperature gradient, the speed should be reduced, and, therefore, the crystallization time should be increased. In the case of growing bismuth telluride single crystals by the Bridgman method in a traditional cylindrical container, a fundamentally different situation occurs. A single crystal in this case is not a set of wide planes, but a set of bars parallel to the vector of earth gravity with a relatively small cross section, whose bypass is a surface of a paraboloid of revolution. In this case, the uncompetitive growth of a single crystal from a single supercritical nucleus takes place no longer, since such a single nucleus, if we ignore the seed, does not exist. Moreover, the presence of a transverse temperature gradient and the resulting dependence of the surface tension coefficient at the “melt-solid phase” boundary on the distance to the cylinder axis can cause the formation of a dendritic structure, especially since using a traditional cylindrical container there are no preferred directions of single crystal growth in the transverse section. Thus, the cleavage planes, as indicated, for example, in the description of patent [3] and in paper [4], can have an arbitrary orientation.

This makes it necessary to obtain thermoelectric legs from incomplete disks, or their sections.

From formula (6) at first glance it may seem that in the case of a cylindrical container it is possible to compensate for the transverse temperature gradient by reducing the diameter of the container. But a sharp decrease in this diameter would force to obtain cylindrical thermoelectric legs, which is not technological. On the other hand, the large diameter of the ingot would, on the contrary, lead to a sharp increase in the transverse temperature gradient, which, due to the temperature dependence of the diffusion coefficient of impurities in the crystal, would lead to a sharp heterogeneity of their radial distribution, and, therefore, not only to a significant variation of the thermoelectric parameters of the resulting legs, but also to the appearance of mechanical stresses, which would lead to the emergence of longitudinal cracks in the ingot, and, consequently, to the destruction of the legs, and thus to a decrease in the yield ratio. Thus, when growing single crystals of bismuth telluride and alloys based on it in traditional cylindrical containers, it becomes necessary to select the optimum diameter of the container.

Let us compare our theoretical results with the results of experiments of other authors who have studied the thermoelectric and strength properties of alloys based on bismuth telluride, including those grown in flat slots [5 – 7].

In [5], the strength of thermoelectric legs made of *p* and *n*-type bismuth telluride based alloys manufactured by three methods was studied. In the first method, the legs were cut from solid plates grown in flat slots of  $41 \times 49 \times 1.4$  mm in size. The size of 1.4 mm corresponded to the size of the leg section. In the second method, the legs were assembled of plates of size  $41 \times 49 \times 0.27$  mm. The plates were connected by soldering from the ends. According to the third method, the plates of  $41 \times 49 \times 0.27$  mm in size were joined by pressing. Each method produced 20 samples.

It turned out that the legs made by the first method (with a standard plate thickness) had an average modulus of elasticity for *p* and *n*-type, respectively, equal to 68.9 and 52.3 MPa with a standard deviation of 27.7 and 14.5 MPa, respectively. The bending strength of these legs was 14.0 and 16.6 MPa, respectively, with a standard deviation of 3.76 and 4.92 MPa, respectively. The combined *p* and *n*-type legs made by the second method had an average modulus of elasticity of 78.4 and 70.2 MPa, respectively, with a standard deviation of 18.0 and 9.7 MPa, respectively. The bending strength of these legs was 15.8 and 19.8 MPa, respectively, with a standard deviation of 3.2 and 1.86 MPa, respectively. The extruded legs, manufactured by the third method, had an average modulus of elasticity of 72.9 and 82.8 MPa, respectively, with a standard deviation of 27.0 and 12.1 MPa, respectively. The bending strength of these legs was 12.5 and 17.8 MPa, respectively, according to the standard deviation of 2.82 and 3.97 MPa, respectively. Thus, we see that reducing the slot width contributes both to improving the mechanical characteristics of the legs, and to improving the reproducibility of these characteristics.

In [6], the influence of conditions for growing ingots of  $Bi_2Te_{2.7}Se_{0.3}$  solid solutions on the anisotropy of their physical properties was studied. It turned out that in the case of growing in flat slots (one of the Bridgman method variants), an ingot structure is observed in which the cleavage planes are not only parallel to the direction of crystal growth, which is typical of traditional zone melting, but also practically parallel to each other and the plane of the plate, that is, the wide edge of the slotted container. This avoids thermoelastic stresses arising from the conjugation of grains with different coefficients of thermal expansion. The ingot was obtained in the form of a plate with a thickness equal to the side of the "leg" section. Such a plate is the most convenient object for performance monitoring and subsequent cutting into legs. The study of the influence of the crystallization rate on the texture was started with a plate 0.5 mm thick.

Then, with the selected crystallization time, the effect of plate thickness on the texture was investigated. It turned out that during rapid crystallization, the normals to the planes deviate by angles from 0 to 250 from the growth axis. In this case, the dendritic structure of the ingot is observed, which is characterized by a random crystallographic orientation of the crystal with respect to the growth axis. The texture along the length of the ingot did not change in principle. An increase in the plate crystallization

time to 120 minutes led to the suppression of the dendritic type of crystallization. The results of the texture study showed that by the middle of the plate, the normals to the planes are oriented along the growth axis with a slight texture spread of 3-40° in the center and on the periphery of the plate. By the nature of the change in the orientation of the grains over the plate section, it was concluded that the crystallization front is almost flat. By the middle of the plate, the type of the texture and its distribution over the cross section did not practically change. At a distance of 30 mm from the beginning of the plate in the central part, the orientation of the grain remained, but at the edges of the plate small grains appeared with an orientation different from the main volume. Further, the deviation of the cleavage planes from the ingot axis at the edges of the plate grows and amounts to 8° on one edge and 10° on the other. This change in the structure indicates a curvature of the crystallization front.

When increasing the crystallization time to 420 min, the normals to the (0001) cleavage planes are parallel to the normal to the plane of the plate or deviate from it by 3° from the plane perpendicular to the growth axis with a slight variation of  $\pm 2^\circ$ . Such orientation has a positive effect on the strength characteristics of the material.

A clear material texture, whereby the cleavage planes are oriented parallel to the growth axis, was observed only for a plate thickness of 0.5 mm. At a plate thickness of 1 mm, the normals to planes  $(11\bar{2}0)$  for different grains deviated from the plate axis by 2, 4, 7, and 9°. A crystallization front bend was observed. Along the length of the plate 1 mm thick, the texture was not fundamentally changed. At a plate thickness of 1.4 mm, the normals to planes  $(11\bar{2}0)$  deviated from the growth axis by the angles up to 10°. A study of the texture along the length of the plate 1.4 mm thick showed that, after the middle of the plate, the deviations of the normals to planes  $(11\bar{2}0)$  from the plate axis increased and reached 15°.

Control of the position of the crystallographic planes (0001) relative to the plane of the plate showed that with an increase in the thickness of the plate, the disorientation of the cleavage planes relative to each other and relative to the plane of the plate increases. Thus, these data also confirm our conclusion that reducing the width of the slot increases the degree of parallelism of the cleavage planes relative to each other and to the wide edges of the slotted container.

In [7, 8], it was shown that on plates 1 mm thick, dendritic growth was suppressed and a clear orientation of the cleavage planes relative to the plate plane with maximum angular declination not more than 5 degrees was obtained only during crystallization times in the interval 210 - 420 min. This confirms the conclusion that the crystallization time increases with a decrease in the temperature gradient.

## **Conclusions**

1. By solving the heat conduction equation it has been established that due to the existence of a transverse temperature gradient in the approximation of a uniform distribution of dopants in a crystal, the crystallization front in the case of a slotted container has the shape of a parabolic cylinder with generators parallel to the wide side of the slot, and in the case of a traditional cylindrical container, the shape of a paraboloid of revolution.
2. Due to such features of the crystallization front, a single crystal in the case of a slotted container is a set of layers parallel to the wide edges of the container which grow with different speeds. So, in order to achieve close to perfect parallelism of cleavage planes of a single crystal to the wide edges of the container, it is proposed to make the narrow side of the slot minimum acceptable, and the wide side, on the contrary, maximum acceptable technologically.
3. When growing single crystals of bismuth telluride and alloys on its basis by the Bridgman method in a traditional slotted container, the negative influence of transverse temperature gradient on the

crystallization front shape through reduction of container diameter cannot be compensated, since it would necessitate making thermoelectric legs of cylindrical shape, which is not technological. On the other hand, an increase in container diameter would result in the increase of maximum transverse temperature gradient. This, due to sharp inhomogeneity of impurity distribution in a crystal, as well as the dependence of surface tension coefficient at “liquid-solid phase” boundary on the distance to container axis would cause formation in the ingot of a dendritic structure, sharp spread in thermoelectric parameters of the resulting legs, as well as reduction of mechanical strength of the legs due to formation in the ingot of longitudinal cracks caused by the increase in mechanical stresses. Therefore, there is a need to select the optimum diameter of the cylindrical container.

4. Thus, there are obvious undeniable advantages of growing single crystals of bismuth telluride and alloys on its basis in a slotted container compared to the traditional cylindrical one.

## References

1. Goltsman B.M., Kudinov V.A., Smirnov I. A. (1972). *Poluprovodnikovyye termoelektricheskiye materialy na osnove  $Bi_2Te_3$*  [Semiconductor thermoelectric materials based on  $Bi_2Te_3$ ]. B.Ya.Moizhes (Ed.). Moscow: Nauka [in Russian].
2. Strutynska L.T., Zhikharevich V.V. (2012). Simulation of  $Bi_2Te_3$  thermoelectric material growth by vertical zone melting method. *J. Thermoelectricity*, 2, P. 79-87.
3. *Patent of RF and Japan* (2000). Belov Yu.M., Maekawa H. Cast plate made of thermoelectric material.
4. Belov Ju. M., Maniakin S.M., Morgunov I.V. (2006). Review of methods of thermoelectric materials mass production. In: *Thermoelectric handbook. Macro to nano*. D. M. Rowe (Ed.). Boca Raton (FL): – Taylor & Francis group, LLC CRC Press.
5. Voronin A.I., Osipkov A.S., Gorbatovskaia T.A. (2010). Mekhanicheskaya prochnost vetvei termoelementov na osnove  $Bi_2Te_3$  pri razlichnykh metodakh ikh polucheniia [Mechanical strength of thermoelement legs based on  $Bi_2Te_3$  with different methods of their production]. *Nano-i mikrosistemnaia tekhnika – Nano- and Microsystems Technology*, 2 (115), P. 17-21.
6. Bublik V.T., Voronin A.I., Vygovskaya E.A., et al. (2010). Vliianiye uslovii vyrashchivaniia slitkov tverdykh rastvorov  $Bi_2Te_{2.7}Se_{0.3}$  na anisotropiiu fizicheskikh svoystv [Influence of conditions for growing  $Bi_2Te_{2.7}Se_{0.3}$  solid solutions on the anisotropy of physical properties]. *Materialy elektronnoi tekhniki – Electronic Materials*, 1, P. 58-62 [in Russian].
7. Alenkov V.V., Belov Yu.M., Bublik V.T., et al. (2008). Vliianiye uslovii kristallizatsii na strukturu plastin tverdykh rastvorov termoelektricheskikh materialov na osnove  $Bi_2Te_3$ , vyrashchennykh iz rasplava [Influence of crystallization conditions on the structure of plates of solid solutions of  $Bi_2Te_3$  based thermoelectric materials]. *Materialy elektronnoi tekhniki – Electronic Materials*, 2, P. 22-25 [in Russian].
8. Voronin A.I., Bublik V.T., Tabachkova N.Yu., Belov Yu.M. (2011). Structure of profiled crystals based on solid solutions of  $Bi_2Te_3$  and their X-ray diagnostics. *J. Electronic Materials*, 40, 5, P. 794-800 (doi: 10.1007/s11664-011-1573-5).

Submitted 01.11.2018

**Горський П. В.,** *докт. фіз.-мат. наук,<sup>1,2</sup>*  
**Разінков В.В.,** *канд. фіз.-мат. наук<sup>1,2</sup>*

<sup>1</sup>Інститут термоелектрики НАН і МОН України,  
вул. Науки, 1, Чернівці, 58029, Україна,  
<sup>2</sup>Чернівецький національний університет імені Юрія  
Федьковича, вул. Коцюбинського 2, Чернівці, 58012, Україна  
*e-mail: anatysh@gmail.com*

## **ВПЛИВ ГЕОМЕТРІЇ КОНТЕЙНЕРА НА ОРІЄНТАЦІЮ ТА СТУПІНЬ ПАРАЛЕЛЬНОСТІ ПЛОЩИН СПАЙНОСТІ МОНОКРИСТАЛІВ ТЕЛУРИДУ ВІСМУТУ**

*В статті шляхом розв'язання рівняння теплопровідності для циліндричного та щілинного контейнерів показано, що за однієї і тієї ж питомої потужності нагрівника і однієї і тієї ж температури зовнішніх стінок контейнера поперечний градієнт температури у розплаві тим більший, чим більшим є діаметр циліндричного або ширина щілинного контейнера. Окрім того показано, що в ідеалізованому випадку фронт кристалізації в разі застосування циліндричного контейнера має форму параболоїда обертання, а в разі застосування щілинного контейнера – форму параболічного циліндра з твірними, паралельними до довгої сторони поперечного перерізу контейнера, яка істотно ближча до плоскої. Але діаметр циліндричного контейнера різко зменшити не можна, в той час, як ширину щілини щілинного контейнера можна зменшити до мінімальної величини, яка є технологічно прийнятною для подальшого розрізання отриманої монокристалічної пластини у вигляді прямокутного паралелепіпеда на гілки. Ця обставина разом з можливістю обертання печі Бріджмена навколо вертикальної вісі з оптимальною кутковою швидкістю з метою згладжування поперечного градієнту температури дає можливість за умови застосування щілинних контейнерів максимально наблизити форму фронту кристалізації до плоскої, і, отже, домогтися максимальної паралельності площин спайності монокристалу до широких граней контейнера та максимальної однорідності розподілу лежучих домішок в отриманому монокристалі. Бібл. 8, Рис. 4.*

**Ключові слова:** щілинний контейнер, циліндричний контейнер, питома потужність нагрівника, форма фронту кристалізації, параболоїд обертання, параболічний циліндр, максимальний градієнт температури, ступінь паралельності площин спайності до широких граней щілинного контейнера, ступінь однорідності розподілу домішок у монокристалі.

**Горский П. В.,<sup>1,2</sup>** *докт. физ.-мат. наук,*  
**Разинков В.В.,<sup>1,2</sup>** *канд. физ.-мат. наук*

<sup>1</sup>Институт термоэлектричества НАН и МОН Украины,  
ул. Науки, 1, Черновцы, 58029, Украина,  
*e-mail: anatysh@gmail.com*  
<sup>2</sup>Чернивецкий национальный университет имени Юрия  
Федьковича, ул. Коцюбинского 2, Черновцы, 58012, Украина

## ВЛИЯНИЕ ГЕОМЕТРИИ КОНТЕЙНЕРА НА ОРИЕНТАЦИЮ И СТЕПЕНЬ ПАРАЛЛЕЛЬНОСТИ ПЛОСКОСТЕЙ СПАЙНОСТИ МОНОКРИСТАЛЛОВ ТЕЛЛУРИДА ВИСМУТА

В статье путем решения уравнения теплопроводности для цилиндрического и щелевого контейнеров показано, что при одной и той же удельной мощности нагревателя и одной и той же температуры внешних стенок контейнера поперечный градиент температуры в расплаве тем больше, чем больше диаметр цилиндрического или ширина щелевого контейнера. Кроме того показано, что в идеализированном случае фронт кристаллизации при применении цилиндрического контейнера имеет форму параболоида вращения, а в случае применения щелевого контейнера - форму параболического цилиндра с образующими, параллельными длинной стороне поперечного сечения контейнера, которая существенно ближе к плоской. Но диаметр цилиндрического контейнера резко уменьшить нельзя, в то время как ширину щели щелевого контейнера можно уменьшить до минимальной величины, технологически приемлемой для дальнейшего разрезания полученной монокристаллической пластины в виде прямоугольного параллелепипеда на ветви. Это обстоятельство вместе с возможностью вращения печи Бриджмена вокруг вертикальной оси с оптимальной угловой скоростью с целью сглаживания поперечного градиента температуры дает возможность при условии применения щелевых контейнеров максимально приблизить форму фронта кристаллизации к плоской, и, следовательно, добиться максимальной параллельности плоскостей спайности монокристалла широким граням контейнера и максимальной однородности распределения легирующих примесей в полученном монокристалле. Библ. 8, Рис. 4.

**Ключевые слова:** щелевой контейнер, цилиндрический контейнер, удельная мощность нагревателя, форма фронта кристаллизации, параболоид вращения, параболический цилиндр, максимальный градиент температуры, степень параллельности плоскостей спайности широким граням щелевого контейнера, степень однородности распределения примесей в монокристалле.

### References

1. Goltsman B.M., Kudinov V.A., Smirnov I. A. (1972). *Poluprovodnikovyye termoelektricheskiye materialy na osnove  $Bi_2Te_3$*  [Semiconductor thermoelectric materials based on  $Bi_2Te_3$ ]. B.Ya.Moizhes (Ed.). Moscow: Nauka [in Russian].
2. Strutynska L.T., Zhikharevich V.V. (2012). Simulation of  $Bi_2Te_3$  thermoelectric material growth by vertical zone melting method. *J. Thermoelectricity*, 2, P. 79-87.
3. *Patent of RF and Japan* (2000). Belov Yu.M., Maekawa H. Cast plate made of thermoelectric material.
4. Belov Ju. M., Maniakin S.M., Morgunov I.V. (2006). Review of methods of thermoelectric materials mass production. In: *Thermoelectric handbook. Macro to nano*. D. M. Rowe (Ed.). Boca Raton (FL): – Taylor & Francis group, LLC CRC Press.
5. Voronin A.I., Osipkov A.S., Gorbatovskaia T.A. (2010). Mekhanicheskaya prochnost vetvei termoelementov na osnove  $Bi_2Te_3$  pri razlichnykh metodakh ikh polucheniia [Mechanical strength of thermoelement legs based on  $Bi_2Te_3$  with different methods of their production]. *Nano-i mikrosistemnaya tekhnika – Nano- and Microsystems Technology*, 2 (115), P. 17-21.
6. Bublik V.T., Voronin A.I., Vygovskaya E.A., et al. (2010). Vliianiye uslovii vyrashchivaniia slitkov tverdykh rastvorov  $Bi_2Te_{2.7}Se_{0.3}$  na anisotropiiu fizicheskikh svoystv [Influence of conditions for growing  $Bi_2Te_{2.7}Se_{0.3}$  solid solutions on the anisotropy of physical properties]. *Materialy elektronnoy tekhniki – Electronic Materials*, 1, P. 58-62 [in Russian].
7. Alenkov V.V., Belov Yu.M., Bublik V.T., et al. (2008). Vliianiye uslovii kristallizatsii na strukturu plastin tverdykh rastvorov termoelektricheskikh materialov na osnove  $Bi_2Te_3$ , vyrashchennykh iz rasplava [Influence of crystallization conditions on the structure of plates of solid solutions of  $Bi_2Te_3$



based thermoelectric materials]. *Materialy elektronnoi tekhniki – Electronic Materials*, 2, P. 22-25 [in Russian].

8. Voronin A.I., Bublik V.T., Tabachkova N.Yu., Belov Yu.M. (2011). Structure of profiled crystals based on solid solutions of  $Bi_2Te_3$  and their X-ray diagnostics. *J. Electronic Materials*, 40, 5, P. 794-800 (doi: 10.1007/s11664-011-1573-5).

Submitted 01.11.2018



V.S. Zakordonets

**V.S. Zakordonets, Cand.Sc. (Physics and Mathematics)**

**N.V. Kutuzova**

Ivan Puyul Ternopil National Technical University,  
56, Rus'ka str., Ternopil, 46001  
e-mail: wladim21@gmail.com



N.V. Kutuzova

## **CALCULATION OF THERMOELECTRIC SYSTEM FOR COOLING LEDs**

---

*In this paper, the thermal mathematical model of thermoelectric cooling system is constructed. The system of equations which includes the stationary thermal conductivity equation, the thermogeneration equation and cold generation equation is solved. The temperature of LED heterojunction is calculated, depending on its power, total thermal resistance of cooling system, ambient temperature and cold productivity of TCM. The analytical dependences of heterojunction temperature on TCM supply current were obtained at different LED powers and at different values of thermal resistance of cooling system. With the given thermal power of LED and thermal resistance of cooling system, an optimal value of the TCM supply current is found, whereby the temperature of LED heterojunction reaches the minimum. It is shown that the use of TCM allows reducing the temperature of LED heterojunction to values lower than ambient temperature. This is particularly relevant under conditions when ambient temperature is close to the critical temperature of heterojunction. It was shown that the efficiency of using TCM decreases with increasing LED power, ambient temperature and total thermal resistance of cooling system. Bibl. 11, Fig. 4, Tabl. 1.*

**Key words:** LED, heterojunction, thermal mode, thermal resistance, thermal stabilization, thermoelectric cooling module, radiator.

### **Formulation of the problem**

Modern semiconductor sources of light have the efficiency of electric into light energy conversion close to 30 % [1, 2]. Thus, almost 70 % of the supplied energy is converted into heat. With increasing the power of LEDs, traditional thermal stabilization systems do not always provide adequate thermal conditions. If thermal energy is not diverted, excessive heating of LED will lead to degradation of the light characteristics and reduce its service life. In addition, the rise in temperature will reduce the brightness and luminous flux.

To improve the efficiency of thermal stabilization of powerful LEDs, active methods of heat dissipation are used, namely fans, liquid cooling, thermoelectric cooling, etc. Thermoelectric cooling systems have several advantages compared with other systems, namely high reliability and no moving parts, compactness and low weight, low inertia and noiseless operation. The use of thermoelectric cooling modules (TCM) provides the heat removal system with a cooling function, that is, makes it possible to reach the temperature of LED heterojunction which is lower than ambient temperature. This becomes especially relevant under conditions when ambient temperature becomes equal to or greater than the temperature of LED heterojunction.

## Analysis of recent research and publications

The problem of stabilizing the thermal mode of LED has already been highlighted in a number of works. In particular, [3, 4] deal with the issues of ensuring the thermal mode of LED. Particular attention is paid to the problem of minimizing thermal resistance when using different models of radiators. The innovative technologies of LED cooling with the use of jet blowing are considered. However, the calculation of the thermal mode was not carried out. In [5], using the well-known heat engineering formulas and experimental observations of temperature modes, a technique for choosing an effective radiator was constructed. In this case, fan cooling was used to intensify the heat exchange of the radiator with an ambient medium. In [6], a theoretical analysis of the thermal mode of LED with a remote radiator and traditional cooling was carried out. The overheat temperature of LED heterojunction was calculated depending on its power and parameters of the heat conductor and radiator. However, thermoelectric cooling of LED was not considered.

**The purpose of the work** is to construct a thermal mathematical model of the thermoelectric cooling system of LED and to calculate on its basis the heterojunction overheat temperature depending on the LED power, the thermal resistance of cooling system and the cooling capacity of TCM.

### Formulation of the task

Through theoretical analysis, to establish the analytical relations between the power of LED, the thermal resistance of cooling system, the cooling capacity of TCM and the LED heterojunction temperature, which will make it possible to rationally choose the cooling circuit of LED in order to provide maximum luminous flux at the minimum heterojunction temperature.

### Presentation of the main material

It is known that LED generates thermal power

$$P_t = (1 - \eta_e) U_f I_f, \quad (1)$$

where  $I_f$  and  $U_f$  are the direct current and direct voltage of LED,  $\eta_e$  is its quantum efficiency.

It is obvious that TCM must absorb the power not less than the thermal power of LED, since, otherwise, the stabilization of the thermal mode will be impossible. If TCM absorbs excess power, condensation will form on its cold surface, which can lead to a short circuit. The only possible way to make the use of TCM efficient is to employ an electronic unit that can regulate the power of the module, depending on the temperature of LED heterojunction.

We assume that the thermal power of LED is completely absorbed by the cold surface of TCM

$$P_t = P_c, \quad (2)$$

and the thermal power  $P_h$  is removed from the hot surface using a radiator.

To calculate the thermal mode of LED, we use the electrothermal analogy method [7]. The thermoelectric cooling system of LED is schematically shown in Fig.1. In the schematic, each element is characterized by its thermal resistance. In particular,  $\Theta_{js}$  is thermal resistance between the heterojunction and the contact pad,  $\Theta_{sc}$  and  $\Theta_{hr}$  are thermal resistances between the contact pad and the cold surface of TCM and between the hot surface of TCM and the radiator,  $\Theta_{ra}$  is thermal resistance between the radiator and the ambient medium,  $\Delta T = T_h - T_c$  is temperature difference between the hot and cold surfaces of TCM which is due to the Peltier effect.

The thermal circuit is matched by thermal equilibrium equation:

$$T_j = T_a + P_c \cdot (\Theta_{js} + \Theta_{sc}) + P_h \cdot (\Theta_{hr} + \Theta_{ra}) - \Delta T, \quad (3)$$

The thermal power which is absorbed by TCM (cooling capacity) is determined by the ratio [8, 9]:

$$P_c = \alpha T_c I - \frac{1}{2} I^2 R - \kappa \Delta T, \quad (4)$$

and the thermal power  $P_h$  is removed from the hot surface using a radiator

$$P_h = \alpha T_h I + \frac{1}{2} I^2 R - \kappa \Delta T, \quad (5)$$

where  $\alpha$ ,  $\kappa$ , and  $R$  is coefficient of differential thermoEMF, thermal conductivity and resistance of semiconductor material of TCM legs,  $T_c$ , and  $T_h$  are the temperatures of the cold and hot surfaces of TCM,  $I$  is the supply current of TCM.

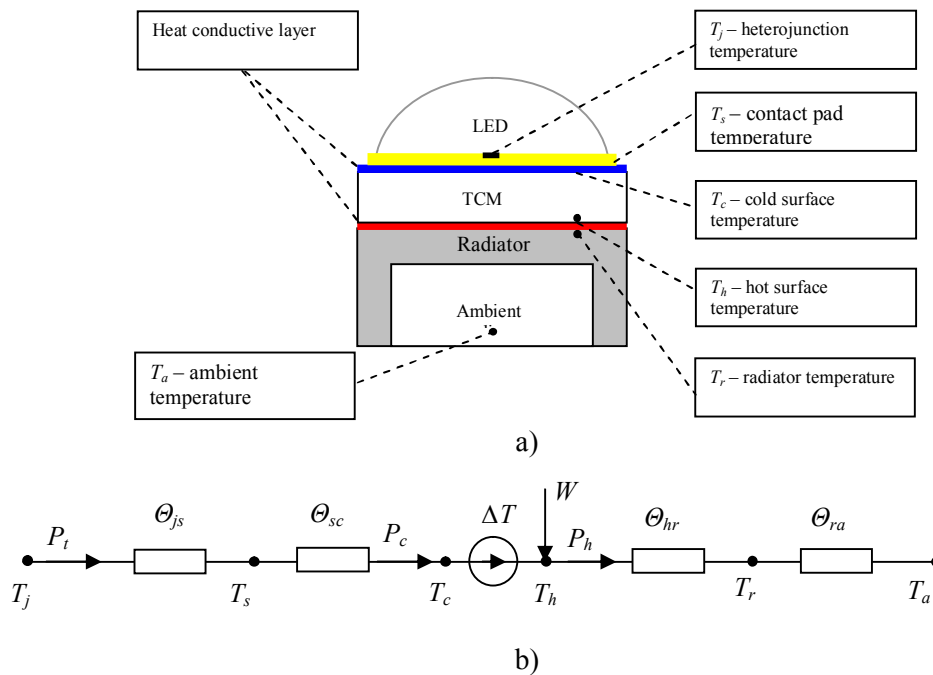


Fig. 1. Schematic of thermoelectric cooling system of LED with TCM and radiator (a) and its thermal circuit (b). Here  $T_j$  is the temperature of LED heterojunction,  $T_s$  is the temperature of the contact pad,  $T_c$  and  $T_h$  is the temperature of the cold and hot surfaces of the TCM, respectively,  $T_r$  is radiator temperature,  $T_a$  is ambient temperature,  $\Delta T$  is temperature difference between the hot and cold surfaces of the TCM.

The power released on the TCM hot surface exceeds the power absorbed by the cold surface by the amount of the power supply's power consumption

$$P_h = P_c + W. \quad (6)$$

The power  $W$  is used to carry out the work on the displacement of charges against the difference in electric potentials that arise in conformity with the Seebeck effect in the thermoelectric circuit, and on the Joule heat losses:

$$W = P_h - P_c = \alpha I \Delta T + I^2 R. \quad (7)$$

From the equation of thermal equilibrium for the overheat temperature of LED heterojunction we get:

$$\Delta T_j = T_j - T_a = P_c \cdot (\Theta_c + \Theta_h) + (\alpha I \Delta T + I^2 R) \cdot \Theta_h - \Delta T \quad (8)$$

where  $\Theta_c = \Theta_{js} + \Theta_{sc}$ , and  $\Theta_h = \Theta_{hr} + \Theta_{ra}$  are thermal resistances on the side of the cold and hot surfaces of TCM,

$$\Delta T = \frac{1}{\kappa} \cdot \left( \alpha T_c I - \frac{1}{2} I^2 R - P_c \right), \quad (9)$$

temperature difference.

In formula (8), the first term describes an increase in the heterojunction temperature during the transfer of thermal power emitted by the LED and the module itself. The last two terms determine the effect of TCM on the temperature of LED heterojunction. Cooling is provided by the temperature difference between the hot and cold TCM surfaces. As a result, the efficiency of the thermoelectric cooling system depends on the mutual ratio of the values of these terms.

The temperature of LED heterojunction is determined by its power, thermal resistance of the cooling system, ambient temperature and the operating mode of TCM. The operating mode of the module is controlled by changing the value of the supply current. In the development and operation of a thermoelectric cooling system, an important issue is the choice of the optimal current at which effective cooling occurs.

### Analysis of the results

Let us consider the effect of TCM supply current on the efficiency of LED cooling at given values of its power and thermal resistance of cooling system. As a source of light we choose a modern LED matrix *XLamp CMA1516*, the parameters of which are given in the table [11].

Table

*Parameters of LED XLamp CMA1516*

Maximum current, <i>A</i>	Maximum voltage, <i>V</i>	Maximum power, <i>W</i>	Light flux, <i>Lm</i>	Thermal resistance of LED $\Theta_{j-s}, K/W$
1.05	39	41	1400-4800	0.4

The power of LED can be controlled over wide range by varying the supply voltage or current. Obviously, the LED power should be no greater than maximum cooling capacity of TCM. For this LED array maximum thermal power is:

$$P_{t \max} = (1 - \eta_e) U_{f \max} I_{f \max} = 30 \text{ W}.$$

The model of TCM will be chosen proceeding from thermal power, dimensions and requirements to temperature operating mode of LED. In the calculations, the characteristics of serial *TEM TB-161* [12] were used with parameters: maximum current  $I_{\max} = 5.7 \text{ A}$ , maximum voltage  $U_{\max} = 18.3 \text{ V}$ , maximum cooling capacity at zero temperature difference  $P_{c,\max} = 66.3 \text{ W}$ , maximum temperature difference at zero cooling capacity  $\Delta T_{\max} = 70 \text{ K}$ .

The use of thermoelectric modules is always associated with the use of particular radiator, which must dissipate not only the heat that the LED emits, but also the Joule heat which is released in the thermoelement when electric current passes through it. The thermal resistance of modern radiators equipped with fans is  $\Theta_{ra} = 0.3 \div 0.6 \text{ K/W}$ . The best samples using heat pipes reach the values  $\Theta_{ra} = 0.1 \text{ K/W}$ . Liquid heat removal systems are even more efficient. Their thermal resistance is  $\Theta_{ra} = 0.1 \div 0.01 \text{ K/W}$ , but they are cumbersome and difficult to install in the lighting system.

As a result of numerical analysis of the obtained relationships a number of graphic dependences were obtained. In particular, Fig. 2 shows a dependence of the overheat temperature of LED heterojunction on TCM current at different values of LED thermal power.

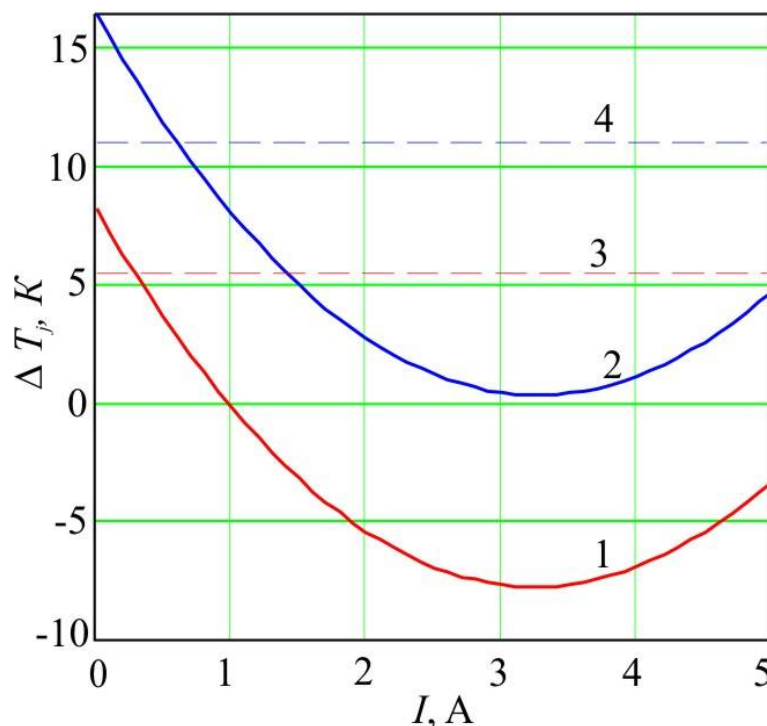


*Fig. 2. The dependence of overheat temperature of LED heterojunction on TCM current at different values of LED power and thermal resistances  $\Theta_c = 0.6 \text{ K/W}$ ,  $\Theta_h = 0.2 \text{ K/W}$ . The solid lines 1 and 2 are at  $P_c = 10 \text{ W}$ , and  $P_c = 20 \text{ W}$ , respectively. The dashed lines 3 and 4 are at the same power and thermal resistances, but in the absence of TCM.*

The minima of the  $\Delta T_j(I)$  lines correspond to the operating modes with the maximum efficiency of the cooling system, whereby which the lowest heterojunction temperature is reached. It is obvious that at currents close to the effective, thermoelectric cooling system yields lower temperatures than the traditional one. The dashed lines in the figure show the temperature dependences for the cooling system without TCM, calculated by formula (7) for the same values of thermal resistance.

The dependence of heterojunction overheat temperature on TCM current at different values of thermal resistance on the hot side of TCM is shown in Fig. 3.

It is obvious that with increasing the value of  $\Theta_h$ , cooling efficiency deteriorates, and the location of the minima of dependences  $\Delta T_j(I)$  shifts to the region of lower current values. At certain ratios between the power of TCM and LED, the heterojunction temperature may decrease to ambient temperature, and sometimes even lower than that. This is particularly relevant in the case when ambient temperature is close to the critical temperature of LED heterojunction.

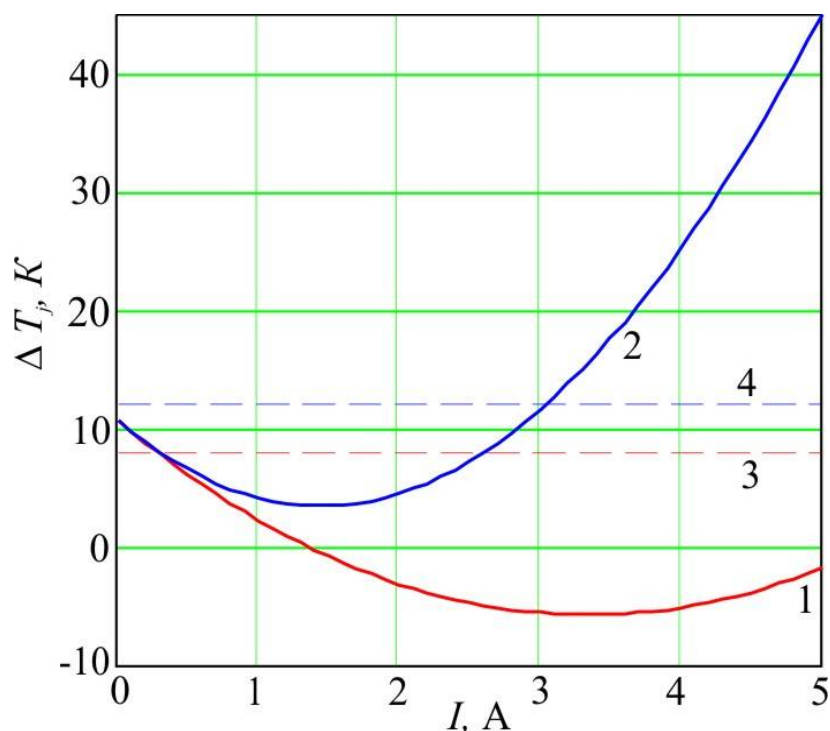


*Fig. 3. The dependence of heterojunction overheat temperature on TCM current at a LED power  $P_c=10$  W and at different values of thermal resistance on the hot side of TCM. The solid lines 1 and 2 are at  $\Theta_h=0.2$ K/W and  $\Theta_h=0.6$ K/W, respectively. The dashed lines 3 and 4 are at the same power and thermal resistances, but in the absence of TCM.*

The dependence of temperature difference on TCM current at different powers of LED is presented in Fig 4.

From the plot it follows that with increasing current, the temperature difference between the hot and cold surfaces of TCM increases. In addition, it depends on the heat load. In particular, with an increase in the thermal power of the LED, the temperature difference decreases and vice versa, with decreasing power it increases.

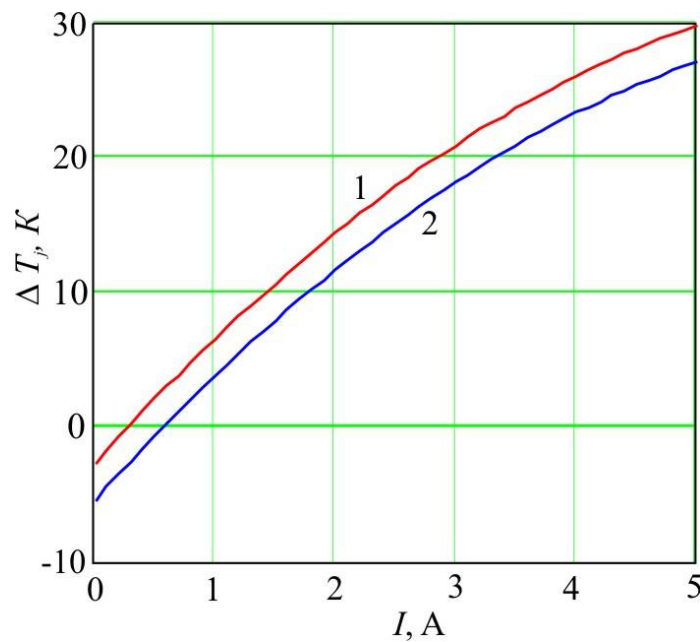


Fig. 4. The dependence of the temperature difference on TCM current at different powers of LED.

Line 1 is at  $P_c=10$  W, line 2 – at  $P_c=20$  W.

The value of thermal resistance of the cooling system is significantly affected by the operating mode of the TCM and the power of the heat load. If the temperature of the LED heterojunction equals the temperature of the medium or becomes lower, the thermal resistance of the system will become zero, or even negative.

## Conclusions

Under conditions when ambient temperature is close to critical temperature of LED heterojunction, to stabilize its thermal mode it is worthwhile to use thermoelectric cooling modules.

With given thermal power of LED and thermal resistance of cooling system, there is an optimal value of TCM supply current whereby the temperature of LED heterojunction reaches the minimum. At currents close to the optimum, thermoelectric cooling system allows obtaining lower values of heterojunction temperature than the traditional one.

With the optimum correlation between the powers of TCM and LED, the thermoelectric cooling system can reduce the temperature of LED heterojunction to the values lower than ambient temperature. The efficiency of using TCM is reduced with increase in the thermal power of LED and total thermal resistance of cooling system.

In the analysis of the efficiency of cooling system operation one should be guided not only by TCM parameters, but also by parameters of the entire LED cooling system, namely the total thermal resistance of cooling system, the thermal load and the operating mode of TCM.

## References

1. Nikiforov S. (2005). Temperatura v zhizni i rabote svetodiodov [Temperature in the life and work of LEDs]. Komponenty i tekhnologii – Components and Technologies, 9, 140-146 [in Russian].



- Gonin M. (2013). Spasitelnaia prokhlada, ili teplootvod dlia moshchnykh svetodiodnykh matrits [Saving coolness, or heat sink for high-power LED arrays]. Novosti elektroniki + svetotekhnika – Electronics News and Illumination Engineering, 2 [in Russian].
- Polishchuk A.A. (2006). Obespecheniie teplovogo rezhima svetodiodnykh lamp pri razrabotke svetotekhnicheskikh ustroystv [Providing thermal mode of LED lamps in the development of lighting devices]. Sovremennaiia elektronika – Modern Electronics, 3, 42-45 [in Russian].
- Staroverov K. (2008). Sistemy okhlazhnediia dlia svedodiodov [Cooling systems for LEDs]. Novosti elektroniki – Electronics News, 17, 21-23 [in Russian].
- Lotar Noel (2010). Okhlazhediie i regulirovanie temperaturnykh rezhimov svetodiodov [Cooling and control of temperature modes of LEDs]. Poluprovodnikovaia svetotekhnika – Semiconductor Illumination Engineering, 3, 13-15 [in Russian].
- Zakordonets V., Natalija Kutuzova (2016). Teoretychnyi analiz teplovykh umov i shliakhy stabilizatsii temperatury svitlodiodiv. [Theoretical analysis of thermal conditions and ways of LED temperature stabilization. Bulletin of TNTU]. Visnyk TNTU – Bulletin of TNTU, 4 (84), 105–112 [in Ukrainian].
- Beliaiev N.M., Riadno A.A. (1982). Metody teorii teploprovodnosti. Chast1. [Methods of thermal conductivity theory. P.1] – Moscow: Vysschaia shkola [in Russian].
- Anatychuk L.I. (1979). Termoelementy i termoelektricheskiie ustroystva [Thermoelements and thermoelectric devices]. Kyiv: Naukova dumka [in Russian].
- Shostakovskii P. (2009). Sovremennyye resheniia termoelektricheskogo okhlazhdeniia [Modern solutions of thermoelectric cooling]. Komponenty i tekhnologii – Components and Technologies, 12, 40-46 in Russian].
- <http://www.cree.com/led-components/media/documents/ds-CMA1516.pdf>.
- <http://kryothermtec.com/ru/standard-single-stage-thermoelectric-coolers.html>.

Submitted 08.10.2018

**Закордонец В.С., канд. фіз.-мат наук**  
**Кутузова Н.В.**

Тернопільський національний технічний університет,  
імені Івана Пуюля, вул. Руська, 56, Тернопіль, 46001, Україна  
*e-mail: wladim21@gmail.com*

## **РОЗРАХУНОК ТЕРМОЕЛЕКТРИЧНОЇ СИСТЕМИ ОХОЛОДЖЕННЯ СВІТЛОДІОДІВ**

*В роботі побудована теплова математична модель термоелектричної системи охолодження. Розв'язана система рівнянь, яка включає стаціонарне рівняння теплопровідності, рівняння термогенерації та рівняння генерації холоду. Розрахована температура гетеропереходу СД в залежності від його потужності, загального теплового опору системи охолодження, температури навколишнього середовища та холодопродуктивності ТЕМ. Отримані аналітичні залежності температури гетеропереходу від струму живлення ТЕМ при різних потужностях СД та при різних значеннях теплового опору системи охолодження. При даній тепловій потужності СД та теплового опорі системи охолодження знайдено оптимальну величину струму живлення*

ТЕМ, при якому температура гетеропереходу СД досягає мінімуму. Показано, що застосування ТЕМ дає можливість зменшити температуру гетеропереходу СД до значень нижчих ніж температура навколишнього середовища. Це особливо актуально в умовах, коли температура середовища близька до критичної температури гетеропереходу. Показано, що ефективність використання ТЕМ знижується при збільшенні потужності СД, температури навколишнього середовища і сумарного теплового опору системи охолодження. Бібл. 11, рис. 4, табл. 1

**Ключові слова:** світлодіод, гетероперехід, тепловий режим, тепловий опір, термостабілізація, термоелектричний модуль охолодження, радіатор.

**Закордонец В.С., канд. физ.-мат. наук, доцент**  
**Кутузова Н.В.**

Тернопольський національний технічний університет,  
імени Івана Пулюя, ул. Русская, 56, Тернополь, 46001, Україна,  
e-mail: wladim21@gmail.com

## **РАСЧЕТ ТЕРМОЭЛЕКТРИЧЕСКОЙ СИСТЕМЫ ОХЛАЖДЕНИЯ СВЕТОДИОДОВ**

В работе построены физическая и математическая тепловые модели термоэлектрической системы охлаждения. Решена система уравнений, включающая стационарное уравнение теплопроводности, уравнение термогенерации и уравнение генерации холода. Рассчитана температура гетероперехода светодиода (СД) в зависимости от его мощности, полного теплового сопротивления системы охлаждения, температуры окружающей среды и холодопроизводительности термоэлектрического охлаждающего модуля (ТЭОМ). Получены аналитические зависимости температуры гетероперехода от тока питания ТЭОМ при различных мощностях СД и значениях теплового сопротивления системы охлаждения. При заданной тепловой мощности СД и тепловом сопротивлении системы охлаждения найдена оптимальная величина тока питания ТЭОМ, при котором температура гетероперехода СД достигает минимума. Показано, что использование ТЭОМ дает возможность уменьшить температуру гетероперехода СД до значений более низких, чем температура окружающей среды. Это особенно актуально в условиях, при которых температура среды близка к критической температуре гетероперехода. Показано, что эффективность использования ТЭОМ снижается при увеличении мощности СД, температуры окружающей среды и полного теплового сопротивления системы охлаждения. Библ. 11, рис. 4, табл. 1.

**Ключевые слова:** светодиод, гетеропереход, тепловой режим, тепловое сопротивление, термостабилизация, термоэлектрический охлаждающий модуль, радиатор.

### **References**

1. Nikiforov S. (2005). Temperatura v zhizni i rabote svetodiodov [Temperature in the life and work of LEDs]. Komponenty i tekhnologii – Components and Technologies, 9, 140-146 [in Russian].

2. Gonin M. (2013). Spasitelnaia prokhlada, ili teplootvod dlia moshchnykh svetodiodnykh matrity [Saving coolness, or heat sink for high-power LED arrays]. *Novosti elektroniki + svetotekhnika – Electronics News and Illumination Engineering*, 2 [in Russian].
3. Polishchuk A.A. (2006). Obespecheniie teplovogo rezhima svetodiodnykh lamp pri razrabotke svetotekhnicheskikh ustroystv [Providing thermal mode of LED lamps in the development of lighting devices]. *Sovremennaia elektronika – Modern Electronics*, 3, 42-45 [in Russian].
4. Staroverov K. (2008). Sistemy okhlazhnediia dlia svetodiodov [Cooling systems for LEDs]. *Novosti elektroniki – Electronics News*, 17, 21-23 [in Russian].
5. Lotar Noel (2010). Okhlazhediie i regulirovanie temperaturnykh rezhimov svetodiodov [Cooling and control of temperature modes of LEDs]. *Poluprovodnikovaia svetotekhnika – Semiconductor Illumination Engineering*, 3, 13-15 [in Russian].
6. Zakordonets V., Natalija Kutuzova (2016). Teoretychnyi analiz teplovykh umov i shliakhy stabilizatsii temperatury svitlodiodiv. [Theoretical analysis of thermal conditions and ways of LED temperature stabilization. *Bulletin of TNTU*]. *Visnyk TNTU – Bulletin of TNTU*, 4 (84), 105–112 [in Ukrainian].
7. Beliaiev N.M., Riadno A.A. (1982). *Metody teorii teploprovodnosti. Chast1.* [Methods of thermal conductivity theory. P.1] – Moscow: Vysschaia shkola [in Russian].
8. Anatyshuk L.I. (1979). *Termoelementy i termoelektricheskiye ustroystva* [Thermoelements and thermoelectric devices]. Kyiv: Naukova dumka [in Russian].
9. Shostakovskii P. (2009). *Sovremennyye resheniia termoelektricheskogo okhlazhdeniia* [Modern solutions of thermoelectric cooling]. *Komponenty i tekhnologii – Components and Technologies*, 12, 40-46 in Russian].
10. <http://www.cree.com/led-components/media/documents/ds-CMA1516.pdf>.
11. <http://kryothermtec.com/ru/standard-single-stage-thermoelectric-coolers.html>.

Submitted 08.10.2018



Максимук Н.В.

**M.V. Maksimuk**

Institute of Thermoelectricity of the NAS and MES  
of Ukraine, 1, Nauky str, Chernivtsi, 58029, Ukraine;  
*e-mail: anatykh@gmail.com*

---

**ECONOMIC ASPECTS OF USING STARTING PREHEATERS  
WITH THERMOELECTRIC HEAT SOURCES**

---

*This paper presents the results of research on the economic indicators of systems for preheating of the internal combustion engine with thermoelectric generators as the sources of electric power. Based on the feasibility study, it was determined that a system with a common heat source is the most efficient option of using thermoelectric power sources for pre-start thermal preparation of vehicle engines for work. The relationship between the unit cost of electric energy and the useful thermal power of the "starting preheater-thermoelectric generator" system with a common heat source is established. It is determined that the peculiarity of using such a system lies in reducing the specific cost of electric energy generation when increasing the thermal output of starting preheaters. Bibl. 11, Table. 3.*

**Keywords:** starting preheater, thermoelectric generator, efficiency.

### **Introduction**

One of the promising methods for solving the problem of battery discharge during the thermal pre-start preparation of vehicle engines is the use of thermoelectric generators (TEG) as power sources for starting preheaters [1 – 7].

In [8], it was shown that the options for using starting preheaters with thermal generators are reduced to three main systems according to the method of supplying and discharging heat flows:

- with individual heat sources;
- with individual heat sources and a common hydraulic circuit;
- with a common heat source.

The choice of the most effective system for applications requires a comprehensive assessment of its energy characteristics and cost indicators. On the basis of studies on the determination of the thermodynamic features of such systems carried out in [8], it was found that the "thermoelectric generator-starting preheater" system with a common heat source and the system in which the starting preheater and TEG are combined by a hydraulic circuit are characterized by the highest efficiency.

The purpose of this work is to further analyze the models of starting preheaters with thermoelectric power sources and to determine the most economically effective option of using thermoelectric generators in systems for preheating of vehicle engines.

### **Technical and economic analysis of the use of starting preheaters with thermoelectric power sources**

The cost  $C$  of systems for preheating of engines will be estimated with the use of the following relationship:

$$C = C_1 + C_2 \tag{1}$$

where  $C_1$ ,  $C_2$  is the cost of starting preheater and thermoelectric generator, respectively. For a system with a common heat source,  $C_1$  is the cost of starting preheater components.

The basic factor which defines the price characteristics of thermoelectric generator is the cost  $C_3$  of generator thermopile:

$$C_3 = n \cdot C_4 \quad (2)$$

Where  $C_4$  is the cost of thermoelectric module of which the thermopile is composed,  $n$  is the number of modules in the thermopile.

The number of modules  $n$  which must be used to assure given level of TEG electric power  $W$  can be found by the relationship:

$$n = \frac{W}{w} \quad (3)$$

Where  $w$  is the electric power of a module.

The cost of systems will be estimated by the example of liquid starting preheater WebastoThermoTopEVO 4, the price specifications of which are given in Table 1.

*Table 1*

*The cost of liquid starting preheater  
WebastoThermoTopEVO 4 and its functional components [9]*

№	Name	Cost $C_i$ , \$USA
1	Starting preheater	850
2	Burner	155
3	Fan	200
4	Fuel pump	110
5	Circulation pump	135

As a thermopile for TEG we will use thermoelectric generator modules "Altec-1061" with electric power output  $w = 10$  W, that are manufactured at the Institute of Thermoelectricity [10]. The cost of one such module is  $\sim 20$  \$. Moreover, to simplify the calculations, it will be assumed that the cost of thermoelectric modules is about 30 % of the total cost of thermoelectric generator.

Since the level of electrical power output which makes it possible to ensure the functioning of the considered systems is about 50 W [8], it is necessary to use six Altec-1061 generator modules in the design of thermal generators. Thus, the total cost of a system with individual heat sources and a system with a common hydraulic circuit will be \$ 1250 with a TEG cost of \$ 400. Accordingly, the cost of the system with a common heat source will be lower by \$ 250.

The estimated cost of system for preheating of engine is presented in Table 2. For a comprehensive assessment of the effectiveness of the systems under consideration, the table below lists the previously obtained values of their total thermal and electrical efficiency.

From the above data it follows that the most rational for preheating of the engine is "starting preheater-thermoelectric generator" system with a common heat source, because with equal values of efficiency, its cost is lower compared to the cost of the system combined by a common hydraulic circuit.

Table 2

*Efficiency of thermoelectric systems for preheating of engine*

№	System type	Efficiency $\eta$ , %	Cost $C$ , \$USA
1	With individual heat sources	60	1250
2	With individual heat sources and a common hydraulic circuit	75	1250
3	With a common heat source	75	1000

Let us estimate the specific cost of electric energy obtained from the use of system for preheating of engine with a common heat source:

$$c = \frac{C}{W} = \frac{C_1 + C_2}{nW} \quad (4)$$

We will perform calculations based on the classification of start equipment according to the level of thermal output and electric power consumed for three types of liquid preheaters: Thermo Top Evo 4, Thermo Pro 90, Thermo E200, oriented for use in vehicles with engine capacity ( $> 2.5$ ) l, (4-10) l and ( $< 10$ ) l [9]. In addition, we establish the dependence of the specific cost of electrical energy on the thermal output of starting preheaters  $Q$  and the efficiency of TEG  $\eta_{TEG}$ , determined by the following relationship:

$$\eta_{TEG} = \frac{W}{Q} \quad (5)$$

The thermal power  $Q$  used for the operation of the thermal generator in a system with a common heat source is equal to the thermal power of starting preheater burner:

$$Q = \eta \cdot A \cdot m, \quad (6)$$

Where  $\eta$  is the efficiency of starting preheater burner;  $A$  and  $m$  is calorific value and consumption of fuel which is used for the operation of starting preheater.

The calculations will be carried out using the information on the technical characteristics of the above models of heaters [9].

The results are presented in Table 3.

Table 3

*Results of calculations of the specific cost of electric energy for "starting preheater-thermoelectric generator" system with a common heat source*

Characteristics	ThermoTopEvo 4	ThermoPro90	ThermoE200
*The cost of functional components $C_1$ , \$	600	700	670
** The cost of thermoelectric generator $C_2$ , \$	670	770	870
The cost of system $C$ , \$	1270	1470	1540
***Output electric power of TEG $W$ , W	100	150	200
Specific cost of electric energy $c$ , \$/W	13	10	8

*Table 3 (continued)*

Thermal output $Q$ , kW	4	9	20
Thermoelectric conversion efficiency $\eta_{TEG}$ , %	2	1.3	1

\* The cost of functional components of liquid starting preheaters was calculated with the use of data given in the pricelists of Webasto [9].

\*\* Due to the fact that the design of thermoelectric generators is made according to one physical model, the cost of thermal generators oriented to high values of electrical power is defined as the sum of the cost of a TEG of the lowest electrical power and the cost of the corresponding number of thermoelectric modules.

\*\*\* The electrical power output of a thermoelectric generator is determined taking into account the possibility of recharging the battery [11].

As follows from the given data, the feature of a system with a common heat source is the reduction of the specific cost of the electrical energy generation, which occurs when the thermal output of starting preheater is increased. The reason for this is the connection between the specific cost and  $\eta_{TEG}$ , and the reduction of the thermoelectric efficiency results in a decrease in the specific cost of the electric energy generation from 13 \$/W for a thermal power of 4 kW to 8 \$/W for power levels of 20 kW, which is another advantage of this system.

## Conclusions

1. It is shown that “starting preheater – thermoelectric generator” system with a common heat source is the most rational for preheating of engine both in terms of energy characteristics and with regard to cost parameters.

2. It is established that the system with a common hydraulic circuit is less effective, since with equal efficiency values, its cost is approximately 1.2 times higher than the cost of a system with a common heat source.

3. It is shown that a system with individual heat sources is least effective for preheating of engine, both in terms of efficiency and from the standpoint of total cost. However, such a system has several advantages, namely the possibility of using a thermoelectric generator as a standby power source in a car.

4. It is determined that the highest values of thermoelectric efficiency in a system with a common heat source should be inherent in starting preheaters of the lowest thermal power. It is established that with the growth of thermal output, the efficiency of the thermoelectric energy conversion reaches 1% for thermal powers of 20 kW. The latter is important because there is a connection between the specific cost of the electricity generated and the efficiency of the thermal generator, and the reduction of the efficiency results in a decrease in the specific cost from 13 \$/W to 8 \$/W.

The author expresses his gratitude to academician L. I. Anatyuk for the topic and idea of scientific research, as well as for valuable advice when writing the paper.

## References

1. Mykhailovsky V. Ya., Maksimuk M. V. (2014). Automobile operating conditions at low temperatures. The necessity of applying heaters and the rationality of using thermal generators for their work. *J. Thermoelectricity*, 3, 20-31.

2. Patent of Ukraine №102303 (2013). Anatyshuk L.I., Mykhailovsky V.Ya.. Thermoelectric power source for automobile [in Ukrainian].
3. Patent of Ukraine №72304 (2012). Anatyshuk L.I., Mykhailovsky V.Ya.. Automobile heater with thermoelectric power source [in Ukrainian].
4. Patent of Ukraine №124999 (2018). Maksimuk M.V. Automobile heater with thermoelectric power source [in Ukrainian].
5. Patent of US6527548B1 (2003). Aleksandr S. Kushch, Daniel Allen. Self-powered electric generating space heater.
6. Patent of US2010/0115968A1 (2010). Jorn Budde, Jeans Baade, Michael Stelter. Heating apparatus comprising a thermoelectric device.
7. Patent of RF 2268393C1 (2006). Prilepo Yu.P. A device to facilitate the start of internal combustion engine.
8. Anatyshuk L.I., Maksimuk M.V. (2018). Efficiency of starting pre-heaters with thermoelectric power sources. *J. Thermoelectricity*, 3.
9. Retrieved from <http://www.webasto.com>
10. Retrieved from <http://www.inst.cv.ua>
11. Mykhailovsky V.Ya., Maksimuk M.V. (2015). Rational powers of thermal generators for starting pre-heaters of vehicles. *J. Thermoelectricity*, 4, 65-74.

Submitted 19.11.2018.

### **Максимук М.В.**

Институт термоэлектрики НАН і МОН України,  
вул. Науки, 1, Чернівці, 58029, Україна,  
e-mail: [anatysh@gmail.com](mailto:anatysh@gmail.com)

## **ПРО ЕКОНОМІЧНІ АСПЕКТИ ВИКОРИСТАННЯ ПЕРЕДПУСКОВИХ НАГРІВНИКІВ З ТЕРМОЕЛЕКТРИЧНИМИ ДЖЕРЕЛАМИ ЕЛЕКТРИКИ**

*Наведено результати досліджень економічних показників систем передпускового розігріву двигуна внутрішнього згорання, в яких джерелами електричної енергії є термоелектричні генератори. На основі техніко-економічного аналізу визначено, що система з сумісним джерелом тепла є найефективнішим варіантом застосування термоелектричних джерел електрики для передпускової теплової підготовки двигунів транспортних засобів до експлуатації. Встановлено взаємозв'язок між питомою вартістю електричної енергії та корисною тепловою потужністю системи "передпусковий нагрівник-термоелектричний генератор" з сумісним джерелом тепла. Визначено, що особливість використання такої системи полягає в зниженні питомої вартості отриманої електроенергії при підвищенні теплопродуктивності передпускових нагрівників. Бібл. 11, Табл. 3.*

**Ключові слова:** передпусковий нагрівник, термоелектричний генератор, ефективність

### **Максимук Н.В.**

Институт термоэлектричества, ул. Науки, 1,  
Черновцы, 58029, Украина  
e-mail: [anatysh@gmail.com](mailto:anatysh@gmail.com)



## ОБ ЭКОНОМИЧЕСКИХ АСПЕКТАХ ИСПОЛЬЗОВАНИЯ ПРЕДПУСКОВОГО ОТОПИТЕЛЯ С ТЕРМОЭЛЕКТРИЧЕСКИМ ИСТОЧНИКОМ ЭЛЕКТРИЧЕСТВА

Приведены результаты исследований экономических показателей систем предпускового разогрева двигателя внутреннего сгорания, в которых источниками электроэнергии являются термоэлектрические генераторы. На основе технико-экономического анализа определено, что система с совместимым источником тепла является самым эффективным вариантом применения термоэлектрических источников электричества для предпусковой тепловой подготовки двигателей транспортных средств к эксплуатации. Установлена взаимосвязь между удельной стоимостью электрической энергии и полезной тепловой мощностью системы "предпусковой отопитель – термоэлектрический генератор" с совместным источником тепла. Определено, что особенность использования такой системы заключается в снижении удельной стоимости полученной электроэнергии при повышении тепловой мощности предпусковых нагревателей. . Библ. 11, Табл. 3.

Установлена взаимосвязь между удельной стоимостью электрической энергии и полезной тепловой мощностью системы "предпусковой отопитель – термоэлектрический генератор" с совместным источником тепла. Определено, что особенность использования такой системы заключается в снижении удельной стоимости полученной электроэнергии при повышении тепловой мощности предпусковых нагревателей. . Библ. 11, Табл. 3.

**Ключевые слова:** предпусковой отопитель, термоэлектрический генератор, эффективность.

### References

1. Mykhailovsky V.Ya., Maksimuk M.V. (2014). Automobile operating conditions at low temperatures. The necessity of applying heaters and the rationality of using thermal generators for their work. *J. Thermoelectricity*, 3, 20-31.
2. Patent of Ukraine №102303 (2013). Anatyshuk L.I., Mykhailovsky V.Ya.. Thermoelectric power source for automobile [in Ukrainian].
3. Patent of Ukraine № 72304 (2012). Anatyshuk L.I., Mykhailovsky V.Ya. Automobile heater with thermoelectric power source [in Ukrainian].
4. Patent of Ukraine № 124999 (2018). Maksimuk M.V. Automobile heater with thermoelectric power source [in Ukrainian].
5. Patent of US6527548B1 (2003). Aleksandr S. Kushch, Daniel Allen. Self-powered electric generating space heater.
6. Patent of US2010/0115968A1 (2010). Jorn Budde, Jeans Baade, Michael Stelter. Heating apparatus comprising a thermoelectric device.
7. Patent of RF 2268393C1 (2006). Prilepo Yu.P. A device to facilitate the start of internal combustion engine.
8. Anatyshuk L.I., Maksimuk M.V. (2018). Efficiency of starting pre-heaters with thermoelectric power sources. *J. Thermoelectricity*, 3
9. Retrieved from <http://www.webasto.com>
10. Retrieved from <http://www.inst.cv.ua>
11. Mykhailovsky V.Ya., Maksimuk M.V. (2015). Rational powers of thermal generators for starting pre-heaters of vehicles. *J. Thermoelectricity*, 4, 65-74.

Submitted 19.11.2018.

**L.I. Anatyhuk**, *acad. National Academy of Sciences of Ukraine*<sup>1,2</sup>

**N.V. Pasechnikova**, *doctor Medical Sciences, Professor*<sup>3</sup>

*Corresponding Member of the National  
Academy of Sciences of Ukraine*

**V.O. Naumenko**, *medical sciences, professor*<sup>3</sup>

**O.S. Zadorozhnyi**, *cand. Medical. of sciences*<sup>3</sup>

**M.V. Havryliuk**, *cand. phys. - math. Sciences*<sup>1,2</sup>

**R.R. Kobylanskyi** *cand. phys. - math. Sciences*<sup>1,2</sup>

<sup>1</sup>Institute of Thermoelectricity of the NAS and MES of Ukraine,

1 Nauky str., Chernivtsi, 58029, Ukraine;

*e-mail: anatyh@gmail.com,*

<sup>2</sup>Yuriy Fedkovych Chernivtsi National University,

2 Kotsiubynsky str., Chernivtsi, 58012, Ukraine;

<sup>3</sup>State Institution "The Filatov Institute of Eye Diseases and Tissue  
Therapy of the NAMS of Ukraine", 49/51 Frantsuzskyi Boulevard,  
Odesa, 65000, Ukraine

## **THERMOELECTRIC DEVICE FOR DETERMINING HEAT FLUX FROM THE SURFACE OF THE EYES**

---

*The paper presents the design and technical characteristics of a newly developed thermoelectric device for determining heat flux from the surface of the eyes. The device is promising for the diagnosis and monitoring of ophthalmic diseases, which makes it possible to increase the efficiency of the early diagnosis of the pathology of the organ of vision, to observe the dynamics of the development of the pathological process in the structures of the eye, as well as to increase the effectiveness of treatment of acute and chronic eye diseases. The developed thermoelectric device allows real-time monitoring of the thermal and temperature state of eye surface, is original and has no world analogues. Bibl. 29, Fig. 8, Tabl. 2.*

**Key words:** thermoelectric device, heat flux, ophthalmology

### **Introduction**

*General characterization of the problem.* The human organism, adapting to changing environmental conditions, can maintain the relative stability of its internal environment (homeostasis). Human thermoregulation is one of the most important aspects of maintaining homeostasis. To ensure the constancy of the human body temperature, it is necessary that the amount of heat energy (heat production) produced in the body is equal to the amount of heat energy emitted to the environment (heat transfer). Generation of thermal energy in the human body occurs continuously in the process of metabolic exothermic reactions of decomposition or oxidation of complex substances (glucose, proteins, lipids, etc.) into simpler ones [1]. The level of heat production, in turn, depends on the activity of the metabolism [2]. The return of heat to the environment is carried out by means of four basic mechanisms: radiation, heat transfer, convection and evaporation [3].

---

Evaluation of the heat exchange processes of the human body is based on the measurement of temperature and heat flux. Temperature characterizes the qualitative side of the thermal phenomenon, and heat flux – the quantitative [4, 5]. The area of temperature measurement, including in ophthalmology, is traditionally well provided with instrumentation and metrology. The temperature in different parts of the eye can be determined by contactless or contact methods. These methods of thermometry have both advantages and certain weak points [6]. As for the local measurement of heat flux from the surface of the human body, tangible success has recently been achieved in the development of modern means of measuring thereof [7 – 14]. Thermoelectric heat flux sensors that combine high sensitivity, accuracy, speed, and stability of parameters in a wide range of operating temperatures and are consistent with modern recording equipment are promising for the study of local heat generation in the human body [15 – 17]. The use of such sensors yields high accuracy of heat measurement [18]. However, it should be noted that there is still no thermoelectric instrument in the world for measuring heat flux from the surface of the eyes.

In the animal and human eye, blood circulation in the choroid is the main source of heat. The blood, entering the eye with a temperature practically equal to the body temperature, forms a thermal gradient that induces the transition of heat from blood to the eye tissues. The more intense the blood circulation, the greater the amount of heat transmitted to the eye tissues. Heat, distributed in the eye tissues, passes into the environment through the outer shells of the eye [6, 19, 20]. Today, in ophthalmology, there is a problem of the early and differential medical diagnosis of various diseases characterized by changes in the intraocular blood circulation (inflammatory processes, choroid tumors, glaucoma, etc.). It is obvious that the disruption of the blood circulation of the eye should be accompanied by a dynamics of heat transfer rates [20, 21]. Thus, the development of new highly sensitive methods for recording changes in the heat exchange of the eye, including the use of thermoelectric heat flux sensors, will improve the effectiveness of the early diagnosis of this pathology.

It is known that a number of acute and chronic ophthalmic diseases are accompanied by changes in the intraocular thermal processes. Thus, in some studies, the relationship of the temperature of the external surface of the eye with the state of the blood circulation of the eye, intraocular pressure, and the presence of an inflammatory process was demonstrated [22, 23]. Changes in the thermal characteristics of the eye tissue can occur in the early phase of the disease before the onset of severe clinical symptoms. Registration of these changes is a promising direction for the early diagnosis of various ophthalmic pathologies. Diagnosis of the pathological process at an early stage of development will lead to an increase in the effectiveness of treatment and a reduction in the risk of complications.

Therefore, *the purpose of this work* is to develop a thermoelectric device for determining the heat flux from the surface of the eyes, which allows increasing the efficiency of the early diagnosis of ophthalmic diseases.

### **Design and technical characteristics of the device**

A thermoelectric device for determining the heat flux from the surface of the eyes was developed at the Institute of Thermoelectricity of the National Academy of Sciences and Ministry of Education and Science of Ukraine as part of a cooperation agreement with the State Institution “The Filatov Institute of Eye Diseases and Tissue Therapy of the NAMS of Ukraine”. The device is designed to diagnose and monitor ophthalmic diseases, which makes it possible to increase the efficiency of the early diagnosis of the pathology of the organ of vision, to observe the dynamics of the development of the pathological process in the structures of the eye, as well as to increase the effectiveness of treatment of acute and chronic eye diseases. The developed thermoelectric device is original and has no world analogues [24]. The

appearance of the device and technical characteristics are shown in Fig. 1 and Table 1.

On the front panel of the device, there is a programmable thermostat of the type RE-202, a connector for connecting a thermoelectric heat flux sensor, a connector for connecting a thermoelectric thermocouple temperature sensor and the device power switch (Fig.1). On the rear panel there is a connector for the charger. It should be noted that it is strictly forbidden to measure the heat flux and temperature of living biological objects when an external mains charger is connected. The device can only be operated with the charger disconnected.

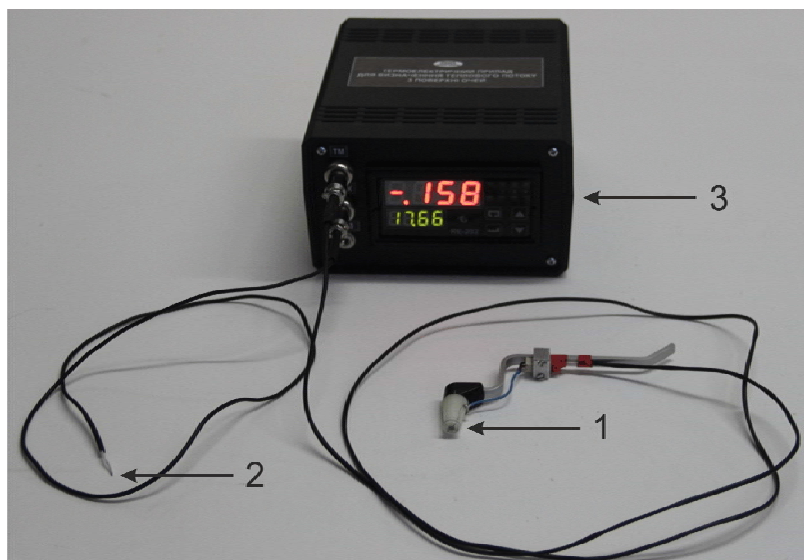


*Fig. 1. Thermoelectric device for determining heat flux from the surface of the eyes: 1 – thermoelectric heat flux sensor, 2 – thermoelectric thermocouple temperature sensor, 3 – electronic control unit.*

*Table 1*

*Technical specifications of the device*

№	Technical specifications of device	Parameter values
1.	Number of measurement channels	4
2.	Number of thermoelectric heat flux sensors	1
3.	Number of thermoelectric temperature sensors	1
4.	Heat flux density measurement range	0.01÷50 mW/cm <sup>2</sup>
5.	Accuracy of heat flux density measurement	± 5 %
6.	Temperature measurement range	0÷50 °C
7.	Temperature measurement resolution	± 0.01 °C
8.	Room temperature measurement range	0÷50 °C
9.	Room temperature measurement resolution	± 0.01 °C
10.	Battery voltage measurement range	3.7÷4.5 V
11.	Time of continuous operation of the device from a charged battery	12 h
12.	Overall dimensions of thermoelectric heat flux sensor	Ø3×0.7 mm
13.	Overall dimensions of electronic control unit	180×140×90 mm
14.	Device weight	0.6 kg

Multichannel thermoelectric device (Fig. 1) is a stand-alone device with a battery power supply, which makes it possible to carry out precise measurements of the heat fluxes and temperatures of biological objects in a contact manner. The block diagram of such a device is shown in Fig. 2.

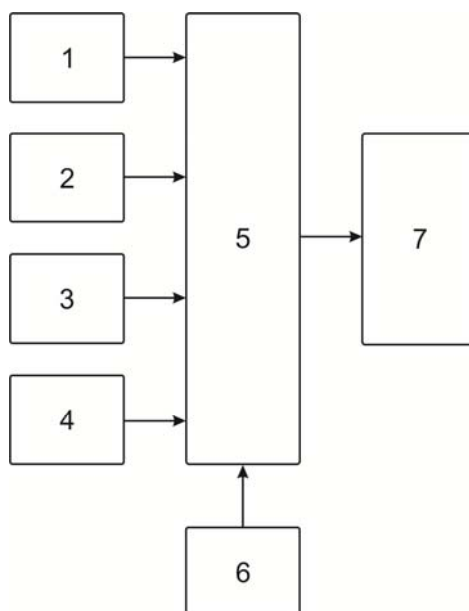


*Fig.2. The block diagram of a thermoelectric device for determining the heat flux from the surface of the eye: 1 - heat flux measurement channel, 2 - temperature measurement channel, 3 - voltage measurement channel on the battery power source, 4 - room temperature measurement channel, 5 - digital microcontroller, 6 - battery pack with a charger, 7 - digital display.*

The device consists of the following functional units: heat flux measurement channel 1, temperature measurement channel 2, voltage measurement channel on the battery power source 3, room temperature measurement channel 4, digital microcontroller 5, battery power supply unit with charger 6 and digital display 7.

The heat flux measurement channel 1 is designed for accurate measurement of the generated voltage of a thermoelectric heat flux sensor and its further transformation into a physical quantity in terms of the heat flux density ( $\text{mW}/\text{cm}^2$ ). The increment of the channel voltage measurement is  $\pm 1 \mu\text{V}$ , which allows for measuring the heat flux with maximum accuracy.

Temperature measurement channel 2 is designed for high-precision temperature measurement by a thermoelectric thermocouple sensor. The peculiarity of the developed device is that for the first time the doctor has an opportunity to measure the temperature of a biological object in increments of  $\pm 0.01 \text{ }^\circ\text{C}$  using a simple standalone portable device. Since chromel-kopel thermocouple is used as a temperature sensor, which can be made with minimal geometric dimensions, this makes it possible to measure the temperature of tiny biological objects at high speed.

Channel 3 is designed to measure and control the voltage on the battery pack. Since the device is powered by a battery, the duration of its continuous operation depends on the battery charge level, which, in turn, depends on the residual voltage on it. If the battery voltage becomes less than 3.7 V, then it should be charged according to the instruction manual of the device.

The room temperature measurement channel 4 is designed to accurately measure the ambient temperature. The temperature sensor is located on the front panel of the device at the connectors. Measurement of room temperature is carried out in increments of  $\pm 0.01 \text{ }^\circ\text{C}$  and this signal is used to compensate for the temperature of the cold junction of the chromel-kopel thermocouple.

The digital microcontroller 5 is designed to control the measuring channels, normalize and convert the generated signals into physical quantities. The digital microcontroller can be programmed using the buttons located on the front of the device, select sensor type and measurement limits.

A battery pack with a charger 6 is designed to electrically isolate the device and the biological object being studied in order to prevent its electric shock. Thanks to the galvanic isolation of the device from the mains, a safe and effective use of the device in ophthalmic practice has been created. The low voltage of the device autonomous power supply (no more than 4.5 V) does not constitute a threat of electric shock to any biological object under study. The charger prevents the lithium-ion battery from failing during its critical operating conditions.

Digital display 7 shows the measurement results (values of heat flux density - in  $\text{mW}/\text{cm}^2$  and temperature - in  $^\circ\text{C}$ ) on the front panel of the device. The digital display is light-emitting diode, large and bright, which makes it possible to carry out measurements in darkened rooms from long distances.

The device is simple, compact, portable, autonomous and reliable in operation, which allows the doctor or medical professional to use it without special training. So, the technical advantages of such a device include: the presence of a highly sensitive specific thermoelectric heat flux sensor, the capability of measuring temperature in increments of  $\pm 0.01 \text{ }^\circ\text{C}$ , the safety of using the device due to its galvanic isolation from the mains and the capability of real-time monitoring the thermal and temperature state of the surface of the human eye.

### **Manufacture and calibration of thermoelectric heat flux sensor**

For this thermoelectric device, a miniature thermoelectric heat flux sensor was developed and manufactured using the special patented technology of the Institute of Thermoelectricity of the National Academy of Sciences and Ministry of Education and Science of Ukraine [25 – 27]. Thermoelectric

micromodule with dimensions  $(2 \times 2 \times 0.5)$  mm contains 100 pcs *n*-type and *p*-type crystals with dimensions  $(0.17 \times 0.17 \times 0.4)$  mm from a highly efficient *Bi-Te*-based thermoelectric material. Such a thermoelectric micromodule is placed between two ceramic plates based on  $Al_2O_3$  with a diameter of 3 mm and a thickness of 0.1 mm each, and the side surface is sealed with a special sealant. Thus, the diameter and height of the manufactured thermoelectric heat flux sensor is 3 mm and 0.7 mm, respectively (Fig. 3). The diameter value of the developed heat flux sensor was determined according to medical requirements [28]. The electrical resistance of such a thermoelectric sensor is  $R = 14 \Omega$ .



*Fig. 3. Thermoelectric heat flux sensor of diameter 3 mm and height 0.7 mm.*

The next stage of the work was the determination of the volt-watt sensitivity of a thermoelectric heat flux sensor [29, 30]. To determine the volt-watt sensitivity of the heat flux sensor of the above device, a blackbody type thermal energy radiator was used as the heat flux source. The schematic of the bench for determining the volt-watt sensitivity of a thermoelectric heat flux sensor is shown in Fig. 4.

The volt-watt sensitivity of thermoelectric heat flux sensor is determined according to the following expression:

$$v = \frac{E}{Q}, \quad (1)$$

where  $v$  is volt-watt sensitivity of thermoelectric heat flux sensor (V/W),  $E$  is thermoEMF of thermoelectric heat flux sensor (V),  $Q$  is the value of heat flux (W).

The value of heat flux radiated by absolutely black body and absorbed by the receiving pad of thermoelectric heat flux sensor is determined as follows:

$$Q = \frac{\varepsilon_1 \cdot \varepsilon_2 \cdot \sigma \cdot (T_1^4 - T_0^4) \cdot S_1 \cdot S_0}{\pi \cdot r^2}, \quad (2)$$

where  $\sigma = 5.67 \cdot 10^{-12}$  W/(cm<sup>2</sup>·K<sup>4</sup>) is the Boltzmann constant,  $\varepsilon_1=1$  for absolutely black body radiator,  $\varepsilon_2=0.82$  for the receiving pad – polished ceramics based on  $Al_2O_3$ ,  $T_1$ , K is the temperature of absolutely black body package,  $T_0$ , K is the temperature of the receiving pad which is actually close to the ambient temperature,  $S_1$ , cm<sup>2</sup> is the area of radiating hole of the absolutely black body,  $S_0$ , cm<sup>2</sup> is the area of the

receiving pad,  $l$ , cm is the distance between the outlet hole of the radiating absolutely black body and the receiving pad which are parallel to each other and their centers are on the same axis.

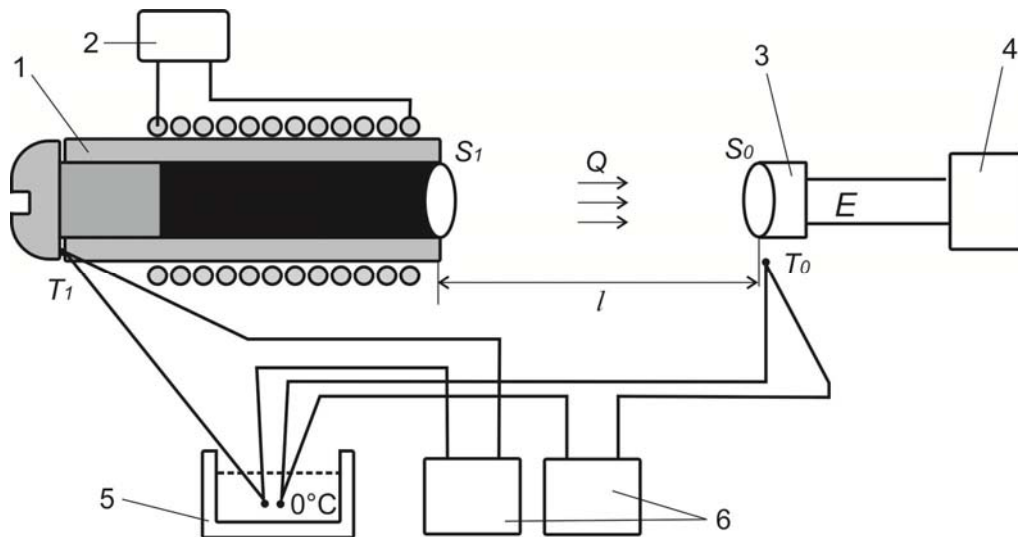


Fig. 4. Schematic of the bench for determining the volt-watt sensitivity of thermoelectric heat flux sensor:  
 1 – absolutely black body, 2 – power supply of absolutely black body heater,  
 3 – thermoelectric heat flux sensor, 4 – millivoltmeter, 5 – zero thermostat of thermoelectric thermocouples, 6 – temperature meters.

For this stand (Fig. 4) we have the following values:  $S_1 = 0.059 \text{ cm}^2$ ,  $S_0 = 0.07065 \text{ cm}^2$ ,  $l = 0.9 \text{ cm}$ .

The results of determining the volt-watt sensitivity of a thermoelectric heat flux sensor are given in Table 2.

Table 2

The results of determining the volt-watt sensitivity of a thermoelectric heat flux sensor

$T_0, ^\circ\text{C}$	$T_1, ^\circ\text{C}$	$E, \text{ mV}$	$Q, \text{ mW}$	$\nu, \text{ V/W}$
18.5	50	0.096	27.9	3.43
18.5	58	0.124	36.44	3.40

Thus, the thermoelectric heat flux sensor was calibrated and the conversion factor ( $k = 4.163 \text{ mW/mV} \times \text{cm}^2$ ) of the generated thermoelectric sensor voltage to a physical value in units of heat flux density ( $\text{mW/cm}^2$ ) was determined.

### The procedure for working with the device

The developed thermoelectric heat flux sensor of the device is fixed on a contact prism and a stand that are similar to standard Goldmann applanation tonometer (medical device used to measure intraocular pressure) [28]. The above contact prism and stand are universal and can be attached to biomicroscopes of



different manufacturers (Fig. 5-8). The unique feature of the contact prism is that it can be removed from the stand for treatment after each patient. The thermoelectric heat flux sensor, fixed in the center of the contact prism, directly contacts the outer surface of the human eye (with the center of the cornea). It should also be noted that the contact surface of the thermoelectric heat flux sensor is made atraumatic (with smoothed edges) and provides for the processing and disinfection of this surface.

Thermoelectric heat flux sensor (diameter 3 mm) is located in the center of the contact prism working surface (diameter 7 mm), and a small optical control zone between them is designed constructively so that the physician looking at the biomicroscope has the possibility to accurately establish the thermoelectric sensor at the center of the cornea of the eye (Fig. 8).



*Fig. 5. Goldmann tonometer stand fixed on a biomicroscope.*

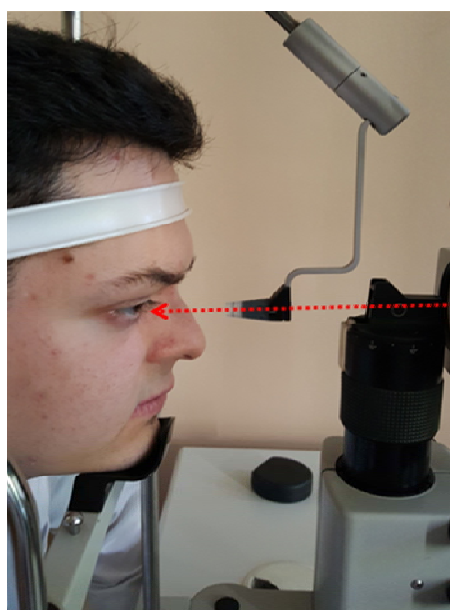


*Fig. 6. Contact prism and Goldmann tonometer. stand fixed on a biomicroscope (the figure shows the direction of the physician's view).*



*Fig. 7. Position of the contact prism fixed in Goldmann tonometer stand in the process of research with the help of a thermoelectric heat flux sensor.*

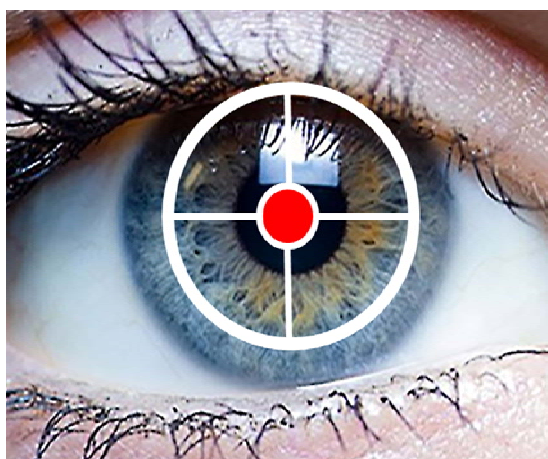


*Fig. 8. Schematic representation of the area of measurement of heat flux from the surface of the cornea of the human eye using the developed device*

## **Conclusions**

1. A thermoelectric device for determining the heat flux from the surface of the eyes was first developed and manufactured. The device is designed to diagnose and monitor ophthalmic diseases, which makes it possible to increase the efficiency of the early diagnosis of the pathology of the organ of vision, to observe the dynamics of the development of the pathological process in the structures of the eye, as well as to increase the effectiveness of treatment of acute and chronic eye diseases. The developed thermoelectric device is original and has no world analogues.
2. The developed thermoelectric device makes possible real-time monitoring of the thermal and temperature state of the surface of the human eyes, which is extremely important for the early diagnosis of ophthalmic diseases.
3. The introduction of the developed thermoelectric device into medical practice will be of extremely important social and economic importance, since it will reduce the risk of ophthalmic complications,

preserve the viability of the patient's eye structures and ensure the provision of highly qualified assistance both in specialized medical institutions and in extreme conditions.

## References

1. Chebyshev N.V., Guzikova G.S., Lazareva Yu.B., Larina S.N. (2011). *Biologiya. Spravochnik.- 2 izdaniie, ispravlennoie i dopolnennoie [Biology. Handbook. 2<sup>nd</sup> ed., revised and enlarged]*. Moscow: GEOTAR-Media [in Russian].
2. Tsarev A.V. (2014). Tselevoi temperaturnyi menedzhment v klinicheskoi praktike intensivnoi terapii kriticheskikh sostoianii [Special-purpose temperature management in the clinical practice of intensive care of critical states]. *Meditsina neotlozhnykh sostoianii – Medicine of Emergencies*, 7, 186-191.
3. Kubarko A.I. (2014). *Normalnaia fiziologiya: Uchebnik. V 2 chastiakh. Chast 2. [Normal physiology: textbook. In 2 parts. Part 2]*. A.I.Kubarko (Ed.). Minsk: Vysheishaiia shkola [in Russian].
4. Dekusha L.V. (2016). Sredstva teplometrii na base termoelektricheskikh preobrazovatelei teplovogo potoka [Heat metering means based on thermoelectric heat flux converters]. *Doctor's thesis (Engineering)*.
5. Grishchenko T.G., Dekusha L.V., Vorobiov L.I. (2017). *Teplometriia: teoriia, metrologiia, praktika. Monografiia v 3 knigakh [Heat flow metering: theory, metrology, practice. Monograph in three books]*. T.G.Grishchenko (Ed.). *Kniga 1: Metody i sredstva izmereniia teplovogo potoka [Book 1: Methods and facilities of heat flow measurement]*. Kyiv: Institute of Engineering Thermophysics [in Russian].
6. Anatyshuk L.I., Pasechnikova N.V., Zadorozhnyi O.S., Nazaretian R.E., Mirnenko V.V., Kobylianskyi R.R., Havryliuk N.V. (2015). Originalnoie ustroistvo i podkhody k izucheniiu raspredeleniia temperatury v razlichnykh otdelakh glaza [Original device and approaches to studying temperature distribution in different sections of eye]. *Ophthalmologicheskii zhurnal - J. Ophthalmology*, 6, 50-53 [in Russian].
7. Gischuk V.S. (2012). Electronic recorder of signals from human heat flux sensors. *J.Thermoelectricity*, 4, 105-108.
8. Gischuk V.S. (2013). Electronic recorder with processing signals from heat flux thermoelectric sensor. *J.Thermoelectricity*, 1, 82-86.
9. Gischuk V.S. (2013). Modernized device for human heat flux measurement. *J.Thermoelectricity*, 2, 91-95.
10. Gischuk V.S., Kobylianskyi R.R., Cherkez R.G. (2014). Bahatokanalnyi prylad dlia vymiriuvannia temperatury i hustyny teplovykh potokiv [Multichannel device for temperature and heat flux density measurement]. *Naukovy visnyk Chernivetskoho Universytetu. Fizyka.Elektronika – Scientific Bulletin of Chernivtsi University. Physics. Electronics*, 3 (1), 96-100 [in Ukrainian].
11. Kobylianskyi R.R., Boichuk V.V. (2015). Vykorystannia termoelektrychnykh teplomiriv u medychnii diagnostytsi [The use of thermoelectric heat flow meters in medical diagnostics]. *Naukovy visnyk Chernivetskoho Universytetu. Fizyka.Elektronika – Scientific Bulletin of Chernivtsi University. Physics. Electronics*, 4 (1), 90-96 [in Ukrainian].
12. Anatyshuk L.I., Ivashchuk O.I., Kobylianskyi R.R., Postevka I.D., Bodiaka V.Yu., Hushul I.Ya. (2016). Thermoelectric device for temperature and heat flux density measurement "Altec-10008". *J.Thermoelectricity*, 1, 76-84.
13. Anatyshuk L.I., Yuryk O.Ye., Kobylianskyi R.R., Roi I.V., Fishchenko Ya.V., Slobodianiuk N.P., Yuryk N.Ye., Duda B.S. (2017). Thermoelectric device for the diagnosis of inflammatory processes

- and neurological manifestations of vertebral osteochondrosis. *J. Thermoelectricity*, 3, 54-67.
14. Anatyshuk L.I., Kobylianskyi R.R., Cherkez R.G., Konstantynovych I.A., Hoshovskiy V.I., Tiumentsev V.A. (2017). Termoelektricheskoe ustroystvo s elektronnyim blokom upravleniia dlia diagnostiki vospalitelnykh protsessov v organizme cheloveka [Thermoelectric device with electronic control unit for diagnostics of inflammatory processes in human organism]. *Tekhnologiya i konstruirovaniye v elektronnoi apparature*, 6, 44-48 [in Russian].
  15. Anatyshuk L.I. (1979). Termoelementy i termoelektricheskiye ustroystva: Spravochnik [Thermoelements and thermoelectric devices: Handbook]. Kyiv: Naukova dumka [in Russian].
  16. Gerashchenko O.A. (1971). *Osnovy teplometrii [Fundamentals of heat flow metering]*. Kyiv: Naukova dumka [in Russian].
  17. Ladyka R.B., Dakaliuk O.N., Bulat L.P., et al. (1996). Primeneniye poluprovodnikovyykh teplomerov v diagnostike i lechenii [The use of semiconductor heat flow meters in diagnostics and treatment]. *Meditsinskaya tekhnika – Biomedical Engineering*, 6, 36 – 37 [in Russian].
  18. Anatyshuk L.I., Ivashchuk O.I., Kobylianskyi R.R., Postevka I.D., Bodiaka V.Yu., Gushul I.Ya., Chuprovskaya Yu.Ya. (2018). Pro vplyv temperatury navkolynshniho seredovyscha na pokazy termoelektrychnykh sensoriv medychnoho pryznachennia [On the effect of ambient temperature on the readings of medical purpose thermoelectric sensors]. *Sensorna elektronika i mikrosystemni tekhnologii – Sensor Electronics and Microsystem Technologies*, 15 (1), 17-29 [in Ukrainian].
  19. Mapstone R. (1968). Determinants of corneal temperature. *Brit. J. Ophthalmol.*, 52, 729-741.
  20. Tan J.H., Ng E.Y.K., Acharya U.R., Chee C. (2009). Infrared thermography on ocular surface temperature: A review. *Infrared Phys. Techn.*, 52, 97–108.
  21. Zadorozhnyi O.S., Guzun O.V., Bratishko A.Iu., et al. (2018). Infrared thermography of external ocular surface in patients with absolute glaucoma in transscleral cyclophotocoagulation: a pilot study. *J. Ophthalmol.*, 2, 23-28.
  22. Galassi F., Giambene B., Corvi A., et al. (2007). Evaluation of ocular surface temperature and retrobulbar haemodynamics by infrared thermography and colour Doppler imaging in patients with glaucoma. *British Journal of Ophthalmology*, 91, 878–881.
  23. Sodi A.A., Giambene B.A.D., Falaschi G.B., et al. (2007). Ocular surface temperature in central retinal vein occlusion: preliminary data. *European Journal of Ophthalmology*, 17, 755–759.
  24. *Application for utility model № u201901535 of 15.02.2019*. (2019). Anatyshuk L.I., Kobylianskyi R.R., Bukharaieva N.R., Havryliuk M.V., Tiumentsev V.A. Termoelektrychnyi prylad dlia vymiriuvannia temperatury i teplovoho potoku z poverhni ochei [Thermoelectric device for measurement of temperature and heat flux from the surface of eyes] [in Ukrainian].
  25. *Patent of Ukraine № 9321* (2014). Anatyshuk L.I., Konstantynovych I.A. Method for manufacturing thermoelectric microthermopile [in Ukrainian].
  26. *Patent of Ukraine № 117719* (2017). Anatyshuk L.I., Kobylianskyi R.R. (2017). Method for manufacturing thermoelectric microthermopile [in Ukrainian].
  27. Anatyshuk L.I., Kobylianskyi R.R., Konstantynovych I.A., Kuz R.V., Manik O.M., Nitsovykh O.V., Cherkez R.G. (2016). Technology for manufacturing thermoelectric microthermopiles. *J. Thermoelectricity*, 6, 49-54.
  28. Kim N.R. (2011). Comparison of Goldmann applanation tonometer, noncontact tonometer, and TonoPen XL for intraocular pressure measurement in different types of glaucomatous, ocular hypertensive, and normal eyes. *Curr. Eye Res.*, 36, 295-300.
  29. Anatyshuk L.I., Kobylianskyi R.R., Konstantynovych I.A. (2014). Hraduiuvannia termoelektrychnykh sensoriv teplovoho potoku [Calibration of thermoelectric heat flow sensors]. *Trudy XV Mizhnarodnoi naukovo-praktychnoi konferentsii “Suchasni informatsiini ta elektronni*

tekhnologii' – Proc. of International scientific and practical conference "Modern Information and Electronic Technologies" (Ukraine, Odessa, May 26-30, 2014). (Vol.2, pp.30-31) [in Ukrainian].

30. Anatyshuk L.I., Kobylianskyi R.R., Konstantynovych I.A., Lysko V.V., Pugantseva O.V., Rozver Yu.Yu., Tiumentsev V.A. (2016). Calibration bench for thermoelectric converters of heat flux. *J. Thermoelectricity*, 5, 71-79.

Submitted 16.10.2018.

**Анатичук Л.І.** акад. НАН України<sup>1,2</sup>  
**Пасечнікова Н.В.** док. мед наук, професор,  
член – кореспондент НАМН України<sup>3</sup>  
**Науменко В.О.** док. мед наук, професор<sup>3</sup>  
**Задорожний О.С.** канд. мед. наук<sup>3</sup>  
**Гаврилюк М.В.,** канд. фіз.-мат. наук<sup>1,2</sup>  
**Кобилянський Р.Р.** канд. фіз.-мат. наук<sup>1,2</sup>

<sup>1</sup>Інститут термоелектрики НАН і МОН України,  
вул. Науки, 1, Чернівці, 58029, Україна,  
e-mail: anatysh@gmail.com;

<sup>3</sup>ДУ "Інститут очних хвороб та тканинної терапії ім. В.П.  
Філатова НАМН України", Французький бульвар, 49/51,  
Одеса, 65000, Україна.

## ТЕРМОЕЛЕКТРИЧНИЙ ПРИЛАД ДЛЯ ВИЗНАЧЕННЯ ТЕПЛООВОГО ПОТОКУ З ПОВЕРХНІ ОЧЕЙ

У роботі наведено конструкцію та технічні характеристики вперше розробленого термоелектричного приладу для визначення теплового потоку з поверхні очей. Прилад є перспективним для діагностики та моніторингу офтальмологічних захворювань, що дає можливість підвищити ефективність ранньої діагностики патології органу зору, спостерігати в динаміці за розвитком патологічного процесу в структурах ока, а також підвищити ефективність лікування гострих і хронічних захворювань ока. Розроблений термоелектричний прилад дозволяє здійснювати моніторинг теплового та температурного стану поверхні очей у режимі реального часу, є оригінальним та не має світових аналогів. Бібл. 29, Рис. 8, Табл. 2.

**Ключові слова:** термоелектричний прилад, тепловий потік, офтальмологія.

**Анатычук Л.И.** акад. НАН Украины<sup>1,2</sup>  
**Пасечникова Н.В.** док. мед наук, професор,  
член – кореспондент НАМН Украины<sup>3</sup>  
**Науменко В.О.** док. мед наук, професор<sup>3</sup>  
**Задорожний О.С.** канд. мед. наук<sup>3</sup>  
**Гаврилюк Н.В.,** канд. фіз.-мат. наук<sup>1,2</sup>  
**Кобылянский Р.Р.** канд. фіз.-мат. наук<sup>1,2</sup>

<sup>1</sup>Институт термоэлектричества НАН и МОН Украины  
ул. Науки, 1, Черновцы, 58029, Украина  
e-mail: anatysh@gmail.com;

<sup>3</sup>ГУ "Институт глазных болезней и тканевой терапии им.  
В.П. Филатова НАМН Украины", Французский бульвар, 49/51,  
Одесса, 65000, Украина.

## ТЕРМОЭЛЕКТРИЧЕСКИЙ ПРИБОР ДЛЯ ОПРЕДЕЛЕНИЯ ТЕПЛОВОГО ПОТОКА С ПОВЕРХНОСТИ ГЛАЗ

В работе приведена конструкция и технические характеристики впервые разработанного термоэлектрического прибора для определения теплового потока с поверхности глаз. Прибор является перспективным для диагностики и мониторинга офтальмологических заболеваний, дающего возможность повысить эффективность ранней диагностики патологии органа зрения, наблюдать в динамике за развитием патологического процесса в структурах глаза, а также повысить эффективность лечения острых и хронических заболеваний глаза. Разработанный термоэлектрический прибор позволяет осуществлять мониторинг теплового и температурного состояния поверхности глаз в режиме реального времени, является оригинальным и не имеет мировых аналогов. Библ. 29, Рис.8, Табл. 2.

**Ключевые слова:** термоэлектрический прибор, тепловой поток, офтальмология.

### References

1. Chebyshev N.V., Guzikova G.S., Lazareva Yu.B., Larina S.N. (2011). *Biologiya. Spravochnik.- 2 izdaniie, ispravlennoie i dopolnennoie [Biology. Handbook. 2<sup>nd</sup> ed., revised and enlarged]*. Moscow: GEOTAR-Media [in Russian].
2. Tsarev A.V. (2014). Tselevoi temperaturnyi menedzhment v klinicheskoi praktike intensivnoi terapii kriticheskikh sostoianii [Special-purpose temperature management in the clinical practice of intensive care of critical states]. *Meditsina neotlozhnykh sostoianii – Medicine of Emergencies*, 7, 186-191.
3. Kubarko A.I. (2014). *Normalnaia fiziologiya: Uchebnik. V 2 chastiakh. Chast 2. [Normal physiology: textbook. In 2 parts. Part 2]*. A.I.Kubarko (Ed.). Minsk: Vysheishaiia shkola [in Russian].
4. Dekusha L.V. (2016). Sredstva teplometrii na base termoelektricheskikh preobrazovatelei teplovogo potoka [Heat metering means based on thermoelectric heat flux converters]. *Doctor's thesis (Engineering)*.
5. Grishchenko T.G., Dekusha L.V., Vorobiov L.I. (2017). *Teplometriia: teoriia, metrologiya, praktika. Monografiia v 3 knigakh [Heat flow metering: theory, metrology, practice. Monograph in three books]*. T.G.Grishchenko (Ed.). *Kniga 1: Metody i sredstva izmereniia teplovogo potoka [Book 1: Methods and facilities of heat flow measurement]*. Kyiv: Institute of Engineering Thermophysics [in Russian].
6. Anatyshuk L.I., Pasechnikova N.V., Zadorozhnyi O.S., Nazaretian R.E., Mirnenko V.V., Kobylanskiy R.R., Havryliuk N.V. (2015). Originalnoie ustroistvo i podkhody k izucheniiu raspredeleniia temperatury v razlichnykh otdelakh glaza [Original device and approaches to studying temperature distribution in different sections of eye]. *Ophtalmologicheskii zhurnal - J. Ophthalmology*, 6, 50-53 [in Russian].
7. Gischuk V.S. (2012). Electronic recorder of signals from human heat flux sensors. *J.Thermoelectricity*, 4, 105-108.
8. Gischuk V.S. (2013). Electronic recorder with processing signals from heat flux thermoelectric

- sensor. *J. Thermoelectricity*, 1, 82-86.
9. Gischuk V.S. (2013). Modernized device for human heat flux measurement. *J. Thermoelectricity*, 2, 91-95.
  10. Gischuk V.S., Kobylanskyi R.R., Cherkez R.G. (2014). Bahatokanalnyi prylad dlia vymiriuvannia temperatury i hustyny teplovykh potokiv [Multichannel device for temperature and heat flux density measurement]. *Naukovy visnyk Chernivetskoho Universytetu. Fizyka. Elektronika – Scientific Bulletin of Chernivtsi University. Physics. Electronics*, 3 (1), 96-100 [in Ukrainian].
  11. Kobylanskyi R.R., Boichuk V.V. (2015). Vykorystannia termoelektrychnykh teplomiriv u medychnii diagnostytsi [The use of thermoelectric heat flow meters in medical diagnostics]. *Naukovy visnyk Chernivetskoho Universytetu. Fizyka. Elektronika – Scientific Bulletin of Chernivtsi University. Physics. Electronics*, 4 (1), 90-96 [in Ukrainian].
  12. Anatyshchuk L.I., Ivashchuk O.I., Kobylanskyi R.R., Postevka I.D., Bodiaka V.Yu., Hushul I.Ya. (2016). Thermoelectric device for temperature and heat flux density measurement “Altec-10008”. *J. Thermoelectricity*, 1, 76-84.
  13. Anatyshchuk L.I., Yuryk O.Ye., Kobylanskyi R.R., Roi I.V., Fishchenko Ya.V., Slobodianiuk N.P., Yuryk N.Ye., Duda B.S. (2017). Thermoelectric device for the diagnosis of inflammatory processes and neurological manifestations of vertebral osteochondrosis. *J. Thermoelectricity*, 3, 54-67.
  14. Anatyshchuk L.I., Kobylanskyi R.R., Cherkez R.G., Konstantynovych I.A., Hoshovskyi V.I., Tiumentsev V.A. (2017). Termoelektricheskoe ustroistvo s elektronnyim blokom upravleniia dlia diagnostiki vospalitelnykh protsessov v organizme cheloveka [Thermoelectric device with electronic control unit for diagnostics of inflammatory processes in human organism]. *Tekhnologiya i konstruirovaniye v elektronnoi apparature*, 6, 44-48 [in Russian].
  15. Anatyshchuk L.I. (1979). Termoelementy i termoelektricheskiye ustroystva: Spravochnik [Thermoelements and thermoelectric devices: Handbook]. Kyiv: Naukova dumka [in Russian].
  16. Gerashchenko O.A. (1971). *Osnovy teplometrii [Fundamentals of heat flow metering]*. Kyiv: Naukova dumka [in Russian].
  17. Ladyka R.B., Dakaliuk O.N., Bulat L.P., et al. (1996). Primeneniye poluprovodnikovyykh teplomerov v diagnostike i lechenii [The use of semiconductor heat flow meters in diagnostics and treatment]. *Meditssinskaya tekhnika – Biomedical Engineering*, 6, 36 – 37 [in Russian].
  18. Anatyshchuk L.I., Ivashchuk O.I., Kobylanskyi R.R., Postevka I.D., Bodiaka V.Yu., Gushul I.Ya., Chuprovska Yu.Ya. (2018). Pro vplyv temperatury navkolyshniho seredovyscha na pokazy termoelektrychnykh sensoriv medychnoho pryznachennia [On the effect of ambient temperature on the readings of medical purpose thermoelectric sensors]. *Sensorna elektronika i mikrosystemni tekhnologii – Sensor Electronics and Microsystem Technologies*, 15 (1), 17-29 [in Ukrainian].
  19. Mapstone R. (1968). Determinants of corneal temperature. *Brit. J. Ophthalmol.*, 52, 729-741.
  20. Tan J.H., Ng E.Y.K., Acharya U.R., Chee C. (2009). Infrared thermography on ocular surface temperature: A review. *Infrared Phys. Techn.*, 52, 97–108.
  21. Zadorozhnyy O.S., Guzun O.V., Bratishko A.Iu., et al. (2018). Infrared thermography of external ocular surface in patients with absolute glaucoma in transscleral cyclophotocoagulation: a pilot study. *J. Ophthalmol.*, 2, 23-28.
  22. Galassi F., Giambene B., Corvi A., et al. (2007). Evaluation of ocular surface temperature and retrobulbar haemodynamics by infrared thermography and colour Doppler imaging in patients with glaucoma. *British Journal of Ophthalmology*, 91, 878–881.
  23. Sodi A.A., Giambene B.A.D., Falaschi G.B., et al. (2007). Ocular surface temperature in central retinal vein occlusion: preliminary data. *European Journal of Ophthalmology*, 17, 755–759.

24. *Application for utility model № u201901535 of 15.02.2019.* (2019). Anatyshuk L.I., Kobylianskyi R.R., Bukharaieva N.R., Havryliuk M.V., Tiumentsev V.A. Termoelektrychnyi pryklad dlia vymiriuvannia temperatury i teplovoho potoku z poverhni ochei [Thermoelectric device for measurement of temperature and heat flux from the surface of eyes] [in Ukrainian].
25. *Patent of Ukraine № 9321* (2014). Anatyshuk L.I., Konstantynovych I.A. Method for manufacturing thermoelectric microthermopile [in Ukrainian].
26. *Patent of Ukraine № 117719* (2017). Anatyshuk L.I., Kobylianskyi R.R. (2017). Method for manufacturing thermoelectric microthermopile [in Ukrainian].
27. Anatyshuk L.I., Kobylianskyi R.R., Konstantynovych I.A., Kuz R.V., Manik O.M., Nitsovych O.V., Cherkez R.G. (2016). Technology for manufacturing thermoelectric microthermopiles. *J. Thermoelectricity*, 6, 49-54.
28. Kim N.R. (2011). Comparison of Goldmann applanation tonometer, noncontact tonometer, and TonoPen XL for intraocular pressure measurement in different types of glaucomatous, ocular hypertensive, and normal eyes. *Curr. Eye Res.*, 36, 295-300.
29. Anatyshuk L.I., Kobylianskyi R.R., Konstantynovych I.A. (2014). Hraduiuvannia termoelektrychnykh sensoriv teplovoho potoku [Calibration of thermoelectric heat flow sensors]. *Trudy XV Mizhnarodnoi naukovo-praktychnoi konferentsii "Suchasni informatsiini ta elektronni tekhnologii" – Proc. of International scientific and practical conference "Modern Information and Electronic Technologies"* (Ukraine, Odessa, May 26-30, 2014). (Vol.2, pp.30-31) [in Ukrainian].
30. Anatyshuk L.I., Kobylianskyi R.R., Konstantynovych I.A., Lysko V.V., Pugantseva O.V., Rozver Yu.Yu., Tiumentsev V.A. (2016). Calibration bench for thermoelectric converters of heat flux. *J. Thermoelectricity*, 5, 71-79.

Submitted 16.10.2018.





*P.D. Mykytiuk*

**P.D. Mykytiuk.** *Cand.Sc. (Physics and Mathematics)*<sup>1,2</sup>

**O.Yu. Mykytiuk.** *Cand.Sc. (Physics and Mathematics), Assistant Professor*<sup>3</sup>



*O.Yu. Mykytiuk.*

<sup>1</sup>Institute of Thermoelectricity of the NAS and MES of Ukraine, 1, Nauky str, Chernivtsi, 58029, Ukraine; e-mail: [anatykh@gmail.com](mailto:anatykh@gmail.com);

<sup>2</sup>Yuriy Fedkovych Chernivtsi National University, 2, Kotsiubynsky str., Chernivtsi, 58012, Ukraine;

<sup>3</sup>Higher State Educational Institution of Ukraine "Bukovinian State Medical University", 2, Theatre Square, Chernivtsi, 58002, Ukraine

---

## IN REFERENCE TO THE CHOICE OF THERMOCOUPLE MATERIAL FOR METROLOGICAL-PURPOSE THERMAL CONVERTERS

---

*Peculiarities of application of thermoelectric material (TEM) in the design of metrological-purpose thermoelectric converters (TC) are considered. Comparison of mathematical expressions for the basic parameters of various thermoelectric devices showed that there are significant differences in the choice of TEM for the TC thermocouple. In particular, the maximum thermoelectric figure of merit  $Z$  for TC TEM is not always decisive in providing the best TC parameters. For TC, in addition to the high values of  $Z$ , the maximum values of thermoelectric material thermoEMF and the rational use of heat released by the TC heater (so-called "constructive factor") are important. Tabl. 2, Fig. 2, Bibl. 6.*

**Key words:** thermoelectric converter, heater, thermocouple, sensitivity, thermoelectric material.

### Introduction

Creation of high-precision instruments for measuring AC values is an important task for modern thermoelectric instrumentation. The increase in the sensitivity of such devices is directly related to the increase in the sensitivity of the metrological-purpose thermoelectric converter (TC) [1].

The increase in the TC sensitivity is mainly achieved by improving parameters of thermoelectric material (TEM). However, along with the search for new TEM and quality improvement of known materials, the possibilities of increasing the figure of merit ( $z$ ) which at this stage are practically exhausted, there are opportunities for enhancement of the TC parameters due to their constructive improvements, optimization of thermal operating modes in order to increase the efficiency of using the heat released by the TC heater. The problem of optimal application of TEM is still valid exactly for the TC, since in this case there is a significant difference from the use of TEM for other thermoelectric devices - thermogenerators (TEG), radiation detectors, coolers, etc.

Therefore, an important task and purpose of this work is to establish the characteristics of using TEM exactly during the development of the TC.

### **Distinctions in the choice of TEM for different types of thermoelectric devices**

It is known [2] that the use of semiconductor material for thermal into electric energy converters has led to a drastic improvement of their efficiency and created good prerequisites for the widespread use of such converters. To a much lesser extent, the possibilities of improving the parameters of metrological-purpose TC have been studied. Often, attempts to use TEM developed for energy applications did not meet with the expected success. This is due to the fact that TEM intended for measuring techniques and metrology must meet a number of additional requirements that are not taken into account when developing TEM for other applications, such as TEG, thermoelectric coolers (TEC) and thermoelectric heating devices.

When choosing TEM for the TC thermocouple, TEM optimization criteria are modified. In TEG, TEC and devices for thermoelectric heating, the main parameter determining their quality is efficiency. For TEG, the efficiency ( $\eta_{max}$ ) in the maximum power mode is determined by the expression [3]:

$$\eta_{max} = \frac{1}{2} \frac{T_1 - T_2}{T_1 + \frac{2}{z} - \frac{1}{4}(T_1 - T_2)}, \quad (1)$$

where  $T_1$  and  $T_2$  are the temperatures of the hot and cold junctions, respectively,  $z$  is thermoelectric figure of merit of TEM, which is determined by the formula:

$$z = \frac{\alpha^2 \sigma}{x}, \quad (2)$$

where  $\alpha$  is the Seebeck coefficient,  $\sigma$  is electric conductivity,  $x$  is thermal conductivity.

To characterize TEC, use is made of coefficient of performance  $\varepsilon_{max}$  which is found from Eq.[4]:

$$\varepsilon_{max} = \frac{T_2}{T_1 - T_2} \cdot \frac{\sqrt{1 + 0.5z(T_1 + T_2)} - T_1/T_2}{\sqrt{1 + 0.5z(T_1 + T_2)} + T_1/T_2}. \quad (3)$$

Heating coefficient  $K_T$  for thermoelectric heating devices is determined as follows [5]:

$$K_T = \frac{1}{4} \left( \frac{T_2}{2} - \frac{T_1 - T_2}{zT_2} \right). \quad (4)$$

Formulae (1), (2), (3), (4) remain valid no matter which type of device from the above mentioned is considered. In these formulae, the main parameter characterizing the efficiency of the device is  $z$ . Therefore, the main requirement for TEM is to achieve the maximum possible value of  $z$ . Another, no less important, requirement is the preservation of the figure of merit of TEM in a wide temperature range.

Only for a small group of measuring devices - radiation detectors, microcalorimeters, thermocouples – the ratios were found, from which the relationship between the TEM parameters and the main characteristics of the device is determined taking into account their ability to reach the boundary values limited only by thermal and temperature noise [5].

The main parameters that describe radiation detectors are the ability to detect the signal and the volt-watt sensitivity. For microcalorimeters, similar parameters are introduced. These parameters have long been investigated and described in [3, 4]. Mathematical expressions for the determination of these parameters do not take into account a number of additional factors inherent in various thermoelectric

devices. Expressions for real constructions are much more complicated [5]. In them, various combinations include the TEM parameters:  $\alpha$ ,  $\sigma$ ,  $x$ . In addition to the requirements for achieving maximum sensitivity, a number of additional requirements are put forward to the TEM for the TC, namely stability in the given temperature range, high temporal stability, and others.

It can be seen from the above that the requirements for TEM intended for TEG, TEO and heat pumps are significantly different from those for TEM intended for the design of the TC as measuring instruments. For example, the figure of merit of TEM is decisive for a TEG, and its efficiency at small values of  $zT$  depends on the figure of merit by a law close to linear. Whereas for measuring devices, the expressions into which  $z$  enters are determined by a power dependence [6] and other coefficients. For this reason, the conditions for optimizing TEM to achieve the maximum value of sensitivity, speed, etc., will differ from each other. In addition, there is a difference in the requirements for TEM and for various measuring devices [7]. Because of this, a universal TEM cannot be created that is equally suitable for different thermoelectric products.

In the measuring system using a TC, the measurement accuracy of these magnitudes of alternating current completely depends on the TC quality, which is largely determined by the properties of TEM. However, the requirements for TEM to achieve the maximum possible TC parameters, are either not fully investigated and defined, or selected from considerations that do not always follow from the physical principles of the TC, and are due to operational approaches. In this connection, it is often difficult to choose the optimal variant of TEM for the TC.

### **The relation between the basic TC parameters and the properties of TEM**

To determine the methodology for the selection and optimization of TEM for the TC, we consider the main TC parameters.

The most influential parameters describing the TC properties are those that determine the relationship between the initial values (current, voltage) and output (thermocouple thermoEMF, thermoelectric current, power in the thermocouple circuit). To describe this relationship, the following is adopted in the literature [8]:

a) sensitivity  $S_I = \partial E_T / \partial I_H$ , as the relation of gain in thermocouple thermoEMF  $E_T$  to gain in current  $I_H$  through the heater;

b) sensitivity  $S_U = \partial E_T / \partial U_H$ , as the relation of gain in thermocouple thermoEMF  $E_T$  to gain in voltage  $U_H$ ;

c) sensitivity  $S_W = \partial E_T / \partial P_H$ , as the relation of  $E_T$  to power  $P_H$ , which is dissipated by the heater.

To determine  $S_I$  and  $S_U$ , the following formulae are used:

$$S_I = 2K_1 I_H, \quad (5)$$

$$S_U = 2K_2 U_H. \quad (6)$$

Conversion factors  $K_1$  and  $K_2$  are related by:

$$K_1 = K_2 R_H^2, \quad (7)$$

where  $R_H$  is the resistance of the heater.

Conversion factor  $K_I$  can be approximately written as:

$$K_1 = \frac{\alpha R_H}{S \lambda}, \quad (8)$$

where  $S$  is heat exchange surface;  $\lambda$  is heat-exchange coefficient.

Expressions (5) and (6) for the sensitivity  $S_I$  and  $S_U$  include only one parameter of TEM, namely  $\alpha$ .

Formulae (5) and (7) are valid only for some types of TC, where heat removed by the heater is much larger than heat removed by the thermocouple.

In most TC designs, the thermocouple and the heater are similar in geometric sizes, as well as in thermophysical parameters of materials. In this case, as shown in [8], the thermal conductivity of the thermocouple affects the temperature distribution along the heater. Therefore, the expressions (5) and (6) do not fully take into account the physical processes taking place in the TC.

The volt-watt sensitivity for small temperature differences is equal to [8]:

$$S_W = \frac{\alpha r_T}{S\lambda}, \quad (9)$$

where  $r_T$  is thermal resistance of thermocouple which is determined by the formula:

$$r_T = \frac{l_T}{\kappa S_T}, \quad (10)$$

where  $l_T$  and  $S_T$  are the length and cross-section of thermocouple leg.

The volt-watt sensitivity is related to conversion factor  $K_1$  by the relationship:

$$S_W = \frac{K_1}{R_H}. \quad (11)$$

With account of (11) the general expression for the TC sensitivity can be written as:

$$S_I = \frac{\alpha r_T R_H I_H}{S\lambda}. \quad (12)$$

Thus, expression (12) determines the relation between the basic parameters of thermocouple. It can be seen from formula (12) that it is possible to determine with greater certainty the dependence of the TC properties on the TEM parameters, however, the sensitivity does not characterize them in full.

To fully determine the dependence of the TC parameters on the TEM properties, we introduce a sensitivity parameter

$$S_\eta = \frac{P}{P_H}, \quad (13)$$

which is the ratio of the power obtained on the thermoelement electrical load to the AC electrical power supplied to the TC. To find  $S_\eta$ , consider the equivalent circuit of a contactless TC with a load  $r_H$ , Fig. 1

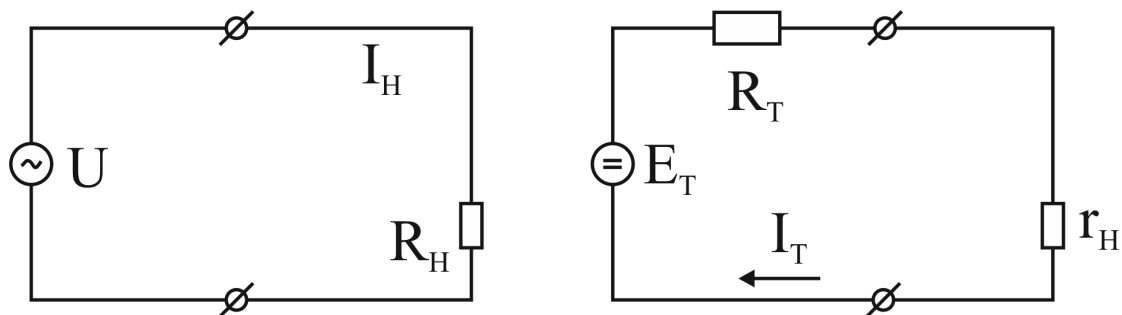


*Fig. 1. Circuit of a contactless TC with a load.*

If the resistance load is matched with the thermocouple load ( $r_H = R_T$ ), then the TC will work in a mode close to maximum efficiency mode and in this case

$$S_{\eta} = \frac{E_T^2}{4R_T R_H I_H^2}. \quad (14)$$

On the other hand, the volt-watt sensitivity  $S_{\eta}$  can be written through thermophysical parameters of thermocouple TEM in the form:

$$S_{\eta} = \frac{z(T_1 - T_2)}{4F_p}, \quad (15)$$

where  $F_p$  is coefficient characterizing the rationality of using heat which is released by the heater in the TC. In so doing

$$F_p = \frac{2P_H r_T}{T_1 - T_2}. \quad (16)$$

Formula (15) according to [3] corresponds to the expression for the efficiency of TEG under the condition of small temperature differences in the thermocouple and provided that TEM parameters for the thermocouple do not depend on temperature. Moreover, the expression for  $S_{\eta}$  can be written [5] in the form:

$$S_{\eta} = \eta = \frac{(T_1 - T_2)\sqrt{1 + zT} - 1}{(T_1\sqrt{1 + zT} - T/T_1)F_p}. \quad (17)$$

From analysis of (15) and (17) it follows that the main operational parameters of TC are set by the thermoelectric figure of merit of the TEM  $z$ , the operating differential  $\Delta T = T_1 - T_2$  and the coefficient  $F_p$  depending on the TC design.

Therefore, an increase in the TC sensitivity can be achieved by increasing  $z$  and  $\Delta T$ , as well as by decreasing the coefficient  $F_p$ . However, an increase of  $\Delta T$  unambiguously impairs the TC parameters: the quadraticity of the conversion (the  $K_1$  coefficient in formula (5) becomes temperature dependent), overcurrent capability, time stability due to aging of the heater metal and acceleration of diffusion processes on thermocouple junctions. Therefore, a significant increase is inappropriate.

Evaluation of the rational TC design, taking into account the possibility of reducing heat losses due to the vacuumization of the TC case or filling it with inert gases with low thermal conductivity (eg, xenon) [10,11], the optimum ratio of the geometric dimensions of the heater and the thermocouple, the use of a variable cross-section heater [12], which optimizes the use of heat from the heater, etc., significantly improves the TC parameters, but the main increase in sensitivity is still achieved by using TEM with the maximum value of  $z$  and thermoelectric coefficient  $\alpha$ .

## Conclusion

The combination of various options for improving the TC parameters with the use of effective materials based on  $Bi_2Te_3$  creates favorable opportunities for the development of TC with the limit values of sensitivity.

## References

1. Anatyshuk L.I., Kuz R.V., Taschuk D.D. (2015). Differential thermoelectric AC converter in the non-simultaneous comparison mode. *J. Thermoelectricity*, 4, 77–82.

2. Anatyshchuk L.I. (1979). *Termoelementy i termoelektricheskiie ustroistva [Thermoelements and thermoelectric devices]*. Kyiv: Naukova dumka [in Russian].
3. Okhotin A.S., Yefremov A.A., Okhotin V.S. (1971). *Termoelektricheskiie generatory [Thermoelectric generators]*. Moscow: Atomizdat [in Russian].
4. Kolenko E.A. (1967). *Termoelektricheskiie okhlazhdaiushchie pribory [Thermoelectric cooling devices]*. Leningrad: Nauka [in Russian].
5. Anatyshchuk L.I. (2003). *Termoelektricheskiie preobrazovateli energii. Tom II. [Thermoelectric power converters. Vol.II]* Kyiv-Chernivtsi: Institute of Thermoelectricity [in Russian].
6. Shol J., Marfon I., Monsh M., et al. (1969). *Priiomniki infrakrasnogo izlucheniia [Infrared radiation receivers]*. Moscow: Mir [Russian transl].
7. Ando E. (1974). Radiation thermocouples with  $(\text{BiSb})_2(\text{TeSe})_3$ . *Jap. J. Appl. Phys.* 13 (5), 363-369.
8. Rozhdestvenskaia T.B. (1964). Metrologicheskiie raboty v oblasti izmereniia toka, napriazheniia i moshchnosti pri povyshennykh chastotakh [Metrological works in the field of measuring current, voltage and power at elevated frequencies]. *Trudy Institutov Goskomiteta - Proceedings of State Committee Institutes*, 76 (136), 65-75 [in Russian].
9. Mykytiuk P.D., Mykytiuk O.Yu. (2018). Impact of thermocouple on temperature distribution in the heater of measuring thermal converter. *J. Thermoelectricity*, 1, 64–59.
10. Anatyshchuk L.I. (2008). *Fizika termoelektrichestva. Tom I [Physics of thermoelectricity. Vol.I]* [in Russian].
11. Mykytiuk P.D. (2017). Factors of influence on the accuracy of thermal converters. *J. Thermoelectricity*, 5, 76–83.
12. Mykytiuk P.D., Mykytiuk O.Yu. (2018). Temperature distribution in a heater with a resistance variable along its length in a thermoelectric converter. *J. Thermoelectricity*, 2, 79–74.

Submitted 08.11.2018

**Микитюк П.Д.** канд. фіз.-мат. наук<sup>1,2</sup>  
**Микитюк О.Ю.** канд. фіз.-мат. наук, доцент<sup>3</sup>

<sup>1</sup>Інститут термоелектрики НАН і МОН України,  
вул. Науки, 1, Чернівці, 58029, Україна,  
*e-mail: anatysh@gmail.com;*

<sup>2</sup>Чернівецький національний університет  
імені Юрія Федьковича, вул. Коцюбинського 2,  
Чернівці, 58012, Україна,

<sup>3</sup>Вищий державний навчальний заклад України  
«Буковинський державний медичний університет»,  
Театральна площа, 2, Чернівці, 58012, Україна

## **ДО ПИТАННЯ ВИБОРУ МАТЕРІАЛУ ТЕРМОПАРИ ДЛЯ ТЕРМОПЕРЕТВОРЮВАЧІВ МЕТРОЛОГІЧНОГО ПРИЗНАЧЕННЯ**

*Розглянуто особливості застосування термоелектричного матеріалу (ТЕМ) при конструюванні термоелектричних перетворювачів (ТП) метрологічного призначення. Порівняння математичних виразів для основних параметрів різних термоелектричних пристроїв показало, що існують суттєві відмінності у виборі ТЕ для термопари ТП. Зокрема, максимальна термоелектрична ефективність ТЕМ Z для ТП не завжди є визначальною у забезпеченні найкращих параметрів ТП. Для ТП, крім високих значень Z, важливими є максимальні значення термоЕРС ТЕМ та раціональне використання тепла, що виділяється нагрівником ТП (так званий "конструктивний фактор"). Бібл. 12, рис. 1.*

**Ключові слова:** термоелектричний перетворювач, нагрівник, термопара, чутливість, термоелектричний матеріал.

**Микитюк П.Д.** канд. физ.-мат. наук<sup>1,2</sup>  
**Микитюк О.Ю.** канд. физ.-мат. наук, доцент<sup>3</sup>

<sup>1</sup>Институт термоэлектричества НАН и МОН Украины,  
ул. Науки, 1, Черновцы, 58029, Украина,  
*e-mail: anatyuch@gmail.com;*

<sup>2</sup>Черновицкий национальный университет  
имени Юрия Федьковича, ул. Коцюбинского 2,  
Черновцы, 58012, Украина

<sup>3</sup>Высшее государственное учебное заведение Украины  
«Буковинский государственный медицинский университет»,  
Театральная площадь, 2, Черновцы, 58002, Украина

## **К ВОПРОСУ О ВЫБОРЕ МАТЕРИАЛА ТЕРМОПАРЫ ДЛЯ ТЕРМОПРЕОБРАЗОВАТЕЛЕЙ МЕТРОЛОГИЧЕСКОГО НАЗНАЧЕНИЯ**

*Рассмотрены особенности применения термоэлектрического материала (ТЭМ) при конструировании термоэлектрических преобразователей (ТП) метрологического назначения. Сравнение математических выражений для основных параметров разных термоэлектрических устройств показало, что существуют существенные отличия в выборе ТЭМ для термопары ТП. В частности, максимальная термоэлектрическая эффективность ТЭМ z для ТП не всегда является определяющей с точки зрения обеспечения наилучших параметров ТП. Для ТП, помимо высоких значений z, важны максимальные значения термоЭДС ТЭМ и рациональное использование тепла, выделяемого нагревателем ТП (так называемый "конструктивный фактор"). Библ. 12, Рис. 1.*

**Ключевые слова:** термоэлектрический преобразователь, нагреватель, термопара, чувствительность, термоэлектрический материал.

## References

1. Anatyshuk L.I., Kuz R.V., Taschuk D.D. (2015). Differential thermoelectric AC converter in the non-simultaneous comparison mode. *J. Thermoelectricity*, 4, 77–82.
2. Anatyshuk L.I. (1979). *Termoelementy i termoelektricheskiie ustroistva [Thermoelements and thermoelectric devices]*. Kyiv: Naukova dumka [in Russian].
3. Okhotin A.S., Yefremov A.A., Okhotin V.S. (1971). *Termoelektricheskiie generatory [Thermoelectric generators]*. Moscow: Atomizdat [in Russian].
4. Kolenko E.A. (1967). *Termoelektricheskiie okhlazhdaiushchie pribory [Thermoelectric cooling devices]*. Leningrad: Nauka [in Russian].
5. Anatyshuk L.I. (2003). *Termoelektricheskiie preobrazovateli energii. Tom II. [Thermoelectric power converters. Vol.II]* Kyiv-Chernivtsi: Institute of Thermoelectricity [in Russian].
6. Shol J., Marfon I., Monsh M., et al. (1969). *Priiomniki infrakrasnogo izlucheniia [Infrared radiation receivers]*. Moscow: Mir [Russian transl].
7. Ando E. (1974). Radiation thermocouples with  $(\text{BiSb})_2(\text{TeSe})_3$ . *Jap. J. Appl. Phys.* 13 (5), 363–369.
8. Rozhdestvenskaia T.B. (1964). Metrologicheskiie raboty v oblasti izmereniia toka, napriazheniia i moshchnosti pri povyshennykh chastotakh [Metrological works in the field of measuring current, voltage and power at elevated frequencies]. *Trudy Institutov Goskomiteta - Proceedings of State Committee Institutes*, 76 (136), 65–75 [in Russian].
9. Mykytiuk P.D., Mykytiuk O.Yu. (2018). Impact of thermocouple on temperature distribution in the heater of measuring thermal converter. *J. Thermoelectricity*, 1, 64–59.
10. Anatyshuk L.I. (2008). *Fizika termoelektrichestva. Tom I [Physics of thermoelectricity. Vol.I]* [in Russian].
11. Mykytiuk P.D. (2017). Factors of influence on the accuracy of thermal converters. *J. Thermoelectricity*, 5, 76–83.
12. Mykytiuk P.D., Mykytiuk O.Yu. (2018). Temperature distribution in a heater with a resistance variable along its length in a thermoelectric converter. *J. Thermoelectricity*, 2, 79–74.

Submitted 08.11.2018





Zaporov S.F.

**S.F. Zaporov**<sup>1</sup>  
**T.V. Zakharchuk**<sup>1,2</sup>



Zakharchuk T.V.

Institute of Thermoelectricity of the NAS  
and MES Ukraine,  
Nauky str., Chernivtsi, 58029, Ukraine  
*e-mail: anatykh@gmail.com*  
<sup>2</sup>Yuriy Fedkovich Chernivtsi National University,  
2, Kotsiubynsky str., Chernivtsi, 58012, Ukraine

## **DEVICE FOR PRODUCING RECTANGULAR SAMPLES OF THERMOELECTRIC MATERIAL**

---

*This paper presents methods and equipment for mechanical cutting of thermoelectric material with the use of free abrasive and by the wires with fixed diamond grains. Trial cuts have shown that the accuracy and most sparing mode of thermoelectric material processing is achieved by cutting tool with the use of tungsten wire of diameter 0.11- 0.14 mm. Bibl. 3, Fig. 9, Tabl. 2.*

**Key words:** cutting device, free abrasive cutting tool, bound abrasive cutting tool

### **Introduction**

The process of thermoelectric material cutting has its unique features, so direct use of up-to-date standard equipment for cutting of semiconductors is not always justified as applied to thermoelectric material.

Cutting technology is an important part of thermoelectric materials processing, cutting quality having a considerable impact on the results and parameters of thermoelectric devices.

The purpose of the work is to study under laboratory conditions cutting of thermoelectric material on a small-sized desktop machine “Altec–13009” for the case when productivity is of minor importance and there is an opportunity to use two methods of thermoelectric material cutting by a tool with free and bound abrasive.

### **Cutting with free abrasive**

Prior to cutting, a billet must be firmly fastened on a fixed base (working table). The most common method is sticking by means of various materials, such as wax, rosin, shellac, glyptal bond.

After machining, the cut samples are washed from picein, slightly heated in specially selected solvents.

Destruction of brittle thermoelectric material on treatment with free abrasive is as follows. Abrasive particles in the form of suspension (boron carbide  $B_4C_3$ , silicon carbide  $SiC$ , aluminum oxide  $Al_2O_3$ ) are fed into cutting zone. Being indented into the surface of processed thermoelectric material, they cause formation of microcracks therein. In the process of treatment these microcracks become larger and propagate deep from the surface. Subsequent processing results in creation of a network of cracks which, when closed, cause chipping out of separate parts of thermoelectric material. The

detached parts are removed from the surface of the initial sample. Thus, there is a layer by layer removal of material and initial sample machining. The presence of liquid facilitates the process of treatment, since abrasive powder is suspended in the liquid and uniformly distributed therein. This, in turn, allows distribution of abrasive grains across the surface to be treated. Abrasive suspension removes heat from cutting zone well enough and does not require special cooling (Fig. 1).

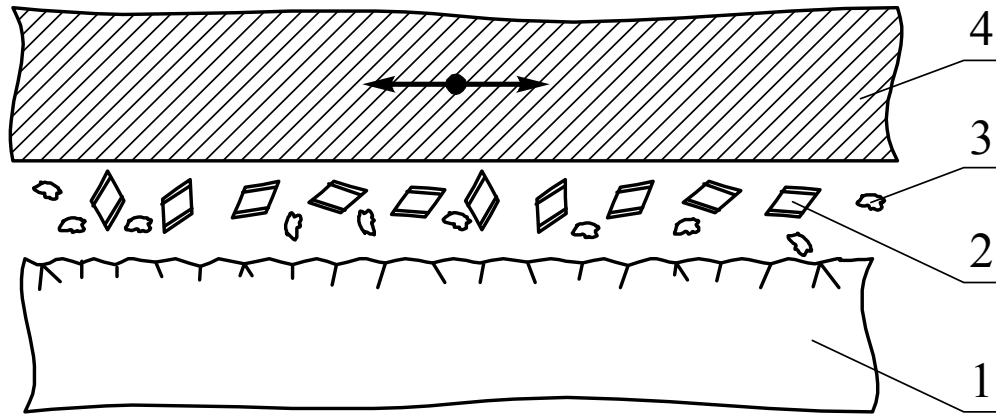


Fig. 1 Schematic of cutting with free abrasive  
1 – thermoelectric material; 2 – abrasive grains;  
3 – detached parts of thermoelectric material; 4 – tool.

Replaceable wire saw, used as cutting tool, is a set of tungsten wires wound on a frame with maximum tension at a pitch assigned by the grooves of spacer bars (Fig 2).

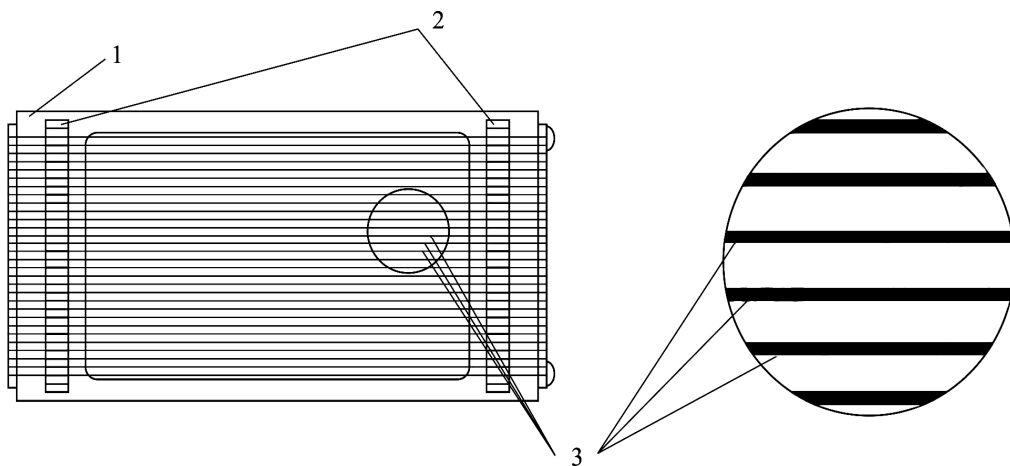


Fig. 2. Cutting tool with the use of free abrasive  
1 – tool; 2 – spacer bars; 3 – wires.

Cutting tool with the use of free abrasive allows simultaneous cutting across the plane of the plate at an accuracy of  $\pm 0.01\text{mm}$ . However, the main advantage of wire cutting is that this method enables one to obtain processed samples with minimum violations of crystal structure arising in the area of contact between the tool and the processed samples of thermoelectric material (the thickness of damaged subsurface layer is  $5 \div 15 \mu\text{m}$ ). However, it also has its limitations (the height of the plates does not exceed  $0.5\text{mm}$ ), which do not allow its broad and efficient use for cutting large billets. Therefore, this method is used for low depth cutting under laboratory conditions (Fig. 3).

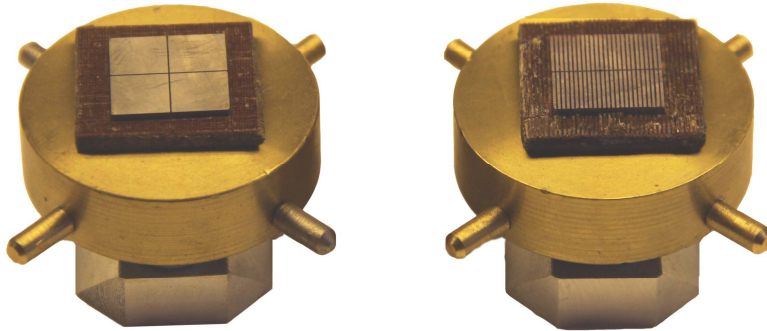


Fig. 3 Free abrasive cutting of thermoelectric material.

### Cutting with bound abrasive

The mechanism of wire saw cutting with bound abrasive is somewhat different from free abrasive treatment. On treatment with bound abrasive, the destruction due to normal force directed perpendicular to the surface (the case of treatment with free abrasive) is supplemented with damages of processed surface due to cutting of micro projections fixed in the cutting edge by diamond grains. Normal forces passed from the working edge through diamond grains to thermoelectric material billet cause the appearance of microcracks which, being enlarged in treatment, propagate deep and close, forming detached parts. Then these detached parts crumble out and are removed from treatment zone. Removal of cutting products and cutting edge cooling is done by water or 3.5% water solution which is fed to treatment zone under pressure (Fig. 4).

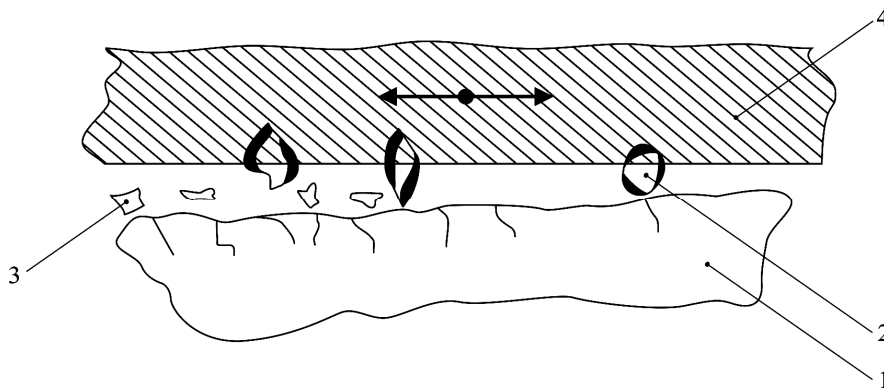


Fig. 4. Schematic of sample cutting with bound abrasive.  
1 – thermoelectric material; 2 – fixed abrasive grains;  
3 – detached parts of thermoelectric material; 4 – tool.

A replaceable wire saw for thermoelectric material cutting is made by the above described principle, but for bound abrasive processing a diamond micropowder ASN 40/28 is deposited on the surface of the wire by electroplating and fixed by deposition of transient group metals (cobalt, nickel, chromium) (Fig. 5).

At the present time cutting with bound abrasive is the most promising and advanced of all the existing methods. Its advantages include good quality of surface treatment, the accuracy of cut  $\pm 0.02$  mm.

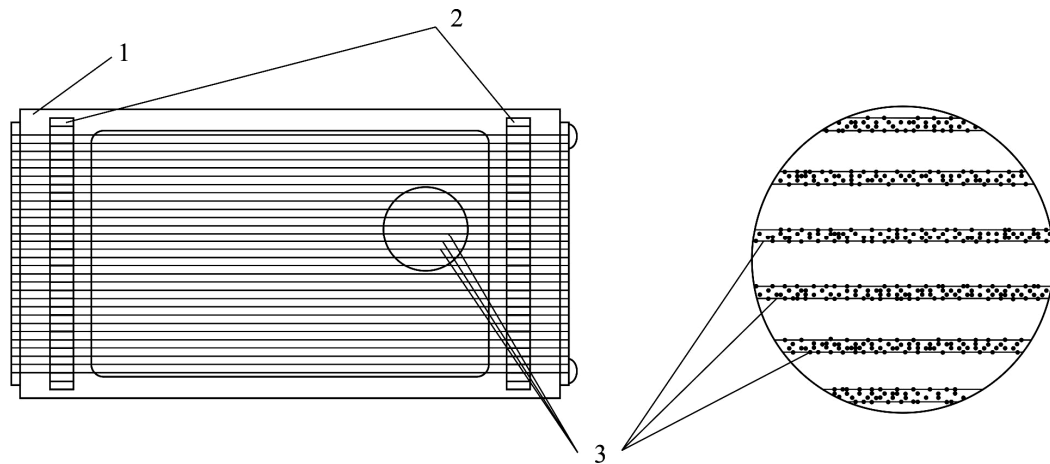


Fig. 5. Tool for cutting by wires with fixed diamond grains.

1 – tool; 2 – spacer bars;

3 – wires with fixed diamond grains.

After mechanical operations, a damaged layer remains on semiconductor surface which significantly affects both subsequent processing treatment (etching, oxidation) and, eventually, parameters of semiconductor devices (Fig. 6).

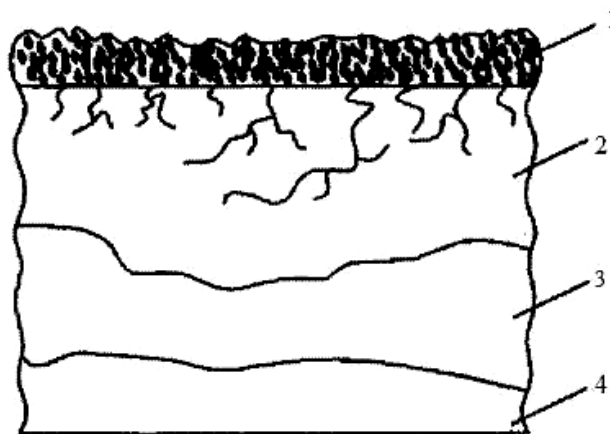


Fig. 6. Structure of surface layer damaged at machining.

1 – relief layer; 2 – microcracks;

3 – dislocation bunch region; 4 – single crystal.

Small-size desktop machine “Altec-13009” is intended for producing rectangular samples of thermoelectric material under laboratory conditions. Cutting process is significantly affected by billet feed velocity (pressing force to the working edge of the tool). At low billet feed velocities (0.1 ÷ 0.3 mm/min) cutting productivity is too low. With increasing feed velocity (0.4 ÷ 0.6 mm/min) the productivity is increased, and processing precision is reduced due to bending of strings. The plate being cut off will have a curved surface. With a low plate thickness it may result in its break during cutting. Therefore, a lower feed velocity is recommended for thin plates and a higher feed velocity for thicker plates, the deterioration of surface layer in this case making 10-25 $\mu$ m (Fig. 7).

The working tool of the machine is a frame with the wires located in parallel. The machine allows cutting under conditions of low deformation effects. Two pressure nuts are used to fasten the frame on the mobile carriage. The same nuts are used to set cutting wires parallel to travel direction of

the tool. Plain bearings of carriage guides provide for the accuracy and ease of their reciprocating motion. On the small-sized desktop machine the beginning and end of thermoelectric material cutting is controlled by dial gauge; table adjuster allows adjustment in the horizontal plane along the  $X$ ,  $Y$  axes.

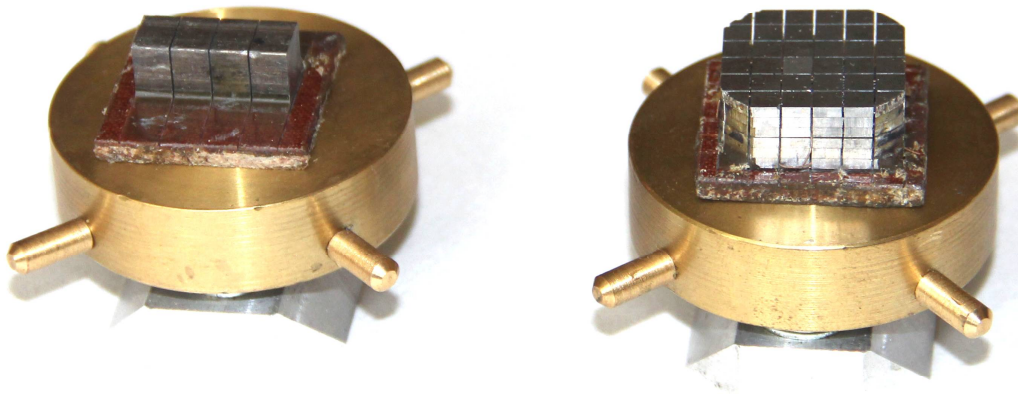


*Fig. 7 Bound abrasive cutting of thermoelectric material.*

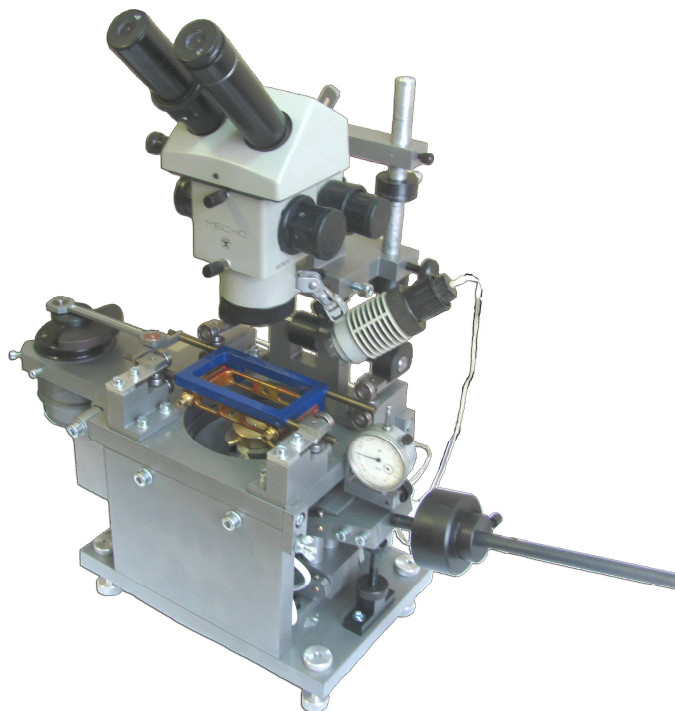


*Fig.8. General view of "Altec-13009" machine.*

The machine consists of a carriage with cutting tool 7 the reciprocating motion of which is realized by means of connecting rod 2 from electric motor 3 (SL-329 24V); carriage attachment points 4; mechanism for raising-lowering table 5, with counterweight of pressure on cutting tool edge; cut depth adjustment system 8, dial gauge 9 for control of cut depth, appliance for cooling liquid feed 11 (Fig. 9).

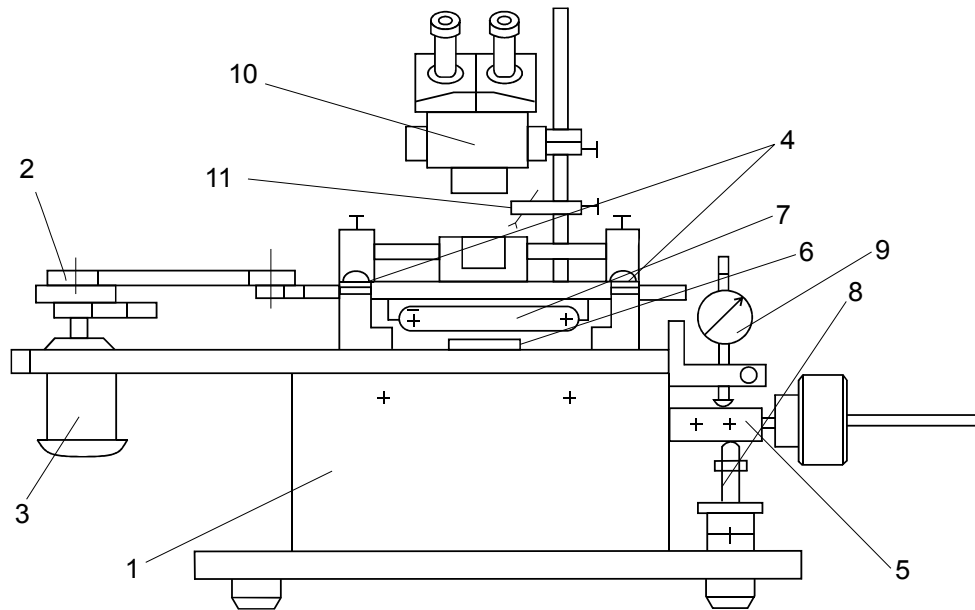


*Fig. 9. Schematic of small-sized desktop machine  
 1-bed; 2- drive unit; 3- electric engine SL-329 24V;  
 4- carriage attachment point; 5- mechanism for raising-lowering the table;  
 6- material; 7-cutting instrument; 8- cut depth adjustment and control system;  
 9- dial gauge; 10- MBS-10 microscope; 11- cooling liquid feed.*

Basic technical data and characteristics are given in Table 1.

*Table 1*

№	Characteristics	
1	Maximum dimensions of billet to be cut, mm	40x40x15
2	Number of wires $\varnothing$ 0.14 on a frame, minimum, pcs.	1
3	Number of wires $\varnothing$ 0.14 on a frame, maximum, pcs.	95
4	Width of cut with diamond coating, mm	0.22
5	Width of cut with free abrasive, mm	0.15
6	Weight, kg, not more	30
7	Electric power requirement, W	60
8	Power supply, CODEGEN 300W	14
9	Dimensions, mm	340 × 690 × 630

### Conclusions

1. Small-sized desktop machine is energy-efficient and does not require large material costs.
2. Wire cutting machine “Altec-13009” is easy to operate for the pursuance of research under laboratory conditions.

### References

1. Z.Yu.Hotra, *Handbook on the Technology of Microelectronic Devices* (Lviv:Kamenyar, 1986), 287p.
2. A.V.Satygo, S.F.Zaporov, The Effect of Various Methods for Cutting  $\text{Bi}_2\text{Te}_3$  on the Properties of Thermoelectric Cooling Modules, *J.Thermoelectricity* 4, 57–60 (2002).

3. Small-Sized Desktop Machine for Cutting Thermoelectric Materials “Altec – 13009”. *Leaflet.*

Submitted 20.11.2018

**Запаров С.Ф.<sup>1</sup>, Захарчук Т.В.<sup>1,2</sup>**

<sup>1</sup>Інститут термоелектрики НАН і МОН України,  
вул. Науки, 1, Чернівці, 58029, Україна,  
*e-mail: anatykh@gmail.com;*

<sup>2</sup>Чернівецький національний університет  
імені Юрія Федьковича, вул. Коцюбинського 2,  
Чернівці, 58012, Україна,  
*e-mail: anatykh@gmail.com*

**ОБЛАДНАННЯ ДЛЯ ОДЕРЖАННЯ  
ЗРАЗКІВ ТЕРМОЕЛЕКТРИЧНОГО МАТЕРІАЛУ  
ПРЯМОКУТНОЇ ФОРМИ**

*У даній роботі наведено методи та описано устаткування для механічного розрізування термоелектричного матеріалу із застосуванням вільного абразиву й струнами із закріпленими алмазними зернами. Пробні різи показали, що точність і найбільш щадний режим при обробці термоелектричного матеріалу досягаються різальним інструментом з використанням вольфрамового дроту діаметром 0.11мм-0.14мм. Бібл. 3, рис. 9, табл. 2.*

**Ключові слова:** обладнання для різання, інструмент для різання вільним абразивом, інструмент для різання зв'язаним абразивом

**Запаров С.Ф.<sup>1</sup>, Захарчук Т.В.<sup>1,2</sup>**

<sup>1</sup>Інститут термоелектричності НАН і МОН України, вул. Науки, 1,  
Черновці, 58029, Україна, *e-mail: anatykh@gmail.com;*

<sup>2</sup>Чернівецький національний університет  
імені Юрія Федьковича, вул. Коцюбинського 2,  
Черновці, 58012, Україна

**УСТРОЙСТВО ДЛЯ ПОЛУЧЕНИЯ  
ОБРАЗЦОВ ТЕРМОЭЛЕКТРИЧЕСКОГО МАТЕРИАЛА  
ПРЯМОУГОЛЬНОЙ ФОРМЫ**

*В настоящей работе приведены методы и оборудования для механического разрезания*

термоэлектрического материала с применением свободного абразива и струнами с закрепленными алмазными зернами. Пробныерезы показали, что точность и наиболее щадящий режим при обработке термоэлектрического материала достигают режущим инструментом с использованием вольфрамовой проволоки диаметром 0.11 мм-0.14 мм. Библ. 3, рис. 9, табл. 2.

**Ключевые слова:** устройство для резки, инструмент для резки свободным абразивом, инструмент для резки связанным абразивом

## References

1. Z.Yu.Hotra, *Handbook on the Technology of Microelectronic Devices* (Lviv:Kamenyar, 1986), 287p.
2. A.V.Satygo, S.F.Zaparov, The Effect of Various Methods for Cutting  $\text{Bi}_2\text{Te}_3$  on the Properties of Thermoelectric Cooling Modules, *J.Thermoelectricity* 4, 57–60 (2002).
3. Small-Sized Desktop Machine for Cutting Thermoelectric Materials “Altec – 13009”. *Leaflet*.

Submitted 20.11.2018



## ARTICLE SUBMISSION GUIDELINES

For publication in a specialized journal, scientific works are accepted that have never been printed before. The article should be written on an actual topic, contain the results of an in-depth scientific study, the novelty and justification of scientific conclusions for the purpose of the article (the task in view).

The materials published in the journal are subject to internal and external review which is carried out by members of the editorial board and international editorial board of the journal or experts of the relevant field. Reviewing is done on the basis of confidentiality. In the event of a negative review or substantial remarks, the article may be rejected or returned to the author(s) for revision. In the case when the author(s) disagrees with the opinion of the reviewer, an additional independent review may be done by the editorial board. After the author makes changes in accordance with the comments of the reviewer, the article is signed to print.

The editorial board has the right to refuse to publish manuscripts containing previously published data, as well as materials that do not fit the profile of the journal or materials of research pursued in violation of ethical norms (for instance, conflicts between authors or between authors and organization, plagiarism, etc.). The editorial board of the journal reserves the right to edit and reduce the manuscripts without violating the author's content. Rejected manuscripts are not returned to the authors.

### **Submission of manuscript to the journal**

The manuscript is submitted to the editorial office of the journal in paper form in duplicate and in electronic form on an electronic medium (disc, memory stick). The electronic version of the article shall fully correspond to the paper version. The manuscript must be signed by all co-authors or a responsible representative.

In some cases it is allowed to send an article by e-mail instead of an electronic medium (disc, memory stick).

English-speaking authors submit their manuscripts in English. Russian-speaking and Ukrainian-speaking authors submit their manuscripts in English and in Russian or Ukrainian, respectively. Page format is A4. The number of pages shall not exceed 15 (together with References and extended abstracts). By agreement with the editorial board, the number of pages can be increased.

To the manuscript is added:

1. Official recommendation letter, signed by the head of the institution where the work was carried out.

2. License agreement on the transfer of copyright (the form of the agreement can be obtained from the editorial office of the journal or downloaded from the journal website – Dohovir.pdf). The license agreement comes into force after the acceptance of the article for publication. Signing of the license agreement by the author(s) means that they are acquainted and agree with the terms of the agreement.

3. Information about each of the authors – full name, position, place of work, academic title, academic degree, contact information (phone number, e-mail address), ORCID code (if available). Information about the authors is submitted as follows:

authors from Ukraine - in three languages, namely Ukrainian, Russian and English;

authors from the CIS countries - in two languages, namely Russian and English;

authors from foreign countries – in English.

4. Medium with the text of the article, figures, tables, information about the authors in electronic

form.

5. Colored photo of the author(s). Black-and-white photos are not accepted by the editorial staff. With the number of authors more than two, their photos are not shown.

### **Requirements for article design**

The article should be structured according to the following sections:

- *Introduction*. Contains the problem statement, relevance of the chosen topic, analysis of recent research and publications, purpose and objectives.
- *Presentation of the main research material* and the results obtained.
- *Conclusions* summing up the work and the prospects for further research in this direction.
- *References*.

The first page of the article contains information:

- 1) in the upper left corner – UDC identifier (for authors from Ukraine and the CIS countries);
- 2) surname(s) and initials, academic degree and scientific title of the author(s);
- 3) the name of the institution where the author(s) work, the postal address, telephone number, e-mail address of the author(s);
- 4) article title;
- 5) abstract to the article – not more than 1 800 characters. The abstract should reflect the consistent logic of describing the results and describe the main objectives of the study, summarize the most significant results;
- 6) key words – not more than 8 words.

**The text** of the article is printed in Times New Roman, font size 11 pt, line spacing 1.2 on A4 size paper, justified alignment. There should be no hyphenation in the article.

**Page setup:** “mirror margins” – top margin – 2.5 cm, bottom margin – 2.0 cm, inside – 2.0 cm, outside – 3.0 cm, from the edge to page header and page footer – 1.27 cm.

**Graphic materials**, pictures shall be submitted in color or, as an exception, black and white, in .obj or .cdr formats, .jpg or .tif formats being also permissible. According to author’s choice, the tables and partially the text can be also in color.

*Figures* are printed on separate pages. The text in the figures must be in the font size 10 pt. On the charts, the units of measure are separated by commas. Figures are numbered in the order of their arrangement in the text, parts of the figures are numbered with letters – a, b, .. On the back of the figure, the title of the article, the author (authors) and the figure number are written in pencil. Scanned images and graphs are not allowed to be inserted.

*Tables* are provided on separate pages and must be executed using the MSWord table editor. Using pseudo-graph characters to design tables is inadmissible.

*Formulae* shall be typed in Equation or MatType formula editors. Articles with formulae written by hand are not accepted for printing. It is necessary to give definitions of quantities that are first used in the text, and then use the appropriate term.

*Captions to figures and tables* are printed in the manuscript after the references.

*Reference list* shall appear at the end of the article. References are numbered consecutively in the order in which they are quoted in the text of the article. References to unpublished and unfinished works are inadmissible.

**Attention!** In connection with the inclusion of the journal in the international bibliographic abstract database, the reference list should consist of two blocks: CITED LITERATURE and REFERENCES (this requirement also applies to English articles):

CITED LITERATURE – sources in the original language, executed in accordance with the Ukrainian standard of bibliographic description DSTU 8302:2015. With the aid of VAK.in.ua

(<http://vak.in.ua>) you can automatically, quickly and easily execute your “Cited literature” list in conformity with the requirements of State Certification Commission of Ukraine and prepare references to scientific sources in Ukraine in understandable and unified manner. This portal facilitates the processing of scientific sources when writing your publications, dissertations and other scientific papers.

REFERENCES – the same cited literature list transliterated in Roman alphabet (recommendations according to international bibliographic standard APA-2010, guidelines for drawing up a transliterated reference list “References” are on the site <http://www.dse.org.ua>, section for authors).

**To speed up the publication of the article, please adhere to the following rules:**

- in the upper left corner of the first page of the article – the UDC identifier;
- family name and initials of the author(s);
- academic degree, scientific title;

begin a new line, Times New Roman font, size 12 pt, line spacing 1.2, center alignment;

- name of organization, address (street, city, zip code, country), e-mail of the author(s);

begin a new line 1 cm below the name and initials of the author(s), Times New Roman font, size 11 pt, line spacing 1.2, center alignment;

- the title of the article is arranged 1 cm below the name of organization, in capital letters, semi-bold, font Times New Roman, size 12 pt, line spacing 1.2, center alignment. The title of the article shall be concrete and possibly concise;
- the abstract is arranged 1 cm below the title of the article, font Times New Roman, size 10 pt, in italics, line spacing 1.2, justified alignment in Ukrainian or Russian (for Ukrainian-speaking and Russian-speaking authors, respectively);
- key words are arranged below the abstract, font Times New Roman, size 10 pt, line spacing 1.2, justified alignment. The language of the key words corresponds to that of the abstract. Heading “Key words” - font Times New Roman, size 10 pt, semi-bold;
- the main text of the article is arranged 1 cm below the abstract, indent 1 cm, font Times New Roman, size 11 pt, line space spacing 1.2, justified alignment;
- formulae are typed in formula editor, fonts Symbol, Times New Roman. Font size is “normal” – 12 pt, “large index” – 7 pt, “small index” – 5 pt, “large symbol” – 18 pt, “small symbol” – 12 pt. The formula is arranged in the text, center aligned and shall not occupy more than 5/6 of the line width, formulae are numbered in parentheses on the right;
- dimensions of all quantities used in the article are represented in the International System of

Units (SI) with the explication of the symbols employed;

- figures are arranged in the text. The figures and pictures shall be clear and contrast; the plot axes – parallel to sheet edges, thus eliminating possible displacement of angles in scaling; figures are submitted in color, black-and-white figures are not accepted by the editorial staff of the journal;

- tables are arranged in the text. The width of the table shall be 1 cm less than the line width. Above the table its ordinary number is indicated, right alignment. Continuous table numbering throughout the text. The title of the table is arranged below its number, center alignment;

- references should appear at the end of the article. References within the text should be

enclosed in square brackets behind the text. References should be numbered in order of first appearance in the text. Examples of various reference types are given below.

### **Examples of LITERATURE CITED**

#### Journal articles

Anatychuk L.I., Mykhailovsky V.Ya., Maksymuk M.V., Andrusiak I.S. Experimental research on thermoelectric automobile starting pre-heater operated with diesel fuel. *J.Thermoelectricity*. 2016. №4. P.84–94.

#### Books

Anatychuk L.I. *Thermoelements and thermoelectric devices. Handbook*. Kyiv, Naukova dumka, 1979. 768 p.

#### Patents

*Patent of Ukraine № 85293*. Anatychuk L.I., Luste O.J., Nitsovykh O.V. Thermoelement.

#### Conference proceedings

Lysko V.V. *State of the art and expected progress in metrology of thermoelectric materials*. Proceedings of the XVII International Forum on Thermoelectricity (May 14-18, 2017, Belfast). Chernivtsi, 2017. 64 p.

#### Authors' abstracts

Kobylianskyi R.R. *Thermoelectric devices for treatment of skin diseases*: extended abstract of candidate's thesis. Chernivtsi, 2011. 20 p.

### **Examples of REFERENCES**

#### Journal articles

Gorskiy P.V. (2015). Ob usloviakh vysokoi dobrotnosti i metodikakh poiska perspektivnykh sverhreshetochnykh termoelektricheskikh materialov [On the conditions of high figure of merit and methods of search for promising superlattice thermoelectric materials]. *Termoelektrichestvo - J.Thermoelectricity*, 3, 5 – 14 [in Russian].

#### Books

Anatychuk L.I. (2003). *Thermoelectricity. Vol.2. Thermoelectric power converters*. Kyiv, Chernivtsi: Institute of Thermoelectricity.

#### Patents

*Patent of Ukraine № 85293*. Anatychuk L. I., Luste O.Ya., Nitsovykh O.V. Thermoelements [In Ukrainian].

#### Conference proceedings

Rifert V.G. Intensification of heat exchange at condensation and evaporation of liquid in 5 flowing-down films. In: *Proc. of the 9<sup>th</sup> International Conference Heat Transfer*. May 20-25, 1990, Israel.

#### Authors' abstracts

Mashukov A.O. *Efficiency hospital state of rehabilitation of patients with color cancer*. PhD (Med.) Odesa, 2011 [In Ukrainian].